GEOLOGY OF THE INTERMOUNTAIN WEST
an open-access journal of the Utah Geological Association
ISSN 2380-7601

Volume 12 ***2025***

DIFFERENTIATING ANKYLOSAUR SPECIES IN THE UPPER JURASSIC MORRISON FORMATION IN LIGHT OF NEWLY RECOVERED SKELETAL ELEMENTS OF *MYMOORAPELTA MAYSI* FROM ITS TYPE LOCALITY

James I. Kirkland, ReBecca K. Hunt-Foster, Kirsty Morgan, Julia B. McHugh, and John R. Foster

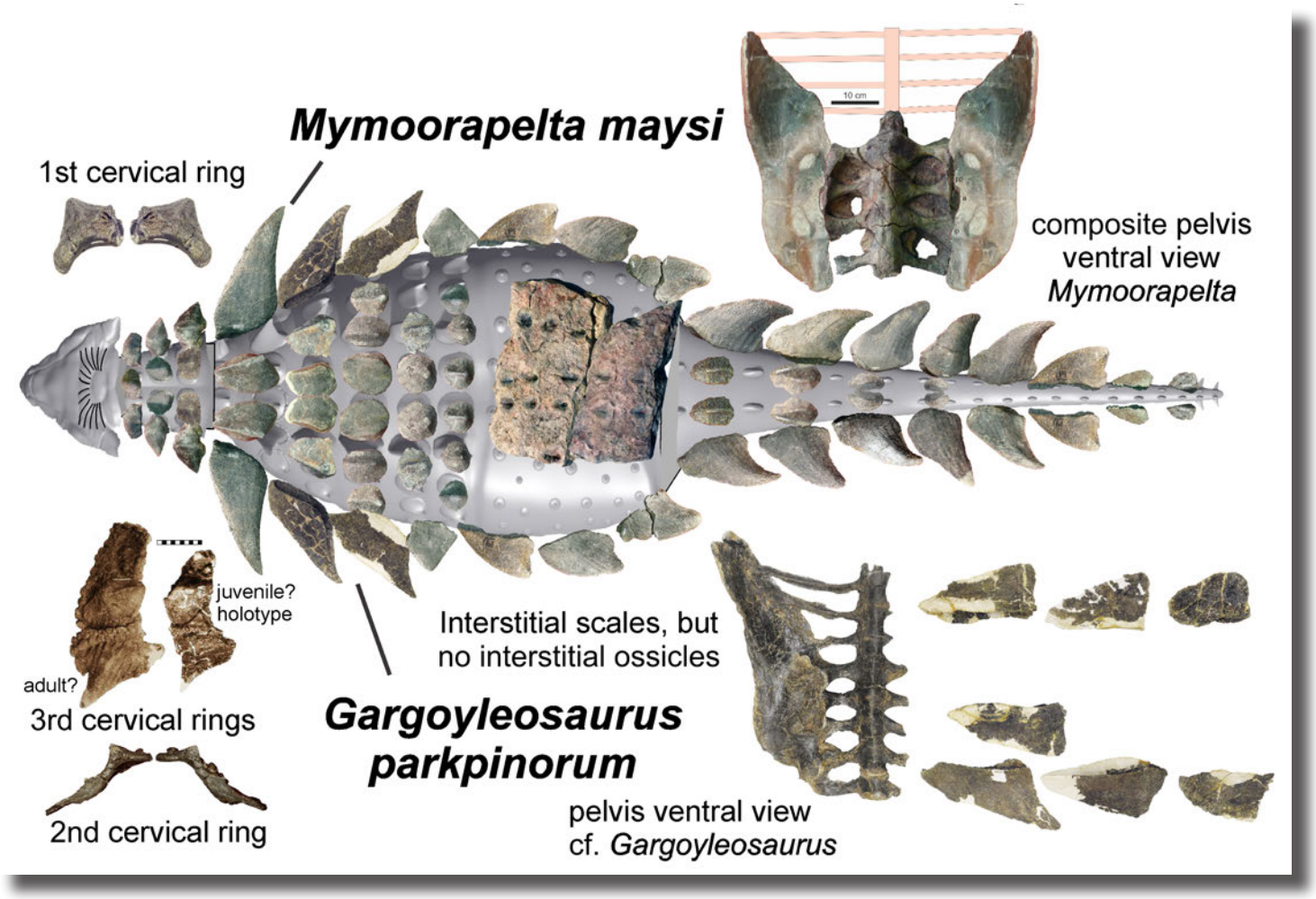

This is an open-access article in which the Utah Geological Association permits unrestricted use, distribution, and reproduction of text and figures that are not noted as copyrighted, provided the original author and source are credited. Email inquiries to GIW@utahgeology.org.

GEOLOGY OF THE INTERMOUNTAIN WEST

an open-access journal of the Utah Geological Association

ISSN 2380-7601

Volume 12 ***2025***

Editors

Douglas A. Sprinkel
Azteca Geosolutions
801.391.1977
GIW@utahgeology.org
dsprinkel@gmail.com

Thomas C. Chidsey, Jr.
Utah Geological Survey, Emeritus
801.824.0738
tomchidsey@gmail.com

Bart J. Kowallis
Brigham Young University
801.380.2736
bkowallis@gmail.com

Steven Schamel
GeoX Consulting, Inc.
801.583.1146
geox-slc@comcast.net

John R. Foster
Utah Field House of Natural History State Park Museum
435.789.3799
johnfoster@utah.gov

William R. Lund
Utah Geological Survey, Emeritus
435.590.1338
williamlundugs@gmail.com

Production

Cover Design and Desktop Publishing
Douglas A. Sprinkel

Cover

Hypothetical reconstruction of the distribution of osteoderm elements of *Mymoorapelta maysi* with reconstructed pelvis in ventral view as compared to that of *Gargoyleosaurus parkpinorum*'s pelvis and lateral osteoderm elements. Scale of fossil elements by reference to figures in manuscript. Comparison of *Gargoyleosaurus* third cervical rings modified after Carpenter et al. (2013).

Geology of the Intermountain West (GIW) is an open-access journal in which the Utah Geological Association permits unrestricted use, distribution, and reproduction of text and figures that are not noted as copyrighted, provided the original author and source are credited.

2025–2026 UGA Board

President	Rob Buehring	robbuehring@yahoo.com	713.412.9269
President-Elect	Trae Boman	traebgeologist@gmail.com	801.648.5206
Program Chair	Mike Arnoff	marnoff@utah.gov	385.303.0431
Treasurer	Will Hurlbut	wdhurlbut@gmail.com	860.733.3190
Secretary	Kylie Arcaris	kaarcaris@gmail.com	801.628.6731
Past President	Keilee Higgs	keileeann@utah.gov	801.678.3683

UGA Committees

Environmental Affairs	Seeking a Volunteer		
Geologic Road Sign	Greg Gavin	greggavin@gmail.com	513.509.1509
Historian	Paul Anderson	paul@pbageo.com	801.364.6613
Outreach	Greg Nielsen	gnielsen@weber.edu	801.626.6394
Public Education	Zach Anderson	zanderson@utah.gov	801.537.3300
	Matt Affolter	gfl247@yahoo.com	
Publications	Paul Inkenbrandt	paulinkenbrandt@utah.gov	801.537.3361
Publicity	Paul Inkenbrandt	paulinkenbrandt@utah.gov	801.537.3361
Social/Recreation	Roger Bon	rogerbon@xmission.com	801.580.1331

AAPG House of Delegates

2023–2026 Term	David A. Wavrek	dwavrek@petroleumsystems.com	801.322.2915

State Mapping Advisory Committee

UGA Representative	Bill Loughlin	bill@loughlinwater.com	435.649.4005

Earthquake Safety Committee

Chair	Seeking a Volunteer		

UGA Website — www.utahgeology.org

Webmaster	Paul Inkenbrandt	paulinkenbrandt@utah.gov	801.537.3361

Scholarship Golf Tournament

Co-Chair	Rick Ford	rford@weber.edu	801.915.3188
Co-Chair	John South	jsouth@utah.gov	385.266.2113

UGA Newsletter

Newsletter Editor	Mike Barber	uga.newsletter@gmail.com	435.640.1382

Become a member of the UGA to help support the work of the Association and receive notices for monthly meetings, annual field conferences, and new publications. Annual membership is $30 and annual student membership is only $5. Visit the UGA website at www.utahgeology.org for information and membership application.

The UGA board is elected annually by a voting process through UGA members. However, the UGA is a volunteer-driven organization, and we welcome your voluntary service. If you would like to participate please contact the current president or committee member corresponding with the area in which you would like to volunteer.

Utah Geological Association formed in 1970 from a merger of the Utah Geological Society, founded in 1946, and the Intermountain Association of Geologists, founded in 1949. Affiliated with the American Association of Petroleum Geologists.

GEOLOGY OF THE INTERMOUNTAIN WEST
an open-access journal of the Utah Geological Association
Volume 12 ***2025***

Differentiating Ankylosaur Species in the Upper Jurassic Morrison Formation in Light of Newly Recovered Skeletal Elements of *Mymoorapelta maysi* from its Type Locality

James I. Kirkland[1], ReBecca K. Hunt-Foster[2], Kirsty Morgan[3], Julia B. McHugh[4], and John R. Foster[5]
[1]*Utah Geological Survey, Salt Lake City, UT 84114-6100 USA; jameskirkland@utah.gov*
[2]*Dinosaur National Monument, Jensen, UT 84035 USA; rebecca.k.hunt@gmail.com*
[3]*Department of Geosciences, University of Arkansas Fayetteville, AR 72701 USA; kirstymorgan08@gmail.com*
[4]*Museum of Western Colorado, Grand Junction, CO 81502 USA; jmchugh@mowc.co*
[5]*Utah Field House of Natural History State Park Museum, Vernal, UT 84078 USA; johnfoster@utah.gov*

ABSTRACT

Since the first Jurassic ankylosaur from North America, *Mymoorapelta maysi,* was described in 1994, considerably more material has been recovered from the type locality in western Colorado. This taxon is the most complete ankylosaur from the Morrison Formation and is completely distinct from *Gargoyleosaurus*. The new material from this and 11 other known Morrison ankylosaur localities justify a new description of the available fossils to better characterize these two Morrison dinosaur genera and better resolve their distribution through the extent of the Morrison Formation. *Mymoorapelta* is restricted to the upper Morrison Formation in Utah, Colorado, and southern Wyoming, whereas *Gargoyleosaurus* is found near the base of the Morrison and up section into the upper Morrison. *Gargoyleosaurus* may well be represented by more than one species through its stratigraphic range.

INTRODUCTION

With its description in the 1990s (Kirkland and Carpenter, 1994; Kirkland et al., 1998), *Mymoorapelta* became the first well-documented ankylosaur from the Upper Jurassic Morrison Formation. This was soon followed by the description of *Gargoyleosaurus* (Carpenter et al., 1998). Although both are from the Morrison and *Mymoorapelta* is better preserved, the nearly complete skull of *Gargoyleosaurus* made it favored with taxonomists. However, continued excavations at the type location, at the Mygatt-Moore Quarry (Foster et al., 2018; Drumheller et al., 2020; McHugh et al., 2020, 2023) in westernmost Colorado, have resulted in the recovery of nearly every skeletal element of *Mymoorapelta*, including much of the skull, making it the most completely represented Morrison ankylosaur. Skull elements include jugal, postorbital, quadrate, braincase, and teeth that compare well with *Gargoyleosaurus*, whose jugals, quadrates, and braincase were damaged during extraction. However, differences in the proportions in the braincase, pelvis, caudal vertebrae, caudal osteoderms, and in the stratigraphic positions of specimens of *Mymoorapelta* and *Gargoyleosaurus* confirms the retention of the latter as a distinct genus. Of the major postcranial skeleton, only the pubis and femur are not represented in the material for *Mymoorapelta* present in the Mygatt-Moore Quarry but are the only skeletal elements known from the hindquarters of the holotype

Citation for this article.
Kirkland, J.I., Hunt-Foster, R., Morgan, K., McHugh, J.B., and Foster, J.R., 2025, Differentiating ankylosaur species in the Upper Jurassic Morrison Formation in light of newly recovered skeletal elements of *Mymoorapelta maysi* from its type locality: Geology of the Intermountain West, v. 12, p. 315–393, https://doi.org/10.31711/giw.v12.pp315-393.

of *Gargoyleosaurus*. All osteoderms of the external carapace are well represented including significant portions of cervical rings. Clearly, *Mymoorapelta* and *Gargoyleosaurus* are similar in nearly every morphological feature of the shared, preserved skeletal elements. *Mymoorapelta* preserves a mosaic of characters relative to more derived ankylosaurs that may provide important information as to what are the primitive character states in Ankylosauria. For instance, the ischium is bent as in polacanthids, nodosaurids, and most stegosaurs indicating that the straight ischium of ankylosaurids is actually a derived character state. The scapular spine forms a vertical ridge opposite the glenoid in *Mymoorapelta* as in ankylosaurids and the only other Morrison ankylosaur scapula from the Dry Mesa Quarry in western Colorado (Kirkland et al., 1998). *Mymoorapelta* has short limbs with even shorter distal limb elements as in ankylosaurids and polacanthids. This new analysis indicates that *Mymoorapelta* and *Gargoyleosaurus* share unique characters with *Polacanthus*, *Hylaeosaurus*, *Gastonia*, and *Hoplitosaurus* (Blows, 2015).

ANKYLOSAUR REMAINS FROM THE MORRISON FORMATION

Ankylosaur remains are now documented in the Upper Jurassic Morrison Formation of Colorado, Utah, Wyoming, and New Mexico (Figure 1). The first Morrison ankylosaur fossils were recognized in 1990 in western Colorado (Kirkland and Carpenter, 1994) at the Mygatt-Moore Quarry and are all curated into the collections of the Museum of Western Colorado (MWC) and by 1998, ankylosaur fossils had been recognized from six localities (Kirkland et al., 1998). There are currently 12 localities recognized across four states. These localities span nearly the entire Morrison outcrop belt (Figure 1).

Colorado Localities

Mygatt-Moore Quarry

The Mygatt-Moore Quarry in western Colorado is near the middle of the Brushy Basin Member of the Morrison Formation (Figures 2A through 2D). The site is the type locality for *Mymoorapelta* (Kirkland and Carpenter, 1994; Kirkland et al., 1998) and is the only site in the Morrison that has yielded the remains of more than one individual ankylosaur. The taphonomy of the quarry has recently been described in detail by Foster et al. (2018). This site is discussed in more detail below.

Cactus Park Ankylosaur

In the early 1990s, Denver high school teacher Kent Hups discovered an ankylosaur skeleton weathering out of a calcite-cemented sandstone ledge in the Brushy Basin Member on the east side of Cactus Park southeast of Grand Junction, Colorado (Figure 2E). The fossil (specimen MWC 2610) is an articulated skeleton lying ventral side down. It was assigned to *Mymoorapelta* based on the morphology of its caudal plates (Kirkland et al., 1998). The curated fossil material consists of broken sandstone blocks collected from the slope below the ledge that revealed much of the posterior portion of the skeleton. This material consists largely of external molds of the bones and unprepared bones within the sandstone blocks.

Much of the anterior portion of the skeleton remains uncollected in the field where it appears to be preserved in a multi-ton block of sandstone that remains in continuity with the sandstone ledge. Requests to bring in heavy equipment to collect this large specimen have been turned down by the Bureau of Land Management, as the site is within the Dominguez-Escalante National Conservation Area. However, during a visit to the site, its discoverer Kent Hups found the skull in the highly cemented sandstone and brought it to the Denver Museum of Nature and Science (DMNH) for preparation. The skull, which initially had been complete, became fragmented during the course of preparation. The highly fragmented skull is in sections coated by sandstone and is undergoing consolidation and preparation in the paleontology lab at Dinosaur Journey, MWC, which is expected to take several years. Hopefully this entire specimen will be collected and studied in the future.

Garden Park Tibia

In 1992, the DMNH collected a partial ankylosaur

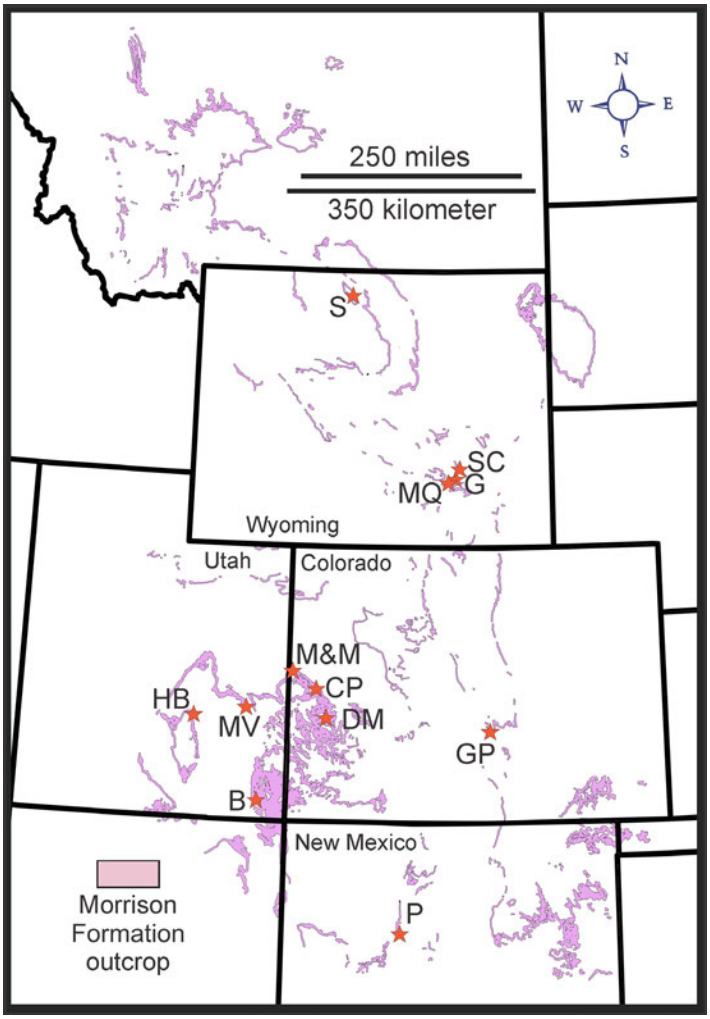

Figure 1. Locality map of the Rocky Mountain region indicating where ankylosaurs have been found in the Morrison Formation. Abbreviations: B = Los Angeles County Museum's Blanding *Mymoorapelta* sacrum locality; CP = Cactus Park, Hups Quarry's *Mymoorapelta* skeleton; DM = Dry Mesa Quarry (scattered *Mymoorapelta* elements); G = type locality of *Gargoleosaurus* at Bone Cabin West Quarry; GP = Denver Museum of Science and Nature's Garden Park *Stegosaurus* site (Ankylosaur tibia); HB = associated skeleton at Hanksville-Burpee Quarry; M&M = Mygatt-Moore Quarry, type locality of *Mymoorapelta*; MQ = Mailyn Quarry (ankylosaur caudal vertebrae and caudal plates); MV = Movie Valley ankylosaur; P = Peterson Quarry (ankylosaur osteoderm); S = Simon Quarry has yielded *Gargoyleosaurus* pelvis and tibia; SC = Sheep Creek; B = Boris Quarry cf. *Mymoorapelta* braincase and perhaps Zane Quarry ankylosaur caudal vertebra.

tibia (specimen DMNH 15162) beneath a *Stegosaurus* skeleton they had been excavating at the locally well-known Small Quarry within the Garden Park area, south-central Colorado. Initially identified as indeterminate (Kirkland et al., 1998), it compares well with the partial tibia from the Mygatt-Moore Quarry and Cactus Park. Given its stratigraphic position in the upper Morrison Formation just above the "clay change," a regional marker horizon where the surface weathering of Morrison mudstone indicates a significant increase in smectitic (swelling) clay and thus input of volcanic ash (Peterson and Turner, 1998; Turner and Peterson 1999, 2004; Demko et al., 2004; Kirkland, 2006; Christiansen et al., 2015; Kirkland et al., 2020), it is now considered to represent a possible occurrence of *Mymoorapelta*.

Dry Mesa Quarry

Field crews from Brigham Young University's Museum of Paleontology (BYU) have collected an abundance of diverse dinosaur remains from the Dry Mesa Quarry in the medial Morrison Formation of western Colorado over many years (Miller et al., 1991); among these are several ankylosaur elements. A well-preserved scapulocoracoid (specimen BYU 725-12963) was collected in 1990 from the Dry Mesa Quarry in the lower Brushy Basin Member by Rod Scheetz (Kirkland et al., 1998); subsequently, a grooved shoulder spine and several caudal plates have been prepared from the site. The co-occurrence of *Allosaurus jimmadseni* suggests that it is temporally equivalent stratigraphically from the type locality in the Salt Wash Member of the Morrison Formation at Dinosaur National Monument and in the lower Morrison of Wyoming (Chure and Loewen, 2020). Stratigraphically, Turner and Peterson (1999) place the Dry Mesa Quarry at a clay composition change (sudden appearance of smectitic clays near base of Brushy Basin) that has been noted by them and others (e.g., Demko et al., 2004; Kirkland, 2006) as forming a distinct surface across the Colorado Plateau associated with a major calcrete horizon. Extending that marker bed into Wyoming and farther north has not been considered possible as smectitic clay in the Morrison vanishes northward across Wyoming (Trujillo, 2006).

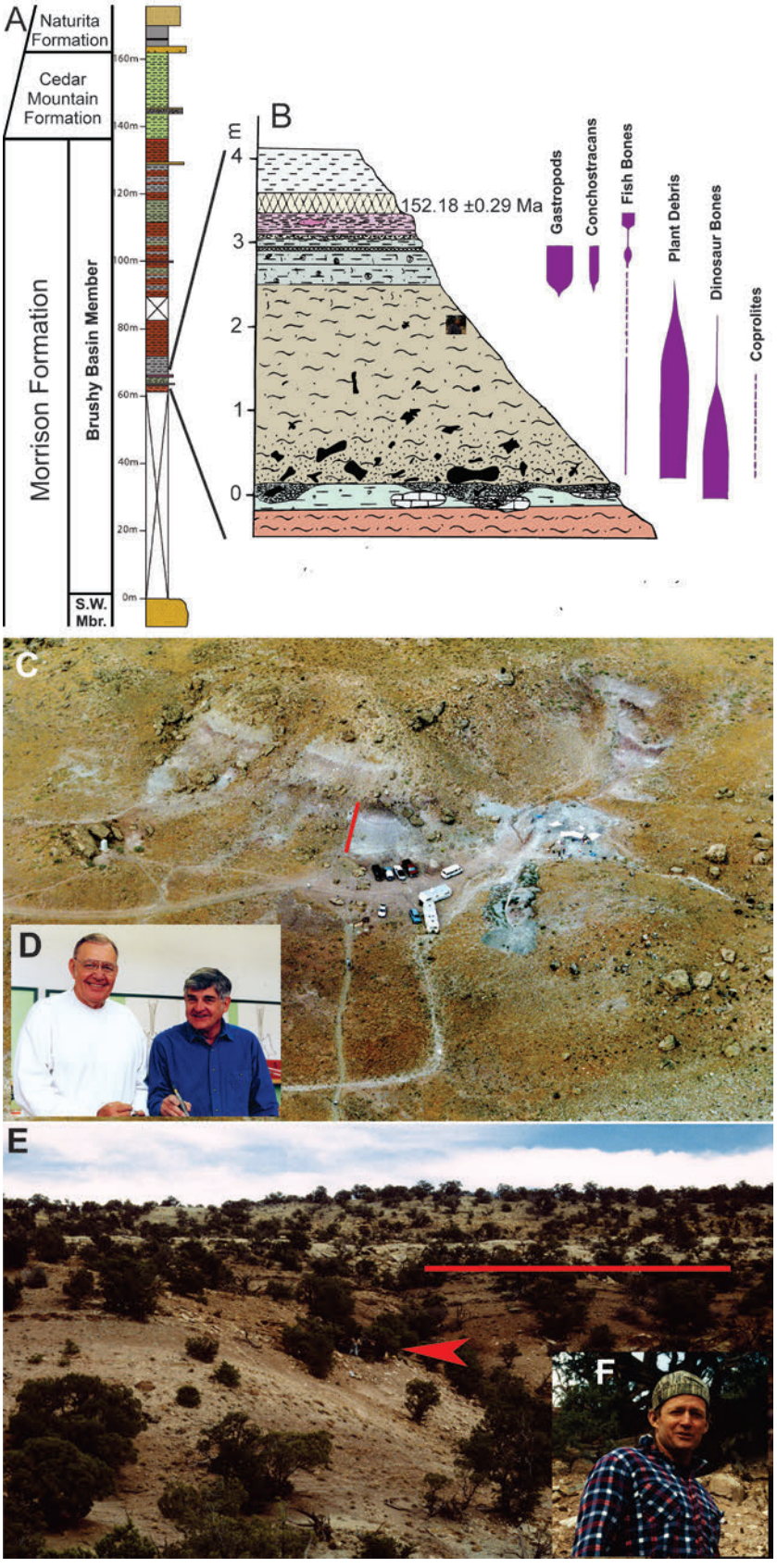

Figure 2. *Mymoorapelta* localities in the Morrison Formation of western Colorado. (A) Brushy Basin Member of Morrison Formation in Rabbit Valley with the position of the Mygatt-Moore Quarry indicated after Foster et al. (2018). (B) Detailed section through Mygatt-Moore Quarry from Chin and Kirkland (1998), scale is in meters. (C) Oblique aerial photograph of the Mygatt-Moore Quarry area. Red bar indicates position of detailed stratigraphic section in B (Google Earth image). (D) J.D. Moore and Pete Mygatt, discoverers of the Mygatt-Moore Quarry. (E) Overview of the Cactus Park *Mymoorapelta* site. Red arrowhead indicates ankylosaur site. Red bar indicates base of the Lower Cretaceous Burro Canyon Formation. Note that much of the Brushy Basin Member of the Morrison Formation has been truncated at the basal Cretaceous unconformity. (F) Kent Hups during the initial excavations of the Cactus Park in the mid-1990s. Figures E and F courtesy of Harley Armstrong, retired, Bureau of Land Management.

Wyoming Localities

Bone Cabin Quarry

Dinosaur excavations have been undertaken at Bone Cabin Quarry since the American Museum of Natural History (AMNH) first opened the quarry in 1898 northwest of Laramie (Colbert, 1968). However, it was not until the mid-1990s that excavations to the west of the main AMNH site by Western Paleontology Labs of Orem, Utah, yielded the remains of a partial ankylosaur skeleton with a well-preserved skull in a subsite referred to as Bone Cabin West. Following their donation of the specimen to the DMNH, it was described as *Gargoyleosaurus parkpinorum* (Carpenter et al., 1998; Kilbourne and Carpenter, 2005). Bone Cabin Quarry is the stratigraphically highest site (Figure 3) from which diagnostic *Gargoyleosaurus* material has been collected (Schmude and Weege, 1996) and it is the only site where it co-occurs with *Allosaurus fragilis* (Turner and Peterson, 1999; Foster, 2003). This occurrence supports overlap in the temporal ranges of *Mymoorapelta* and *Gargoyleosaurus*.

Boris Quarry

A water-worn ankylosaur braincase at the University of Wyoming, specimen UW 21869 was recovered during the excavation of an *Apatosaurus* femur at the "Boris" locality, specimen UW V-93101, near Sheep Creek in south-central Wyoming by Robert T. Bakker and volunteers on a Dinamation International Society dig in July of 1993. Bakker's field notes indicate that stratigraphically, the locality is situated about 19 m below the base of the Dakota Formation (Muddy Formation) in smectitic mudstone well above the regional calcrete marking the "clay change" in the upper Morrison Formation of this region. This site was referred to as the Mummy Quarry in Kirkland et al. (1998).

The specimen includes the braincase and skull roof overlying it. Abrasion on the margins of the fossil suggests wear during transport prior to burial in the bone lag accumulation represented by the "Boris" locality at Sheep Creek as interpreted by Bakker (field interpretation on file at the University of Wyoming Geological Museum). The proportions of the basicranium and its stratigraphic position suggest this specimen represents an example of *Mymoorapelta* from Wyoming.

Meilyn Quarry

Excavations in the 1990s at the Meilyn Quarry northwest of Medicine Bow in southern Wyoming (Figures 1 and 3) undertaken by Western Paleontology Labs has yielded two caudal vertebrae and three caudal plates. The Meilyn Quarry is situated 7 m above the base of the Morrison Formation (Schmude and Weege, 1996) even farther to the southwest than the Boris Quarry along the west flank of the Medicine Bow anticline. These interesting specimens were sold to private collectors with the caudal plates going to one unknown collector and a medial caudal vertebra going to another unknown collector (Jason Cooper, Dinosaurs of America LLC., verbal communication, 2000). One proximal caudal vertebra has been curated into the collections of the Elizabeth Dee Shaw Stewart Museum of Paleontology at the George S. Eccles Dinosaur Park, Ogden, Utah. Although we have been able to view photographs of the specimens in private hands, access to future researchers is not likely. Perhaps future excavations at the Meilyn Quarry will yield additional material.

Zane Quarry

Kirkland et al. (1998) reported on a partial mid-caudal vertebra collected by Robert T. Bakker from the Zane Quarry near the base of the Morrison Formation near Sheep Creek in south-central Wyoming and reported as curated at the Tate Museum, Casper College, Casper, Wyoming. Turner and Peterson (1999) record several sites at the Zane quarries as WY-92, but no known records exist as to their specific location, but they may be near the Boris Quarry. The low stratigraphic occurrence of this locality suggests that it may be nearly correlative with the Meilyn Quarry. Following up with the Tate Museum, it was revealed that no specimen had ever been curated into their collections from the Zane Quarry.

Simon Quarry

The most recently discovered ankylosaur material

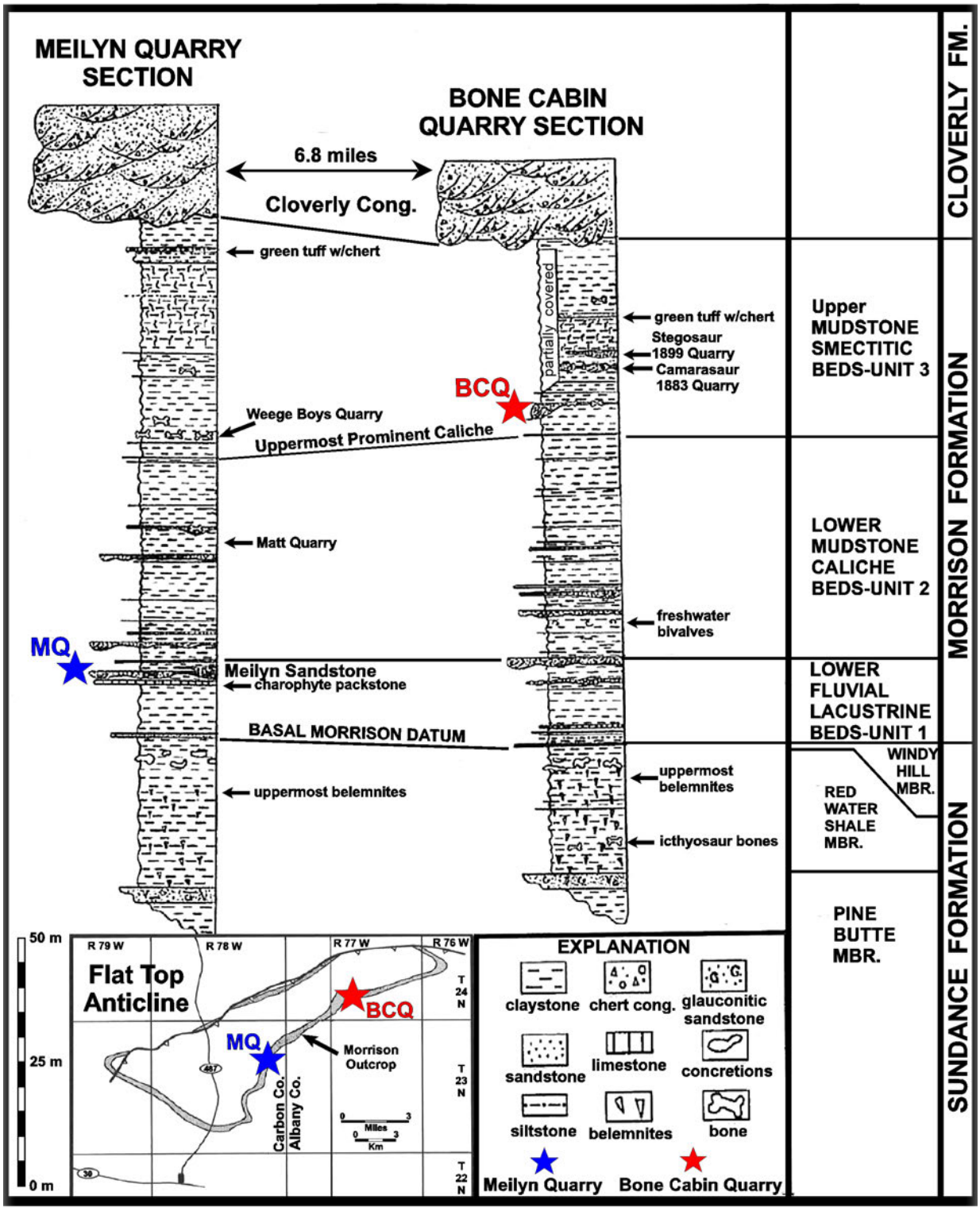

Figure 3. Relative stratigraphic position of *Gargoyleosaurus* localities in southern Wyoming. Red star is holotype *Gargoyleosaurus parkpinorum* locality at Bone Cabin Quarry. Blue star is the oldest Morrison ankylosaur in Meilyn Quarry. Modified after Schmude and Weege (1996).

in Wyoming is from the Bob Simon's Red Ranch Quarries about 20 to 30 m above the base of the Morrison Formation on the northeast side of the Big Horn Basin (Maidment et al., 2015). Specimen DMNH 58831 consists of a complete sacrum with right ilium and the right second cervical half ring. Carpenter et al. (2013) assigned this specimen to *Gargoyleosaurus parkpinorum* based on its similar cervical half ring,

The differences in the stratigraphic level of the Simon and Bone Cabin Quarries could bring the specific identification of the Simon Quarry specimen as *Gargoyleosaurus parkpinorum* into question. However, as discussed below, given the great disparity in the characters of the sacrum and ilium of this specimen and *Mymoorapelta*, we agree that it is most parsimonious to assign this specimen to the genus *Gargoyleosaurus* based on the similarities of the cervical ring.

Utah Localities

Movie Valley Ankylosaur

During the 1970s, Jim Jensen of BYU excavated several associated dorsal vertebrae and rib fragments from a site in the southern part of Little Valley near the Cat Ballou movie set west of Arches National Park. Although the original site has not been relocated, it is assumed the fossils are from the Brushy Basin Member, as much of the valley is formed by erosion of these strata and the preservation of the bone suggests that the fossils were collected from the Morrison Formation. These fossils compare well with those of *Mymoorapelta*, but as they are not in themselves diagnostic and the stratigraphic position of the site has been in question, they can only be questionably referred to as *Mymoorapelta*. Recently, Matt Wedel (Western University of Health Sciences) found a bone and wood scatter in the medial part of the Brushy Basin, which includes a diagnostic ankylosaur rib section near the south end of this valley that may pertain to the specimen. Subsequent exploration resulted in more ankylosaur fragments and the specific identification of Wedel's site. Because we are unable to prove that this is the original Movie Valley ankylosaur site, the specimen has been assigned its own locality number within the State of Utah's paleontological locality database (Matt's Ankylosaur in the Woods Gr1381v [see Gr335v: Movie Valley Ankylosaur]).

Los Angeles County Museum Sacrum

While conducting excavations at a dinosaur site (LACM Locality 7683) in the medial Brushy Basin Member near Blanding in southwestern Utah, the Los Angeles County Museum (LACM) uncovered an ankylosaur sacrum. It has been identified as *Mymoorapelta* based primarily on the presence of a groove along the ventral surface of the sacral centra as in the material assigned to the holotype individual. Additionally, this specimen lacks a fused series of dorsal vertebrae to form a synsacrum.

Hanksville-Burpee Ankylosaur

In June of 2014, Kirkland was asked to examine ankylosaur material being uncovered by the Burpee Museum in a huge dinosaur site in the Brushy Basin Member northeast of Hanksville, Utah. Numerous dorsal osteoderms and several ribs were collected from what may be an associated ankylosaur specimen. Additional material is still being recovered from the locality and under study at the Burpee Museum. Initially the fossils were attributed to *Mymoorapelta* (Tremaine et al., 2015). Subsequently, Large (2023) proposed that these fossils pertain to *Gargoyleosaurus* on the basis of sharing a lateral depression on the lateral side of the dorsal osteoderms.

New Mexico Locality

A single keeled ankylosaur osteoderm has been curated into the collections of the New Mexico Museum of Natural History and Science (NMMNH). Specimen NMMNH P-58749 was collected from the Peterson Quarry in west-central New Mexico, 26 m below the top of Brushy Basin Member (Heckert et al., 2003; Burns and Lucas, 2015). It was hypothesized as being closer to *Mymoorapelta* as the base of the osteoderm was only shallowly excavated. However, its external surface is smooth without the fine vascular pits and grooves characteristic of *Mymoorapelta*, although morphologi-

cally, it appears to be more similar to *Gargoyleosaurus* in superficial appearance. Given such limited material, we agree that Ankylosauria indeterminant is a suitable taxonomic identification.

MATERIALS AND METHODS

All of the ankylosaur materials discussed within were examined first hand by the senior author with the assistance of several of the coauthors. All of the ankylosaur fossils from the Mygatt-Moore Quarry up through the end of the 2025 field season were photographed and described first hand by the senior author with measurements made using calipers. All other photographs were also made by the senior author during his research except those of ankylosaur sacrum from southeastern Utah, which were provided by Luis Chiappe at the Dinosaur Institute at the LACM. No attempt was made to undertake a phylogenetic analysis as the senior author thinks the construction of a completely new character matrix would be essential in properly establishing an up-to-date phylogeny of the Ankylosauria and is beyond the scope of this review. Thus, only a differential diagnosis was performed in the description the Jurassic ankylosaurid fossils presented herein.

TERMINOLOGY

We employed the monophyletic clade Polacanthidae of Carpenter (2001) to facilitate comparison with and discussion of a number of similar taxa (*Gargoyleosaurus*, *Mymoorapelta*, *Hylaeosaurus*, *Polacanthus*, *Horshamosaurus*, *Hoplitosaurus*, and *Gastonia*). The analysis of polacanthids as a monophylogenetic subfamily of nodosaurids was by Yang et al. (2013), who similarly defined them as the most inclusive clade containing *Polacanthus foxii* but not *Ankylosaurus magniventris*or and *Panoplosaurus mirus.* While in the phylogenetic analysis of the Thyreophoria, Raven (2021) and Raven et al. (2023) recovered a clade identified as Polacanthidae. However, they never formally described it, excluded *Gargoyleosaurus*, and included several taxa, that we would not include within the Polacanthidae; as such, their definition will not be considered further here.

Osteoderm is used in reference to nearly all dermal elements of the fossils described herein, along with the term ossicle for simple ovoid dermal bones of approximately 1 cm or less in diameter following Burns (2015). Cervical half rings may be fused or unfused and for Jurassic polacanthids consist of one to two dorsal osteoderms and laterally a solid spine. Dorsal armor is ventrally flat to moderately concave with larger crested, subrectangular- to teardrop-shaped elements interpreted to be situated anteriorly; smaller, more posterior dorsal osteoderms are more circular with a low crest or low apical prominence. The larger osteoderms in the sacral region are also round with low apical prominences surrounded by fused ossicles. Simple elongate crested osteoderms are considered to be situated on the legs or along the tail and/or on the lateral margins of the body posterior to the posteriorly grooved shoulder spines and anterior to the sacral-caudal plates. The bases of the grooved shoulder spines and sacral-caudal plates are deeply excavated with medial vascular openings a few mm in diameter (Kirkland et al., 1998). The caudal plates appear to be of taxonomic utility (Kirkland et al., 2016; Morgan et al., 2016) and readily distinguish *Mymoorapelta* and *Gargoyleosaurus* (Figure 4). We use the term caudal rib instead of the misused term caudal transverse process.

INSTITUTIONAL ABBREVIATIONS

We employ the following institutional abbreviations: AMNH, American Museum of Natural History, New York, New York; BYU/ BYU VP, Museum of Paleontology, Brigham Young University, Provo, Utah; CEUM, Prehistoric Museum, Utah State University Eastern, Price, Utah; DMNH, Denver Museum of Nature and Science, Denver, Colorado; EDP-SM, Elizabeth Dee Shaw Stewart Museum of Paleontology at the Eccles Dinosaur Park, Ogden, Utah; FCPTD/ MAP, Fundación Conjunto Paleontológico de Teruel-Dinópolis/Museo Aragonés de Paleontología, Teruel, Spain; IVPP, Institute of Vertebrate Paleontology and Paleoanthropology, Beijing, China; KUVP, Kansas Museum of Natural History, Lawrence, Kansas; LACM, Natural History Museum of Los Angeles County, Los

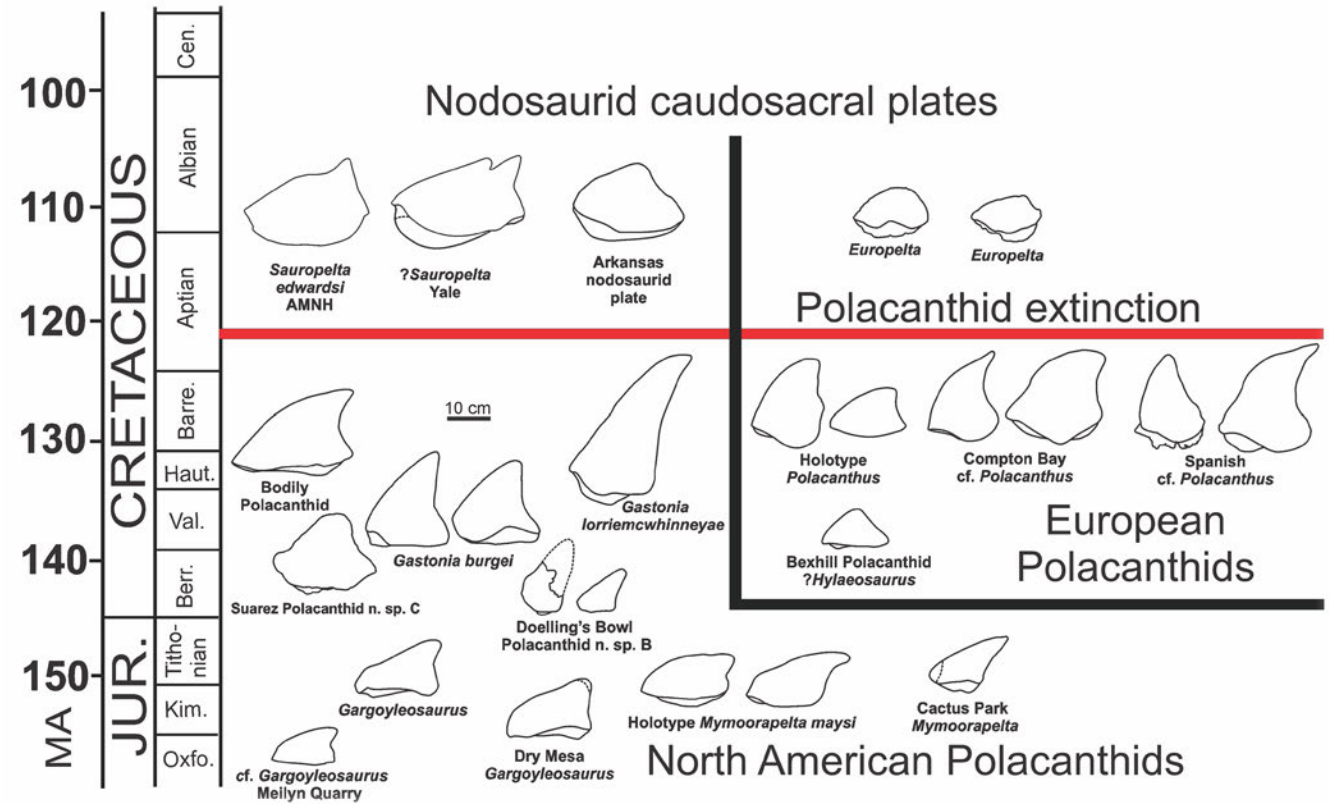

Figure 4. Comparison of North American and European polacanthid ankylosaur proximal caudal plates. From Kirkland et al. (2016) and Morgan et al. (2016).

Angeles, California; MPC, Mongolian Paleontological Center, Ulaan Baatar, Mongolia; MWC, Dinosaur Journey, Museums of Western Colorado, Fruita, Colorado; NHMUK, formally BMNH, Natural History Museum, London, England; NMC, National Museum of Canada, Ottawa, Canada; NMW, National Museum of Wales, Cardiff, Wales; NOVA-FCT, NOVA School of Sciences and Technology, Lisbon Portugal; QM, Queensland Museum, Queensland, Australia; ROM, Royal Ontario Museum, Toronto, Canada; SDNHM, San Diego Natural History Museum, San Diego, California; SGDS, Saint George Dinosaur Discovery Site at Johnson Farm, St. George, Utah; SMP, State Museum of Pennsylvania, Harrisburg, Pennsylvania; SMU, Schuler Museum, Southern Methodist University, Dallas, Texas; USNM, National Museum of Natural History, Smithsonian Institution, Washington, D.C.

SYSTEMATIC PALEONTOLOGY

Dinosauria Owen, 1842
Ornithischia Seeley, 1887
Thyreophora Nopcsa, 1915
Ankylosauria Osborn, 1923 (undefined, p. 3)
Polacanthidae Haekel, 1910

Diagnosis: The most inclusive clade containing *Polacanthus foxii* but not *Ankylosaurus magniventris* or *Panoplosaurus mirus* (Yang et al., 2013).

Gargoyleosaurus Carpenter et al., 1998

Diagnosis: As for species.

Gargoyleosaurus parkpinorum
Carpenter et al., 1998
(modified Carpenter, 2001)

Diagnosis: Differs from all other polacanthid ankylosaurs except *Mymoorapelta* in the possession of premaxillary teeth. Differs from *Mymoorapelta* in having a relatively narrower basicranium with smaller basitubera, in possessing a ventrally keeled sacrum, more elongate vertebral centra, possessing more fully excavated dorsal osteoderms, and in having more expansive, less reclined caudal osteoderms.

Type locality: Bone Cabin Quarry west; 33 m west of original AMNH Bone Cabin Quarry. This locality was mistakenly described as being in the lower part of the Morrison Formation in strata equivalent to the Salt Wash Member on the Colorado Plateau by Turner and Peterson (1999). They report the site as being east of the main Bone Cabin Quarry, when it is actually to the west. This important locality is stratigraphically high (Figures 1 and 3) in the Morrison (Schmude and Weege, 1996; Kelly Trujillo, Univeristy of Wyoming, written communication, 2018) in strata equivalent to the Brushy Basin Member on the Colorado Plateau.

Type material: Specimen DMNH 27726, a partial, articulated skeleton preserving a nearly complete skull (minus articular ends of both quadrates, left jugal, left quadratojugal and most of right, posterior portion of left maxilla, and posterior palate), right mandible, proatlas, first three cervical vertebrae, six caudal vertebrae, fragmentary cervical, and dorsal ribs, fragments of several ossified tendons, partial right scapula and coracoid, partial right humerus, partial pubis, right femur, and an abundance of dermal armor including left and right first cervical half rings, left second cervical half ring, two grooved lateral shoulder spines, caudal plates, and fused sacral shield fragments.

Referred specimen: Specimen DMNH 58831, a partial pelvis and cervical ring were described from the Simon Quarry in the lower Morrison Formation of the northwestern Bighorn Basin in northern Wyoming (Carpenter et al., 2013). The similarities of the cervical ring with that from the holotype specimen were used for the specific identification. The somewhat larger cervical ring from the Simon Quarry had small ossicles fused to the surface between the larger osteoderms. This was interpreted as being an ontogenetic feature of no taxonomic importance. However, Arbour and Currie (2013b) have noted that intermediate fused osteoderms in Late Cretaceous of Western North America are of taxonomic significance in the Ankylosauridae. Therefore, it is probably safer to regard this specimen as *Gargoyleosaurus* sp. *cf. G. parkpinorum,* given that the fusion of additional ossicles to the cervical half ring may be a specifically significant character, as opposed to being a purely ontogenetic character.

Gargoyleosaurus sp.

A well-preserved, fused scapulocoracoid (BYU 725-12963) from BYU's Dry Mesa Quarry (Figure 1) was described by Kirkland et al. (1998) as genus indeterminate. Subsequent examination of the caudal plates from the Dry Mesa Quarry reveals that they are most readily comparable in overall morphology to those from the holotype of *Gargoyleosaurus parkpinorum* (Figure 4). Additional material from this locality includes a reclined, posteriorly grooved shoulder spine. The co-occurrence of *Allosaurus jimmadseni* suggests that it is temporally equivalent to stratigraphic occurrences of *Allosaurus jimmadseni* from the type locality in the Salt Wash Member at Dinosaur National Monument and in the lower Morrison Formation of Wyoming (Chure, 2000; Chure and Loewen, 2020).

Excavations at the Meilyn Quarry northwest of Medicine Bow in southern Wyoming (Figures 1 and 3) have yielded two caudal vertebrae and three caudal plates, that were situated about 15 m above the base of the Morrison Formation (Schmude and Weege, 1996). These fossils were part of a traveling exhibit put together by Western Paleontology Labs in Orem, Utah. Subsequently, these fossils were sold off piecemeal. The proximal caudal vertebra was curated into the collections of the EDP-SM (EDP-SM 2017.01.096). Fortunately, although most of these fossils have been lost to science, photographs of these fossils exist (Figure 5).

Discussion: Initially, the senior author assumed that *Gargoyleosaurus* was the same taxon as *Mymoorapelta*. The discovery of additional fossil material (Carpenter et al.,

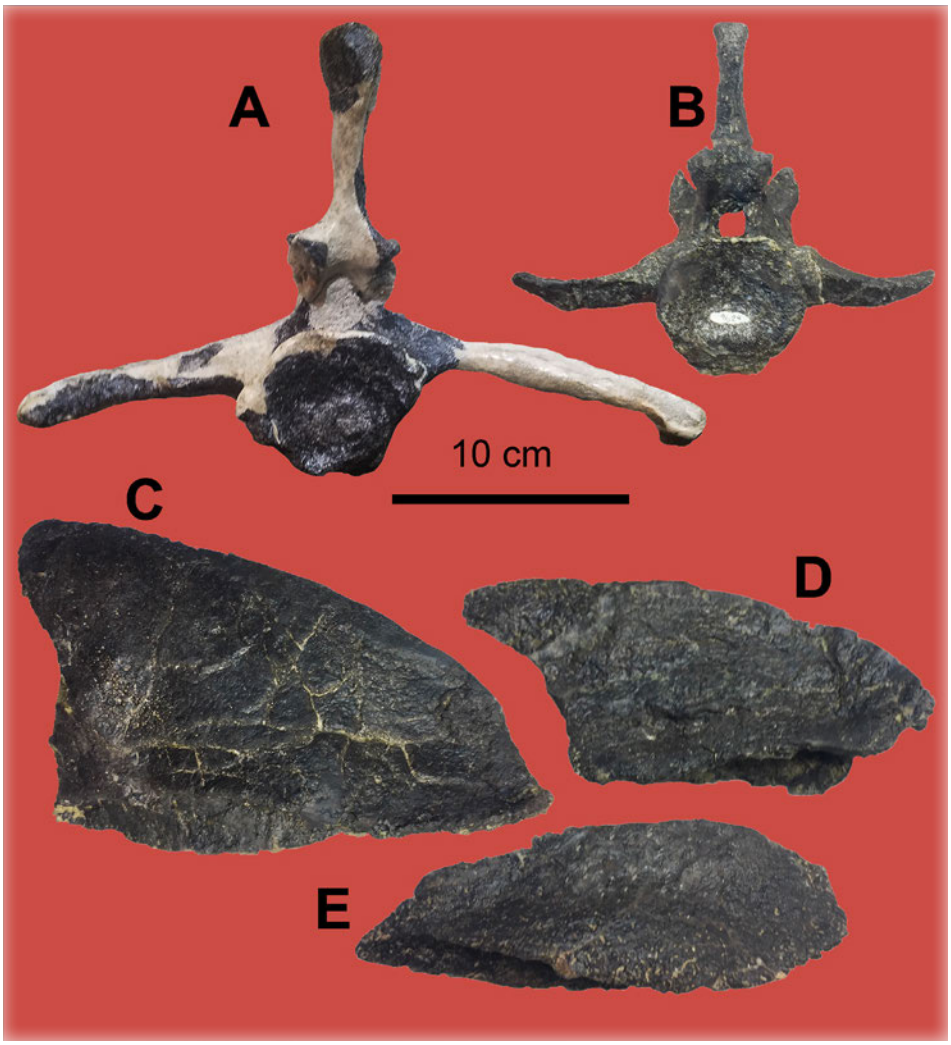

Figure 5. Polacanthine ankylosaurs remains from the basal Morrison Meilyn Quarry in southern Wyoming. (A) Proximal caudal vertebra EDP-SM 2017.01.096 in posterior view. (B) Posterior view of caudal vertebra in private hands. (C through E) Caudal plates reside in private hands.

2013; Kirkland et al., 2016), made it clear that these genera were distinctly different in a number of important diagnostic characters. Specimens assigned to *Gargoyleosaurus* from other localities are all represented by limited fossil material and their assignment to *Gargoyleosaurus* has been based primarily on the comparison of their osteoderms. The presence of more than one species of *Gargoyleosaurus* cannot be disproved with the fossil material at hand. It is therefore possible that *Gargoyleosaurus parkpinorum* is a species from the upper Morrison associated with the co-occurrence of *Allosaurus fragilis* and a second species with lower caudal plates and cervical rings ornamented by larger osteoderm elements separated by numerous ossicles occurs in the lower Morrison, where it is associated with *Allosaurus jimmadseni*. Until additional discoveries are made, it is impossible to test this speculation.

Mymoorapelta Kirkland and Carpenter, 1994

Diagnosis: As for species.

Mymoorapelta maysi Kirkland and Carpenter, 1994

Type locality: MWC loc. 2; Mygatt-Moore Quarry. The quarry is about 48.5% up section into the Brushy Basin Member (Figure 2) as measured by Foster (see Trujillo et al., 2014; Foster et al., 2018). Turner and Peterson (1999) place the site at around 42% up section in the Brush Basin Member. One of the most refined radiometric dates from the Morrison Formation has been published by Trujillo et al. (2014) from volcanic ash in the Mygatt-Moore Quarry. It is a ura-

nium-lead date of 152.18 ± 0.29 Ma from zircons.

The main bone level at the Mygatt-Moore Quarry preserves portions of two ankylosaurs (Figure 6). A partial abraded sacrum from the basal "pebble" bed represents a third individual since an erosive surface (Figure 2A) separates this interval from the overlying bonebed (Chin and Kirkland, 1998; Kirkland et al., 2005; Foster et al., 2018). The east pit preserves an associated partial skeleton of the holotype ilium, MWC 1815; individual elements from this skeleton are among the most pristinely preserved skeletal elements in the Mygatt-Moore Quarry.

Type material: The expanded hypodigm includes a number of skull elements: jugal, specimen MWC 5435; quadrate, MWC 4035; postorbital, MWC 6744; and braincase, MWC 5435; one possible premaxillary tooth, MWC 6740; two cheek teeth, MWC 6741 and 6742; the axis, MWC 1933; one cervical vertebra, MWC 6738; nine dorsal vertebrae, MWC 1800, 1801, 1802, 1803, 3613, 4032, 5940, 6737, and 6739; one sacral centrum, MWC 5104; one caudosacral vertebra, MWC6736; nine isolated caudal vertebra, MWC 1804,1805, 1806, 1807, 1808, 1839a, 1839b, 1907, 1913, 5019, 5104, and 5820; one isolated caudal vertebra with a fused chevron, MWC 1907; two pairs of fused distal caudal vertebrae with fused chevrons, MWC 1818 and 1819; one proximal chevron, MWC 1912; 19 partial ribs, MWC 1810, 1811, 1812, 1840, 1905, 1915, 3568, 3620, 3652, 3747, 3763, 4329, 5013, 5094, 5720, 6729 (three sections), and 6923; one partial scapula, MWC 6743; one humerus, MWC 6745; both ulnae, MWC 1814 and 5638; one radius, MWC 5438; three metacarpals, MWC 10638, 1908, and 1816; one manual phalanx, MWC 3616; one possible manual ungula, MWC 939; one left ilium (original holotype element), MWC 1815; one ischium,

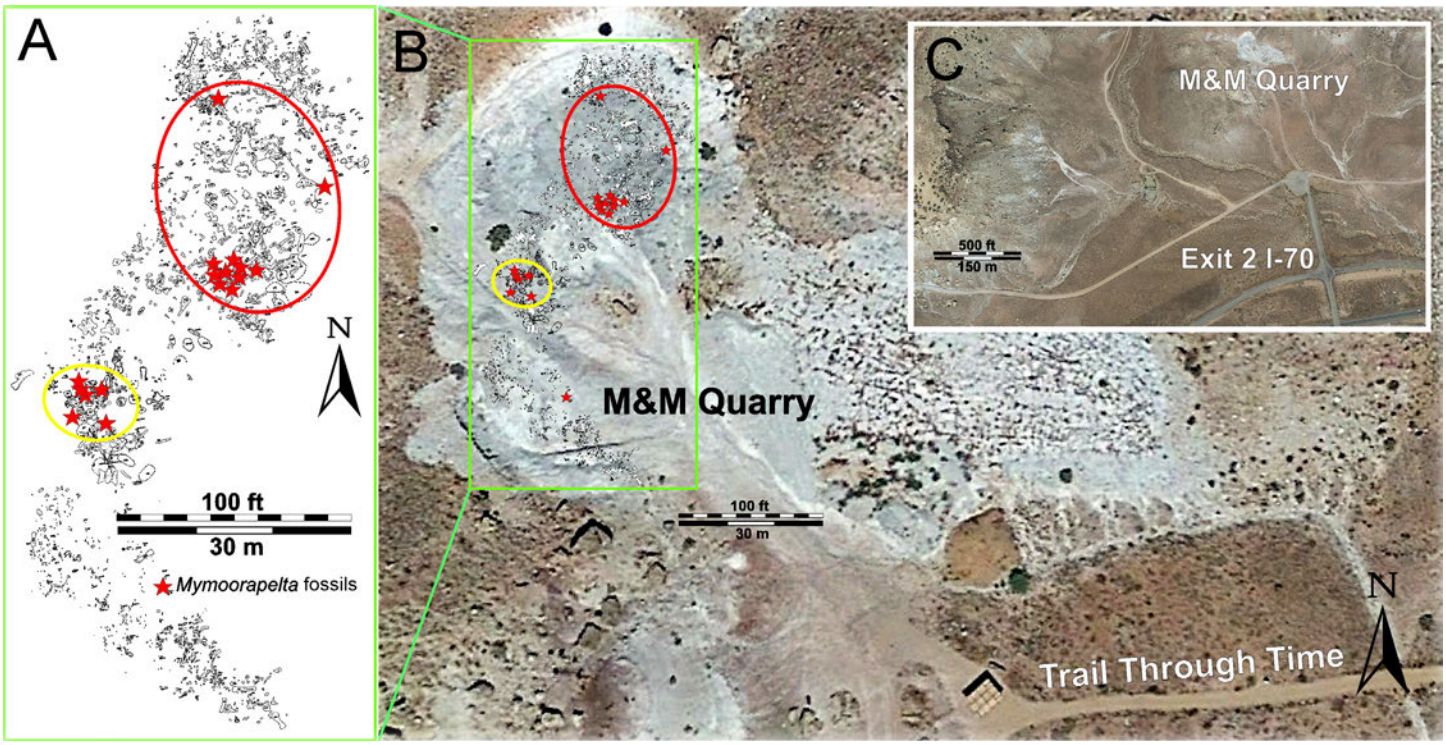

Figure 6. Google Earth images of the Mygatt-Moore Quarry area. (A and B) The Mygatt-Moore Quarry at the beginning of the "Trail through Time" with Mygatt-Moore Quarry map (Foster et al., 2018) superimposed. Area of the excavation where the holotype was recovered indicated by red oval and that of the larger paratype animals indicated by a yellow oval. (C) Overview of northwest side of Rabbit Valley showing relation of Mygatt-Moore Quarry with Colorado Exit 2, Interstate 70. M&M = Mygatt-Moore Quarry.

MWC 4027; one partial tibia, MWC 6746; one metatarsal, MWC 4028; two pedal phalanxes, MWC 1932 and 3615; three pedal unguals, MWC 3714, 3752, and 6728; four dorsal cervical ring elements, MWC 1834, 3744, 5320, and 6977; two cervical spines, MWC 1825 and 6752; one shoulder spine, MWC 1818; ten dorsal caudal spines, MWC 1819, 1820, 1821, 1822, 1823, 2678, 2867, 2868, 5148, and 5642; five lateral caudal spines, MWC 1824, 2677, 6747, 4226, and 5479; seven large dorsal scutes, MWC 1835, 1836, 1837, 4018, 4030, 4223, and 6761; two sacral shield fragments, MWC 1838 and 6751; dorsal scutes, MWC 7064 (cut for histological study [Burns, 2010], under field # MWC 211), 1023, 1813, 1826, 1827, 1828, 1829, 1830, 1831, 1833, 1834, 1841, 1842, 1843, 1844, 1845, 1852, 1909, 1910, 1911, 1914, 1937, 2737, 3629, 3860, 4022, 4029, 4196, 4228, 4229, 4344, 5016, 5099, 5320, 5479, 5838, 5894, 5920, 5928, 6749, 6752, 6754, 6755, 6756, 6757, 6758, 6759, 6760, 6761, 6762, 6763, 6764, 6765, 6766, 6767, 6768, 6769, 6785, 6786, 6787, 6788, 6789, 6790, 6791, 6793, 6794, 6795, 6796, 6797, 10486, and 10487.

Referred elements not assigned to the hypodigm: The north pit preserves elements from a skeleton that is significantly larger (about 133%) and more poorly preserved. The referred specimens include four dorsal vertebrae, MWC 5705, 6733, 6734, and 6735; an isolated sacral centrum, MWC 3613; a partial sacrum, MWC 6932; four isolated caudal vertebra, MWC 5705, 6733, 6734, and 6735; and one rib, MWC 5061. An isolated spine may be from a third individual largely because it is a considerable distance from the other skeletal associations. A partial synsacrum, MWC 10347 from the underlying "pebble" bed, represents a separate individual.

Referred Specimens from other Sites

Cactus Park ankylosaur, MWC loc. 197: In the early 1990s, Denver high school teacher Kent Hups discovered an ankylosaur skeleton weathering out of a calcite-cemented sandstone ledge in the Brushy Basin Member on the east side of Cactus Park southwest of Grand Junction, Colorado. The fossil (MWC 2610) is an articulated skeleton lying ventral side down assigned to *Mymoorapelta* (Kirkland et al., 1998). The curated fossil material consists of broken sandstone blocks collected from the slope below the ledge and preserve much of the posterior portion of the skeleton. This material consists largely of external molds of the bones and unprepared bones within the sandstone blocks. These described materials include unfused posterior dorsal vertebra with associated ossified tendons, the articulated pelvis with sacrum, portions of the hind limbs including four articulated metatarsals, a mold of a nearly complete sacral shield, and caudal and dorsal armor. The articulated proximal ischium and pubis demonstrates the presence of a long post-public rod extending along the ischium (Gaston et al., 2001), and that the spacing of the caudal plates appears to be only about 2 cm apart (Kirkland et al., 1998).

Los Angeles County Museum sacrum: While conducting excavations at LACM Locality 7683 in the medial Brushy Basin Member near Blanding in southeastern Utah, the LACM uncovered an ankylosaur sacrum. It has been identified as that of *Mymoorapelta* based primarily on a ventral groove like that in the expanded hypodigm material and because it lacks a fused series of dorsal vertebrae. Additionally, it is from a nearly correlative stratigraphic position.

University of Wyoming braincase: A water-worn ankylosaur braincase, UW 21869, was recovered during the excavation of an *Apatosaurus* femur at the "Boris" Locality UW V-93101 near Sheep Creek in south-central Wyoming by Robert T. Bakker and volunteers on a Dinamation International Society dig in July of 1993. Stratigraphically, the locality is situated about 19 m below the base of the Dakota Formation (currently Muddy Sandstone) in smectitic mudstone, well above the regional calcrete marking the "clay change" in the upper Morrison Formation of this region. This site was referred to as the Mummy Quarry in Kirkland et al. (1998).

The specimen includes the braincase and skull roof overlying it. Abrasion on the margins of the fossil suggest wear during transport prior to burial in the bone lag accumulation represented as discussed above. The proportions of the basicranium (Table 1) and its strati-

Table 1. Measurements of landmarks on North American polacanthid ankylosaur basicrania.

MYMOORAPELTA CRANIAL MEASUREMENTS IN MM						
	Mymoorapelta maysi	*Gargoyleosaurus parkpinorum*	*Gastonia burgei*	*Gastonia lorriemcwhinnyae*	Cactus Park Ankylosaur	Boris Braincase
		DMNH 27726	CEUM 1307	DMNH 53000	MWC loc. 197	UW 21869
Postorbital Cornice	MWC 6744					
Cornice Width	55.1	56.8	82.3			
Cornice length from base to apex	38.7	48.7	40.8			
Jugal Cornice	MWC 2843					
Anterioposterior length below orbit	40.1	39.1	46.6			
Cornice length orbit to apex	42.3	45.3	43.3			
Quadrate	MWC 4035					
Length	106.1					
Width of mandibular condyles	28.3		22.8		30.8	
Width of squamosal condyle	19.6					
Braincase	MWC 5435					
Width occipital condyle	46.8	53.5	55.3	45.4	52.5	90.9
Height occipital condyle below foramen magnum	27.4	24.2	22.1	21.4	26.3	73.3
Width foramen magnum	25.3	26.5	28.7	24.7	24.8	71
Height foramen magnum	27.0	22.2	26.0		23.2	68.1
Width across basitubera	57.7	46.6	60.1	52.65	48.2	97.3
Midline length of ventral braincase	72.7	81.2	83.1	83	79.4	114.8
total length with basipterygoids	78.3	86.1	109.2	97.1	86.7	

graphic position suggest this specimen represents an example of *Mymoorapelta* from Wyoming.

Diagnosis

Mymoorapelta's skull differs from that of *Gargoyleosaurus* in having a narrow, rounded head on the quadrate having no indication of fusion with the squamosal or paraoccipital process. *Mymoorapelta* is wider across its more robustly developed basitubera and the robust keel on the ventral side of the basiocciput does not extend as far posteriorly as it does in *Gargoyleosaurus*. Buccal teeth are lower crowned than those in *Gargoyleosaurus*. The cervical rings are anterioposteriorly narrow and more massive with the medial pair of osteoderms having keels only extending anteriorly from the apex of osteoderm. Sacral vertebrae are wide with a ventral depression, absent in *Gargoyleosaurus*. Neural spines of posterior dorsal vertebrae are lined by flattened, spindle-shaped ossified tendons. The preacetabular processes of the ilia flex ventrolaterally to form a vertical, lateral surface that gives the ilia a rectangular appearance in dorsal view. Proximal caudal osteoderms (plates) are relatively narrow and reclined posteriorly such that the apex of the plate would overlap the anterior margin of following caudal plate. The dorsal surfaces of the lateral plates are ornamented by faint parallel ridges absent in *Gargoyleosaurus*.

Description of Skull Material

For comparative descriptive purposes the isolated skull elements in Figure 7 are oriented like the skull of its sister taxon *Gargoyleosaurus* (Carpenter et al., 1998).

Postorbital (Figures 7D through 7H)

The wedge-shaped, right postorbital (MWC 6744) has a vertical break anteriorly behind the orbit along a straight medial to lateral line approximately 3 cm forward of the posterior margin of the postorbital horn. As

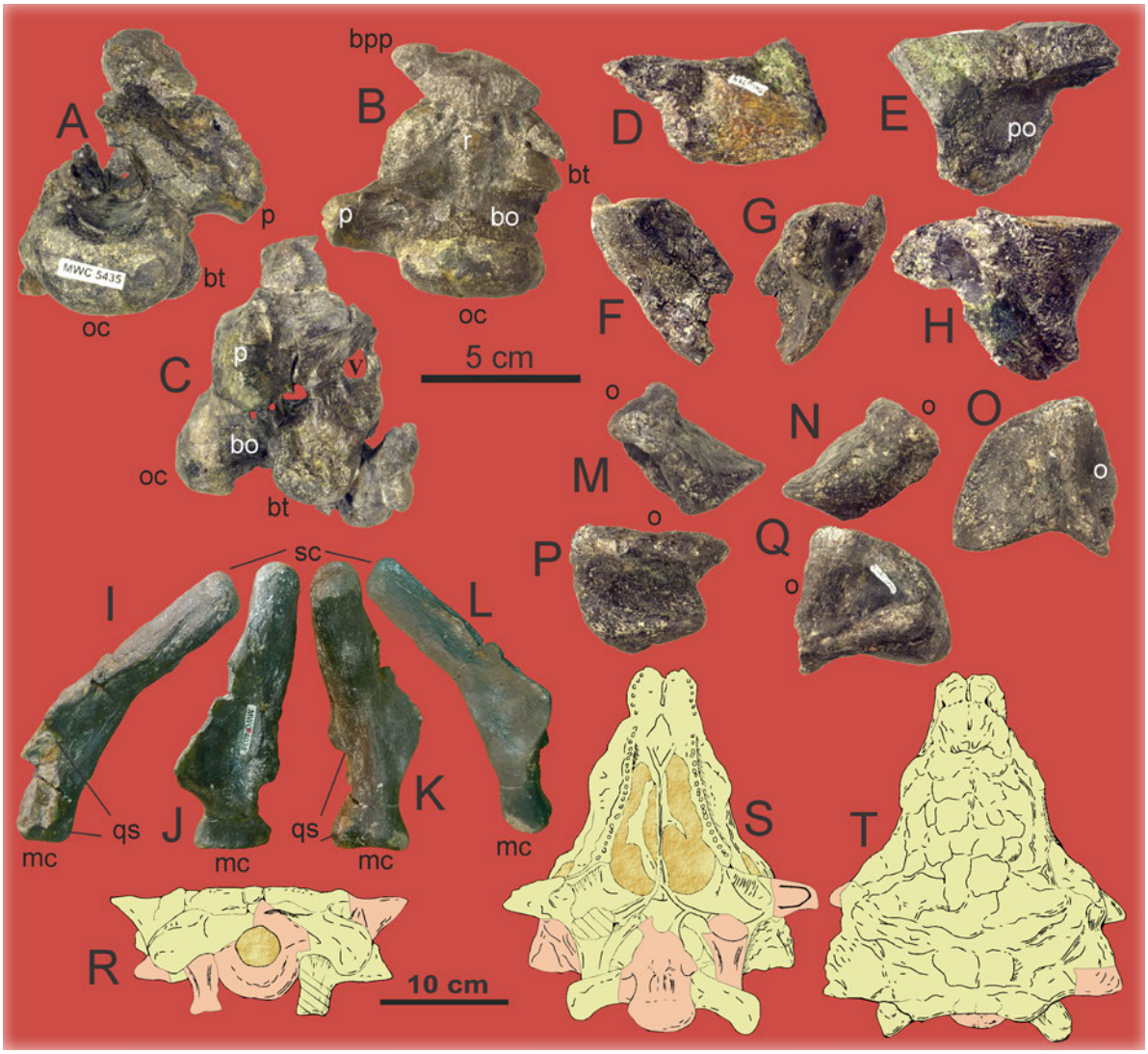

Figure 7. Skull material from revised hypodigm of *Mymoorapelta*. Partial braincase specimen MWC 5435 in (A) caudal, (B) ventral, and (C) right lateral views. Right postorbital MWC 6744 in (D) dorsal, (E) rostral, (F) lateral, (G) medial, and (H) caudal views. Left quadrate MWC 4035 in (I) lateral, (J) rostral, (K) caudal, and (L) medial views. Left jugal MWC 2843 in (M) rostral, (N) caudal, (O) dorsal, (P) medial, and (Q) ventral views. Sketch of *Gargoyleosaurus* skull with skull elements known from holotype of *Mymoorapelta* in pink in (R) caudal, (S) ventral, and (T) dorsal views. Abbreviations: bo = basioccipital, bpp = basipterygoid process, bt = basitubera, mc = mandibular condyle, o = position of orbit, oc = occipital condyle, p = paraoccipital process, po - posterior surface of the orbit, qs = qudratojugal suture, sc = squamosal condyle, V = fifth cranial nerves.

preserved, the shape of the well-vascularized, postorbital horn is nearly identical in size and shape with that of *Gargoyleosaurus* (Carpenter et al., 1998; Kilbourne and Carpenter, 2005) and compares well with that of *Gastonia* (Kirkland, 1998) in that it is pyramidal in shape. Kilbourne and Carpenter (2005) report that the postorbital horn extends onto the squamosal, but on the isolated postorbital of *Mymoorapelta*, this is not the case and indicates that the squamosal is more posterior and medial in both skulls, in keeping with the position of the nearly horizontally directed proximal end of the quadrates anteriorly to the paroccipital processes in *Gargoyleosaurus* (Figure 8). The horizontal dorsal surface forms one face with the posterior face inclined

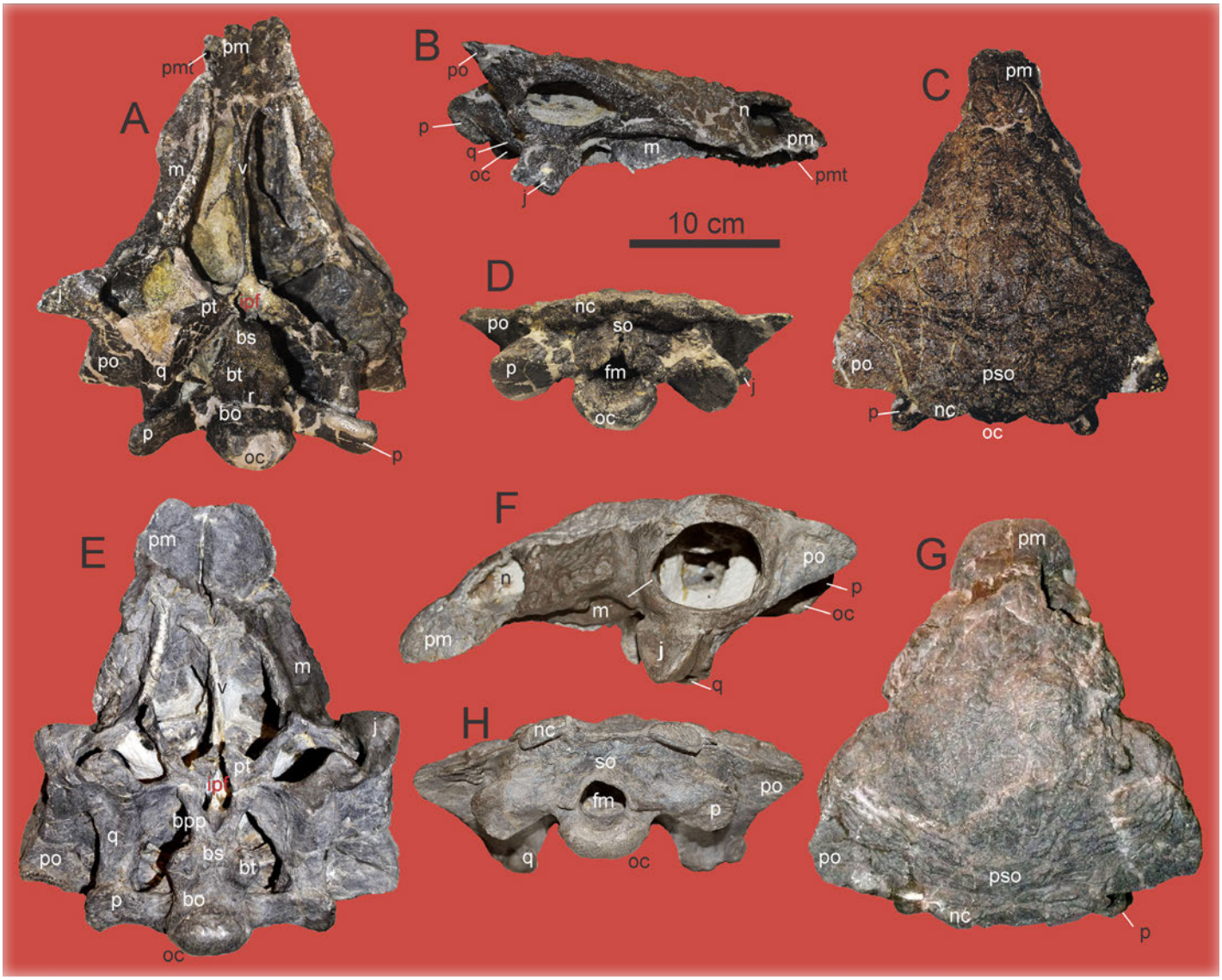

Figure 8. Skulls *Gargoyleosaurus* and *Gastonia*. *Gargoyleosaurus parkpinorum* holotype skull DMNH 27726 in (A) ventral, (B) right lateral, (C) posterior, and (D) dorsal views. *Gastonia burgei* CEUM 1307 in (E) ventral, (F) left lateral, (G) posterior, and (H) dorsal views. Abbreviations: bo = basioccipital, bpp = basipterygoid process, bs = basisphenoid, bt = basitubera, fm = foramen magnum, ipf = interpterygoid fossa, j = jugal, m = maxilla, n = narial opening, nc = nuchal caputegulae, oc = occipital condyle, p = paraoccipital process, pm = premaxilla, pmt = premaxillary tooth, po = postorbital, pso = parietal "spider" ornament, pt = pterygoid, q = quadrate, so = supraocccipital, v = vomer.

anteriorly and the lateral face inclined medially. The bone extends medially between the squamosal and perhaps the parietal. Below this and extending laterally is a rostrally convex sheet of bone separating the posterior surface of the orbit from the lower temporal opening posteriorly. Unfortunately, the total ventral extent of this postocular septum cannot be determined as the thin ventral margin is broken away, but it extends ventrally as much as 8 mm as preserved. A sutural contact with the jugal is visible on the postorbital below the horn on the lateral side indicating the postorbital makes up entire posterior margin of the orbit. Posterior-medially to the horn, a shallow fossa is visible about 2 cm across with a laterally directed vascular opening. A second ventrally directed vascular opening enters the bone just lateral to the fossa and medial to the postorbital horn. A

third dorsally directed vascular opening enters the bone about 1 cm ventrally at the medial margin of the horn.

Jugal (Figures 7M through 7Q)

The left jugal (MWC 2843) is well preserved. It makes up the ventral margin of the orbit, and unlike most ankylosaurs (Vickaryous, 2001; Vickaryous et al., 2001, 2004) the triangular suborbital horn is formed exclusively by the jugal as in *Gargoyleosaurus* (Carpenter et al., 1998) and *Gastonia* (Kirkland, 1998). Kilbourne and Carpenter (2005) describe the only preserved jugal in *Gargoyleosaurus* as pathologic (Figure 8B), but this right jugal is a mirror image of the left jugal of *Mymoorapelta*, suggesting that the *Gargoyleosaurus* jugal is not pathologic. As with *Gargoyleosaurus,* the well-vascularized jugal horn extends ventrally and recurves to an apex ventrolaterally. Unlike most other ankylosaurs, except *Gargoyleosaurus* (Carpenter et al., 1998; Kilbourne and Carpenter, 2005) and *Gastonia* (Kirkland, 1998), there is no sign that the buccal emargination of the maxilla extended up onto the lateral margin of the jugal. Medial to and below the broken inner margin of the orbit, there is a large depression into much of the base of the jugal horn as in *Gargoyleosaurus*. Posterior to the ventral surface of the orbit, there is an irregular sutural surface for the postorbital in the same position as in *Gargoyleosaurus* (Kilbourne and Carpenter, 2005). The sutural surface for the quadratojugal extends ventrally along the posterior margin of the medial depression. The quadratojugals in *Gastonia*, *Gargoyleosaurus*, and *Mymoorapelta* would appear to be small mediolaterally directed bones between the jugals and quadrates based on this interpretation, whereas these are situated posterior to the jugal primitively as in *Scelidosaurus* (Norman, 2020a) and in most other ankylosaurs (Vickaryous et al., 2004). The quadratojugals do not support any of the suborbital horn as in other ankylosaurs (Vickaryous et al., 2004). Superficially it appears that the suborbital horn resides solely on the jugal in the basal nodosaurid *Pawpawsaurus* (Lee, 1996), but in that taxon, the suborbital horn is also supported by the quadratojugal ventrally.

Close examination of the jugal and quadrate of *Mymoorapelta* reveals that, in contrast to most other ankylosaur skulls (Vickaryous et al., 2004), the quadratojugal is situated medially to the jugal as in *Gargoyleosaurus* and *Gastonia* (Kirkland, 1998; Kilbourne and Carpenter, 2005). This is also the case in the nodosaurid *Texasites* (=*Pawpawsaurus*) (Lee, 1996).

Quadrate (Figures 7I through 7L)

The isolated left quadrate (MWC 4035) is well preserved. It is anteriorly arched as in many ankylosaurs and as in both *Gargoyleosaurus* and *Gastonia* (Figure 9A), the slender dorsal ramus would have been directed nearly horizontally. The articular surface for expanded mandibular condyles is well developed and proportionally more massive than in *Gastonia*. It is ovoid in shape and is deeper medially, reflecting the anterioposterorly elongate medial mandibular condyle, which is separated from the low lateral mandibular condyle by a broad but shallow intercondylar groove. A deeply recessed suture for the quadratojugal extends dorsally up the lateral side from the mandibular condyles for 3 cm, much like *Gastonia* and is unknown in *Gargoyleosaurus*. A thin and triangular pterygoid process extends medially from the quadrate shaft at this point as opposed to the more dorsally situated subrectangular pterygoid process in *Cedarpelta* (Carpenter, 2001). Immediately posterior to the quadratojugal suture, a distinct groove is present as reported in *Gargoyleosaurus* and many other dinosaurs (Kilbourne and Carpenter, 2005). The distinct, rounded head forming the dorsal end of the ramus would articulate with the articular surface of the squamosal and the distal end of the paroccipital process as in *Cedarpelta* (Carpenter et al., 2001) and unlike the apparently expanded sutural contact in *Gargoyleosaurus* (Kilbourne and Carpenter, 2005). In lateral view, the ramus is thicker anteroposteriorly than in either *Gargoyleosaurus* or *Gastonia*.

Braincase (Figures 7A through 7C, 9, and 10)

An undistorted braincase (MWC 5435) was recovered from a spoils bucket by the sharp eyes of Rodney Scheetz (BYU), who recovered additional fragments. It consists of the lower portion and right side of the braincase with the paroccipital process broken off at its neck. The absence of

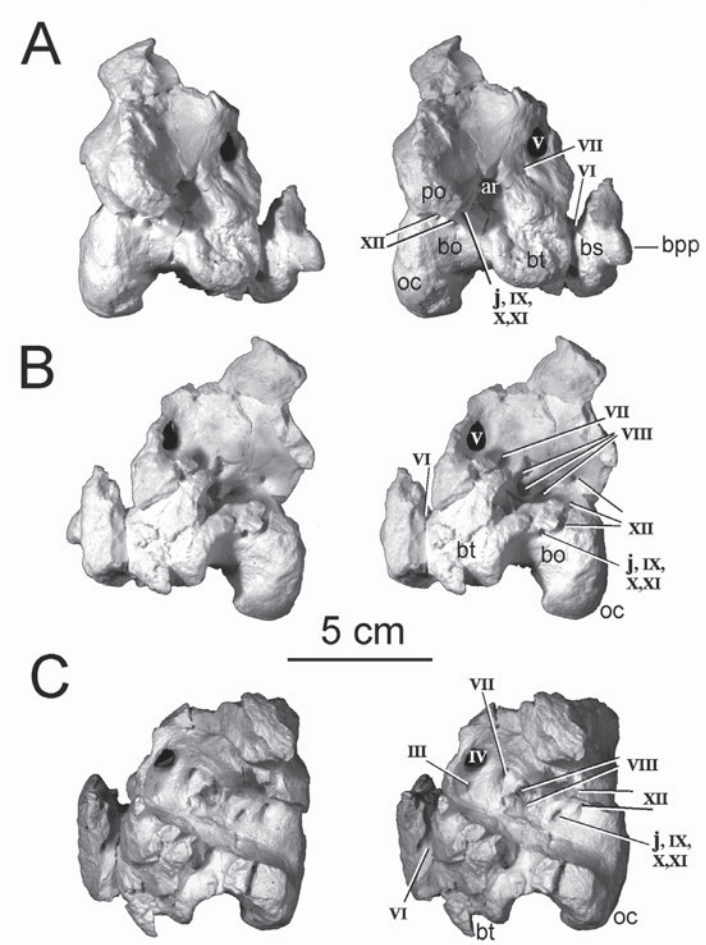

Figure 9. Stereo views of the braincase MWC 5435 of *Mymoorapelta* in (A) lateral, (B) medial, and (C) dorso-medial views. Abbreviations: ar = auditory recess, bo = basioccipital, bpp = basipterygoid process, bs = basisphenoid, bt = basitubera, j = jugular, oc = occipital condyle, po = paraoccipital process, and III, IV, V, VI, VII, VII, IX, X, XI, XII = cranial nerves.

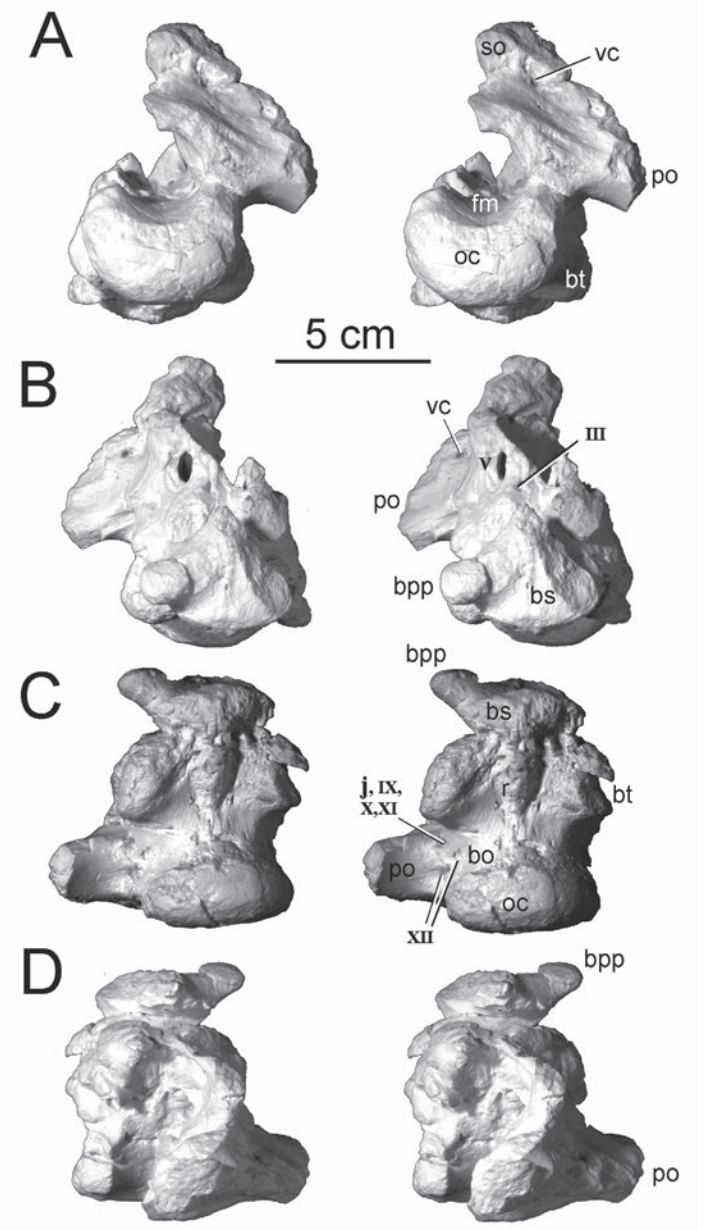

Figure 10. Additional stereo views of the braincase MWC 5435 of *Mymoorapelta* in (A) caudal, (B) rostral, (C) ventral, and (D) dorsal views. Abbreviations: bo = basioccipital, bpp = basipterygoid process, bs = basisphenoid, bt = basitubera, j = jugular, oc = occipital condyle, p = paraoccipital process, po = post ocular shelf, r = ridge on basicranium, so = suproccipital, vc = vesicular canal, and III, V, IX, X, XI, XII = cranial nerves.

the left side permitted the inside of the braincase to be prepared such that the entrance and exit points of the cranial nerve are readily observable. The endocranial impression extends forward to the position of the pituitary fossa at the posterior margin of the parasphenoid. The sutures between individual elements of the braincase are almost completely fused and their relative position and extent are best determined by comparison of the strikingly similar braincases of *Gargoyleosaurus* (Carpenter et al., 1998; Kilbourne and Carpenter, 2005) (Figures 8A through 8D) and *Gastonia* (Kirkland, 1998) (Figures 8E through 8G).

The supraoccipital is broken vertically just to the left of the midline. Its suture with the exoccipital is completely obscured by fusion so the extent to which it makes up

the dorsal margin of the foramen magnum is unknown. Dorsally, it is broken off just below the nuchal shelf of the parietal. Below this break, a shallow, horizontally oriented depression extends across the midline into a deep pit unlike the shallow depressions on either side of the nuchal crest, as observed in many other ankylosaurs such as the nodosaurids *Pawpawsaurus* (Lee, 1996), *Animantarx* (Carpenter and Kirkland, 1998), and Sauropelta. About 1.5 cm laterally above the base of the paroccipital process, a small post-temporal foramen (Lee, 1996) enters the bone and angles medially before exiting on the upper surface of the braincase above the area of the opisthotic. A horizontal flexure below the nuchal shelf due to crushing may be obscuring this area in *Gargoyleosaurus*. The post-temporal foramen is also well expressed in *Gastonia* (Kirkland, 1998) and *Pawpawsaurus* (Lee, 1996). Unlike many ankylosaurs (Vickaryous et al., 2004), no nuchal or medial crest is developed above the foramen magnum. The supraoccipital is dorsoventrally expanded and divided at the midline above the foramen magnum in *Gargoyleosaurus* (Carpenter et al., 1998; Kilbourne and Carpenter, 2005) reflecting the fusion of the proatlas to the supraoccipital as in *Animantarx*, whereas it is smooth across this area as in *Gastonia* (Kirkland, 1998). Although the supraoccipital is nearly vertical below the nuchal shelf in *Gastonia*, it slopes caudoventrally in *Mymoorapelta* and *Gargoyleosaurus*.

The foramen magnum is circular and angled caudoventrally (Figures 9 and 10). The occipital condyle is wide transversely and extends ventrally below the foramen magnum in the form of a broad lip as described for the braincase of *Polacanthus* (Norman and Faiers, 1996). It is posteriorly more flattened than that of *Gargoyleosaurus* (Figure 8D) and not as medially depressed on its ventral surface to suggest two low condyles as in *Gastonia* (Figure 8E). Its strong ventral inclination suggests that *Mymoorapelta*'s cranium was angled down from the horizontal.

The right exoccipital is broken such that only the proximal portion of the paroccipital process is preserved and the left paroccipital process is broken off through cranial nerve openings IX-XII. The exoccipital makes up the lateral margin of the foramen magnum and a portion of the lateral margin of the occipital condyle as it does in *Gargoyleosaurus* (Carpenter et al., 1998; Kilbourne and Carpenter, 2005), *Gastonia* (Kirkland, 1998), and many ankylosaurids (Vickaryous et al., 2004). Ventrally at the base of the paroccipital process (Figure 11C), the foramen for cranial nerves XII-IX forms a nearly equilateral triangle, whereas they are linearly arranged in the braincase tentatively assigned to *Polacanthus* by Norman and Faiers (1996) and are intermediate in configuration in *Gastonia* (Kirkland, 1998). Unfortunately, the braincase in *Gargoyleosaurus* was crushed and sheared such that the cranial nerve openings have all been obscured (K. Carpenter, Museum of Natural History, University of Colorado, personal communication, 2025). Anteriorly, the foramen for the combined passage of cranial nerves XI-IX and the jugular vein is separated from the auditory recess by a narrower strut of bone than it is in *Polacanthus* (Norman and Faires, 1996). Additionally, in lateral view, a line drawn through this cranial nerve opening extending anteriorly through the cranial nerve openings for VII and V angles upward at about 40˚ relative to the plane formed by the occipital condyle and the basitubera as in *Silvisaurus* (Eaton, 1960), whereas this line is nearly parallel with the base of the braincase in *Gastonia* (Kinneer et al., 2016), *Polacanthus* (Norman and Faires, 1996), *Pawpawsaurus* (Lee, 1996), Sauropelta (Parson and Parson, 2009), *Bessektipelta* (Parish and Barrett, 2004), *Saichania* (Maryańska, 1977), and *Euoplocephalus* (Coombs, 1978a; Vickaryous, 2001).

The ventral surface of the braincase between the occipital condyle and the basitubera is constricted with a weak keel originating in its middle and strengthening anteriorly to a rugose crest between the basitubera. This keel is better developed and extends posteriorly to the base of the occipital condyle in *Gargoyleosaurus* and is absent in *Gastonia* and *Polacanthus,* which are depressed between the basitubera. The basitubera are more widely spaced than in *Gargoyleosaurus* (Figure 8) and are large as in *Gastonia* (Figure 9) but are more rugose with a well-developed rugose depression in their anteriolateral margins unlike other ankylosaurs. The pterygoid processes are well developed (Figures 7B and 10) diverging anteriolaterally and end in expanded pads

Figure 11. Boris Quarry at Sheep Creek ankylosaur braincase UW 21869 in (A) caudal, (B) rostral, (C) right lateral, (D) ventral, (E) dorsal, and (F) left lateral views. Abbreviations: ar = auditory recess, bo = basioccipital, bs = basisphenoid, bt = basitubera, fm = foramen magnum, j = jugular, ltf = lower temporal fossa, oc = occipital condyle, p = paraoccipital process, po = post ocular shelf, r = ridge on basicranium, vid = vidian canal, and I, II, III, IV, V, VI, VII, IX, X, XI, XII = cranial nerves.

indicating they could freely articulate with the pterygoids as in *Gastonia* and *Gobisaurus* (Vickaryous et al., 2001). As preserved, there is no indication that elongate pterogoid processes were present in *Gargoyleosaurus* (Figure 8A). The pterygoid processes of *Mymoorapelta* are much shorter than those in *Gastonia* (Figure 9) and are proportionally more divergent, suggesting that *Mymoorapelta* had a wide and anterioposteriorly shorter interpterygoid fossa. There is no visible parasphenoid rostrum unlike the condition in *Sauropelta, Peloroplites*, and *Cedarpelta* (Carpenter et al., 2008).

In general proportions, the holotype braincase is similar to the Boris Quarry braincase (Figure 11), although it represents a larger individual (Table 1) comparable to the larger *Mymoorapelta* vertebral material described below. UW 21869 is a water-worn skull composed of a braincase and posterior skull roof. It was buried with the anterior broken surface down such that the

"high" points of the skull, such as the posterior surface of the occipital condyle, the supraoccipital and the posteriorly projecting lateral margins of the nuchal shelf were worn flat. The left paraoccipital process is completely broken away and the ventrolaterally directed right paraoccipital process is broken at the medial constriction as in the holotype braincase (Figures 11A, 11B, and 11D). The skull roof is truncated near the posterior margin of the left orbit extending medially to midline before angling posteriorly to the right posterior corner of skull. Both postorbital horns are mostly broken away. In anterior view, only the left postocular shelf is largely undamaged, the front of braincase is open at the constriction between the brain and the olfactory bulb, and the basicranium is broken at the basipterygoid processes. The basicranium was broken away perhaps in preparation along a line formed by the cranial nerve openings and then subsequently repaired.

UW 21869 compares well with the holotype braincase of *Mymoorapelta* (MWC 5435). As in the type specimen, in lateral view, a line drawn through the openings for cranial nerve XII extending anteriorly through the cranial nerve openings for VII and V angles upward at about 40˚ relative to the plane formed by the occipital condyle and the basitubera. It differs from *Gargoyleosaurus* and is more like *Mymoorapelta* in its proportionally wider basicranium with larger and more rugose basitubera and a ventral midline ridge does not extend as far posteriorly. Not known in the type material of *Mymoorapelta*, the ornamentation of the posterior skull roof is similar to that of *Gargoyleosaurus* except it is not so sharply defined. As in both *Gargoyleosaurus* and *Gastonia*, the parietal ornamentation is centered on a small, raised area near the center of the parietal about the size of the occipital condyle with transverse ridges less than 1 cm wide leading away from it, in a pattern reminiscent of a crab or spider. Although damaged, the nuchal shelf appears to be considerably dorsoventrally thicker with a squamosal that extends laterally farther beyond it than in *Gargoyleosaurus*.

Because UW 21869 lacks quadrates to obscure the ventral side of the skull roof on either side of the braincase, the postocular shelf clearly divides the vaulted chamber formed by the closure of the supratemporal opening to form the large supratemporal fossa above the recessed lower temporal opening (Figures 11B and 11D).

As initially recovered, the braincase of the fragmented Cactus Park *Mymoorapelta* skull (MWC 2610), although still coated in matrix, was largely intact (Figure 12A). The overall skull beneath the matrix revealed that it compared well with other polacanthines such as *Gastonia* (Figures 12A through 12D). The skull roof is less vaulted than in *Gastonia* and appears to be similar to *Gargoyleosaurus* in lateral profile (Figure 12D). Preliminary preparation has revealed the basic proportion of the Cactus Park braincase (Figures 12G through 12I, Table 1) are similar to those of *Mymoorapelta*. However, the basicrania appears to be narrower and although of similar length the anterior ends of the pterygoid processes are not expanded (Figure 12H). The parocciptal process is not preserved on any other braincases assigned to *Mymoorapelta* and appears to be more laterally expanded than in either *Gargoyleosaurus* or *Gastonia* (Figure 8). The mandibular condyles of the left quadrate are exposed (Figure 12I) and are notable wider (Table 1) than in the quadrate preserved at the Mygatt-Moore Quarry (MWC 4035). Future preparation and analysis of CT data will hopefully reveal more of this important specimen.

Description of Teeth

Three isolated teeth are assigned to the holotype of *Mymoorapelta* (Figures 13A through 13I). All three have anterioposteriorly expanded crowns with a cylindrical, somewhat barrel-shaped root constricted below the crown. Additionally, no secondary ridges extend down the faces of the crown from the denticles as in many stegosaurs, nodosaurids, and ankylosaurids (Blows and Honeysett, 2014a). Two teeth are from the buccal region of either the dentary or maxilla based on their low crown height. The best preserved of these teeth (MWC 6741) has a somewhat damaged crown (Figures 13E through 13H). The total tooth height preserved with root is 18.0 mm. Following the orientation of the teeth of *Gargoyleosaurus* (Kilbourne and Carpenter, 2005), the lingual margin of the tooth is swollen but does not quite form a cingulum. Its crown is 6.7 mm

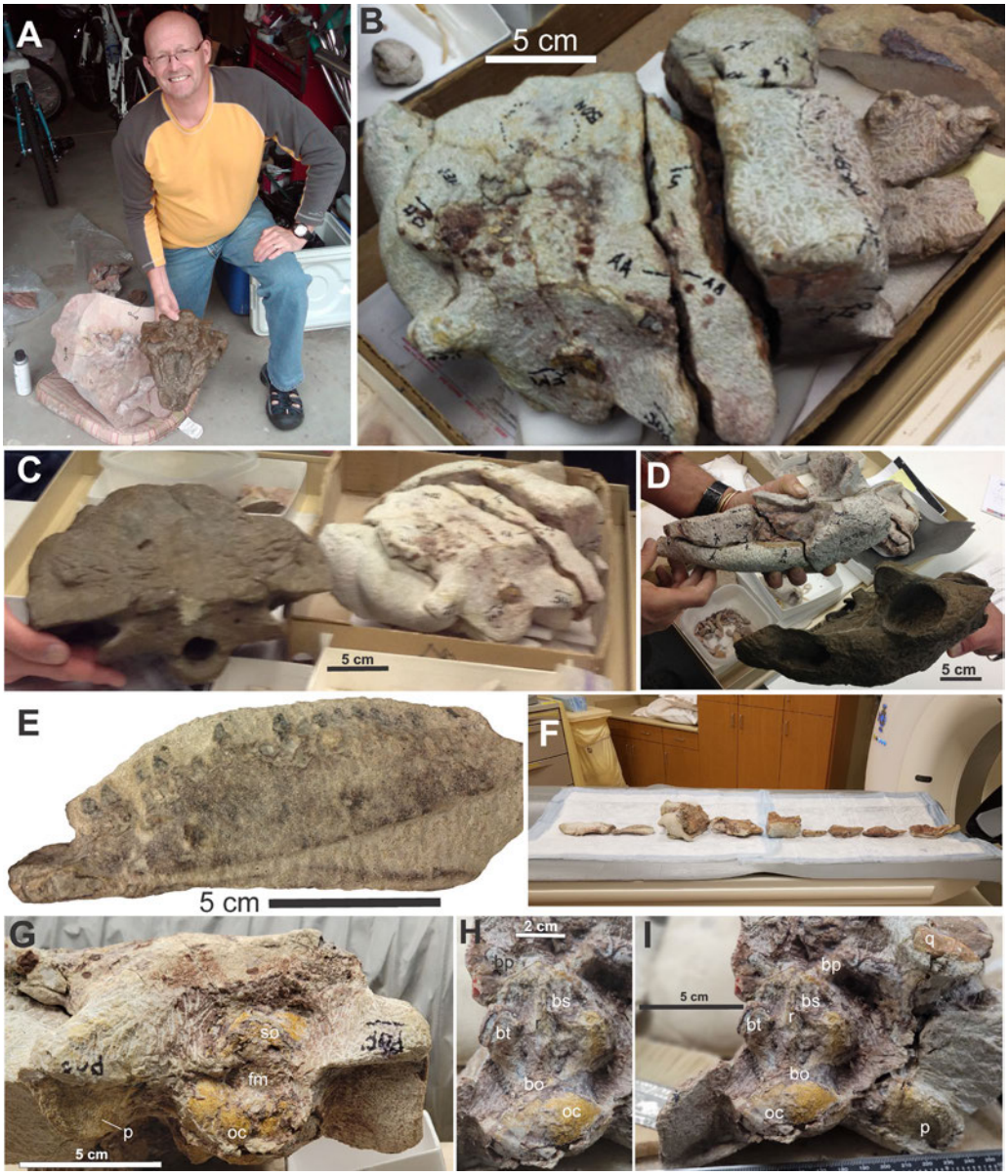

Figure 12. Cactus Park skull MWC 2610. (A) Kent Hups comparing Cactus Park skull within sandstone block with *Gastonia* cast skull. (B through E) Cactus Park skull at Denver Museum of Nature and Science Preparation Lab in (B) dorsal, (C) posterior, (D) lateral, and (E) left dentary views. (F) Cactus Park skull fragments being CT scanned following return to Museum of Western Colorado. (G through I) Braincase following initial preparation in (G) posterior view, (H) basicranium in ventral view, and (I) ventral view. Abbreviations: bo = basioccipital, bp = basipterygoid process, bs = basisphenoid, bt = basitubera, fm = foramen magnum, oc = occipital condyle, p = paraoccipital process, q = quadrate, r = ridge on basicranium, so = supraoccipital. Figures 12A through 12E courtesy of Harley Armstrong, retired, Bureau of Land Management.

long, 4.0 mm wide, and a minimum of 4.8 mm tall as the apex of the crown is damaged. Eight denticles are preserved on what is interpreted as the anterior carina with space for as many as ten. A transversely oriented, sloping wear facet has removed all the preserved denticles on the posterior carina of the tooth except for the two at the base of the crown. The second example of this tooth form (MWC 6742) is significantly smaller with a minimum root height of 14.0 mm (Figures 13E through 13H). Its crown is more damaged and no denticles are

Figure 13. Teeth from revised hypodigm of *Mymoorapelta*. Premaxillary tooth MWC 6740 in (A) rostral, (B) medial, (C) caudal, and (D) lateral views. Maxillary tooth MWC 6741 in (E) rostral, (F) medial, (G) caudal, and (H) lateral views. MWC 6742 in (I) lateral view. Typical tooth from *Gargoyleosaurus parkpinorum* holotype skull DMNH 27726 in (J) medial and (K) lateral views. Tooth CEUM 5145 from within *Gastonia burgei* holotype skull in (L) lateral view.

preserved; it is a minimum of 4.5 mm long.

One well-preserved tooth (MWC 6740) kept little of the root (Figures 13A through 13D). By comparison to *Gargoyleosaurus* (Kilbourne and Carpenter, 2005), this larger, taller, and more asymmetric crown suggests that it represents a premaxillary tooth. The crown is 5.3 mm long, 4.0 mm wide, and 7.8 mm tall. No cingulum is present, although the lateral side of tooth is thicker, as in *Gargoyleosaurus*. There are seven denticles preserved on the anterior carina below the apex with six slightly worn denticles preserved on the posterior carina below apex. The denticles decrease in size apically. The medial side of the tooth is finely wrinkled with an apically directed groove toward the anterior and posterior margins of the crown setting off the carina from the central portion of the tooth.

The teeth of stegosaurs, nodosaurids, and ankylosaurids possess fewer denticles and well- developed cingulae (Coombs, 1990; Galton and Upchurch, 2004; Blows and Honeysett, 2014a). The teeth of the Jurassic ankylosaurs *Scelidosaurus*, *Sarcolestes*, and *Priodontognathus* are higher crowned with well-developed cingulae (Galton, 1983a, 1983b; Blows and Honeysett, 2014a; Norman, 2020a). Teeth from the Valanginian and Barremian (Early Cretaceous) of southern England tentatively assigned to *Hylaeosaurus* and *Polacanthus*, respectively, are higher crowned with fewer denticles (Blows and Honeysett, 2014a). The teeth appear to be proportionally lower crowned and have one to two more denticles than those of *Gargoyleosaurus* (Kilbourne and Carpenter, 2005) (Figures 13J and 13K). Overall, the buccal teeth compare best with those of *Gastonia* (Figure 8L) in the lateral profile of the crown and the number of denticles (Kirkland, 1998; Blows and Honeysett, 2014a).

Description of Axial Skeleton

There are numerous vertebrae from throughout the skeleton assigned to the expanded hypodigm of *Mymoorapelta* and several larger and more poorly preserved vertebrae from a larger referred specimen (Table 2). The vertebral column of ankylosaurs has not been described as a complete unit by previous authors except for a few papers on ankylosaurids (Carpenter, 2004; Carpenter et al., 2011). Particular attention has been made relative to the function of the tail club of the Ankylosauridae (Arbour 2009; Arbour and Currie, 2013a). Descriptions for other less derived taxa are generally restricted to discussing isolated vertebra and/or select representative vertebra from various points along the vertebral column.

Cervical Vertebrae

It has been observed that all vertebrae in *Mymoorapelta* from at least the anterior cervical vertebrae to the

Table 2. Vertebral measurements of *Mymoorapelta* material from the Mygatt-Moore Quarry (measurements in mm).

		Anterior Centrum		Poserior Centrum		Centrum	Neural Canal		Total		
		width	height	width	height	length	width	height	Height	(from neural canal)	Length from neural spine
Cervical Vertebrae											
MWC 1933	axis	48.1	22.2	55.2	25.7	21.2					
MWC 6738	anterior cervical	48.3	36.8	47.52	37.8	35.1	22.6	21.5	89.7	33.3	32.2
MWC 6737	posterior cervical	52.6	38.9	48.9	41.3	37	21.1	16.2	96.1	39.4	61.5
Dorsal Vertebrae											
MWC 1800	1st dorsal	48.5		49	37.7	43.5	16.8	19.4			69.4
MWC 5705	anterior dorsal	56.3	51.9		47.4	52.7	14.8	24.2			
MWC 1802	medial dorsal	45.4	47.5	42.5	49.1	52.6	14.5	19.1			
MWC 1801	medial dorsal	38	46.2	42.3	44.7	52.6	15.4	18.2			
MWC 1803	posterior dorsal		46.4	38.1	45.4	57.9	14	26.7			
MWC 6734	large dorsal referred specimen	51.9	46.9	47.1	53.2	60.9	17.9	25.4			
MWC 6733	large dorsal referred specimen		60.1		57.2	68.9	16.6	17.3			
MWC 6735	large dorsal referred specimen		54.2	52.5		72.9	16	17.6			
	large dorsal referred specimen										
MWC 5940	large dorsal referred specimen										
Sacral centra											
MWC 6932	large					56.5	29				
MWC 3616	large sacrocaudal	51.8	59.4			67.3					
MWC 6736	? caudosacral			52.4			14	14.5			
MWC 5104	small sacrocaudal										
Caudal Vertebrae											
MWC 5070	large proximal caudal referred specimen	67.1	68.1	69.7	70.8	60	18.9	18.7			
MWC 1804	first caudal	56.5		56.4	54	53.7	13.9	12.8			
MWC 1806	second caudal	58.8	44.9	57.6	50.7	42.4	10.9	13.2	122.7	60.9	115.1
MWC 1805	third caudal	58.9	44.8	60.1	49.2	43.3	12.6	13.8	122.1	58.4	118.5
MWC 4036	large medial caudal referred specimen	64.3	63.7	67.3	61.1	54.3	15.7	16.2			
MWC 3651	large medial caudal referred specimen	57	55.2	57.4	58.1	57.3	12.1	15.6			
	large medial caudal referred specimen										
MWC 6732	large medial caudal referred specimen	58.3	50.7	59.7	55.2	51.3	9.2	12.1			
MWC 1807	medial caudal	45.5	39.7	46.1	39.9	44.4	7.2	9.3	94.6	42.5	63.1
MWC 6739	medial caudal	40.5				43.9					
MWC 1913	posterior medial caudal	42	36.8	38.2	34.4	49.7	7.2	6.7	67.9	24	42.1
MWC 1907	posterior medial caudal	39.4	33.1	42.6		47	8.4				
	posterior medial caudal										
MWC 5830	large distal caudal referred specimen		33.3			61.4	5				
MWC 1808	distal caudal					51.8					
MWC 5819a	fused extremely distal caudal	34.2	29.3	32.3	29	47.9	4				
MWC 5819b	fused extremely distal caudal	32.6	27.2	33.3	26.7	44.5					
MWC 5820a	fused extremely distal caudal	27.6					4				
	fused extremely distal caudal										
MWC 5820b	fused extremely distal caudal					38					

medial caudal vertebrae possess a deep anterioposteriorly elongate fossa extending into the centrum from the central midline of the ventral surface of the neural canal. This fossa extends approximately one-third the length of the centrum. It has only recently been described in ankylosaurs perhaps because the fossa is obscured by the neural canal (Barrett and Maidment, 2011; Blows and Honeysett, 2014b; Blows, 2015). It has been figured without comment by previous authors; Carpenter (2004, Figure 11A*) figures this feature in a cervical vertebra of *Ankylosaurus* and it is figured for *Stegopelta* (Carpenter and Kirkland, 1998, Figure 22C). Written communications (2015) by Larry Witmer (Witmer Lab, Ohio University) and Matt Wedel (Western University Health Sciences) note that this feature is widespread in the Archosauria for the vascularization of the centrum from the basivertebral vein and suggest calling it the basivertebral venous fossa. This fossa is paired in Crocodilia (L. Witmer, Witmer Lab, Ohio University, personal communication, 2015).

The *Mymoorapelta* atlas intercentrum is represented by MWC 1933 (Figures 14A through 14E). It is wedge shaped in cross section and 55.2 mm across laterally. The *Gargoyleosaurus* holotype atlas intercentrum (Figure 15A) is considerably larger at 72.1 mm wide (Kilbourne and Carpenter, 2005). The *Mymoorapelta* ventral surface of the atlas is flattened, and the dorsal margin is notched to receive the odontoid of the atlas. Its neural arch is not attached but has not been broken off; either indicating lack of fusion due to ontogeny or a different character state.

MWC 6738 is a complete medial cervical vertebra (Figures 14F through 14K). The vertebra is platycoelan with the faces of the centrum shallowly excavated. The anterior and posterior centrum faces are parallel, but the posterior face is lower than anterior face as they are in many nodosaurids (Gilmore, 1930; Carpenter and Kirkland, 1998) and ankylosaurids (Maleev, 1954, 1956; Maryanska, 1977; Carpenter, 2004) but not *Saichania* (=*Pinacosaurus*; Carpenter et al., 2011, although debated in Kinneer et al., 2016). The centrum is broadly depressed in cross section with the ventral surface of the centrum mostly rounded transversely, with a pair of facets similar in appearance to the chevron facets on the caudal vertebrae present on the ventral margin of the posterior face of centrum. The third cervical centrum of *Gargoyleosaurus* (Figure 15B) has more evenly positioned faces of the centrum and is proportionally more elongate (Kilbourne and Carpenter, 2005). Two vascular foramina enter the centrum of *Mymoorapelta* approximately 1 cm from each side of the midline on ventrolateral surface of the centrum, the right foramen is better developed than the left. The neural canal is expansive and wider (2.6 mm) than tall (21.5 mm). The basivertebral venous fossa is well developed below the neural canal extending for approximately half the length of the centrum. A keel extends up the anterior and posterior sides of the low, posteriorly inclined neural spine. The ventral surfaces of the transverse processes are rounded. The prezygapophysial facets are angled medially 105˚ toward each other. The postzygapophysial facets are slightly cupped to overlap adjoining zygapophyses and angled at 115˚ away from each other. A tapering ridge extends down the posterior neural spine pinching out between zygapophyses. The transverse processes are rounded in cross section extending from below the level of zygapophyses bowing ventrally with these lightly expanded diapophyses oriented anterioventrally at 15˚ and facing ventrolaterally. The parapophyses are located near the anterior margin of the centrum close to the dorsal margin.

MWC 6737 is a posterior cervical vertebra (Figures 14L through 14O). It is platycoelous with the anterior face of the centrum more deeply excavated than the posterior face. The posterior face of the centrum is parallel and even with the anterior face of the centrum. The ventral margin of the centrum is more narrowly rounded, giving it a more heart-shaped cross section. The neural canal is smaller than in MWC 6738 (Table 2), but still wider (21.1 mm) than tall (16.2 mm) and subrectangular in anterior view. The basivertebral venous fossa is well developed below neural canal and two asymmetrical nutritive foramina enter the lower ventrolateral surface of the centrum. The parapophyses are in the same position as MWC 6738. The centrum is about as long as tall, but the neural arch is significantly taller than MWC 6738, although the neural spine is still short. A weak keel extends up the anterior and posterior sides of the

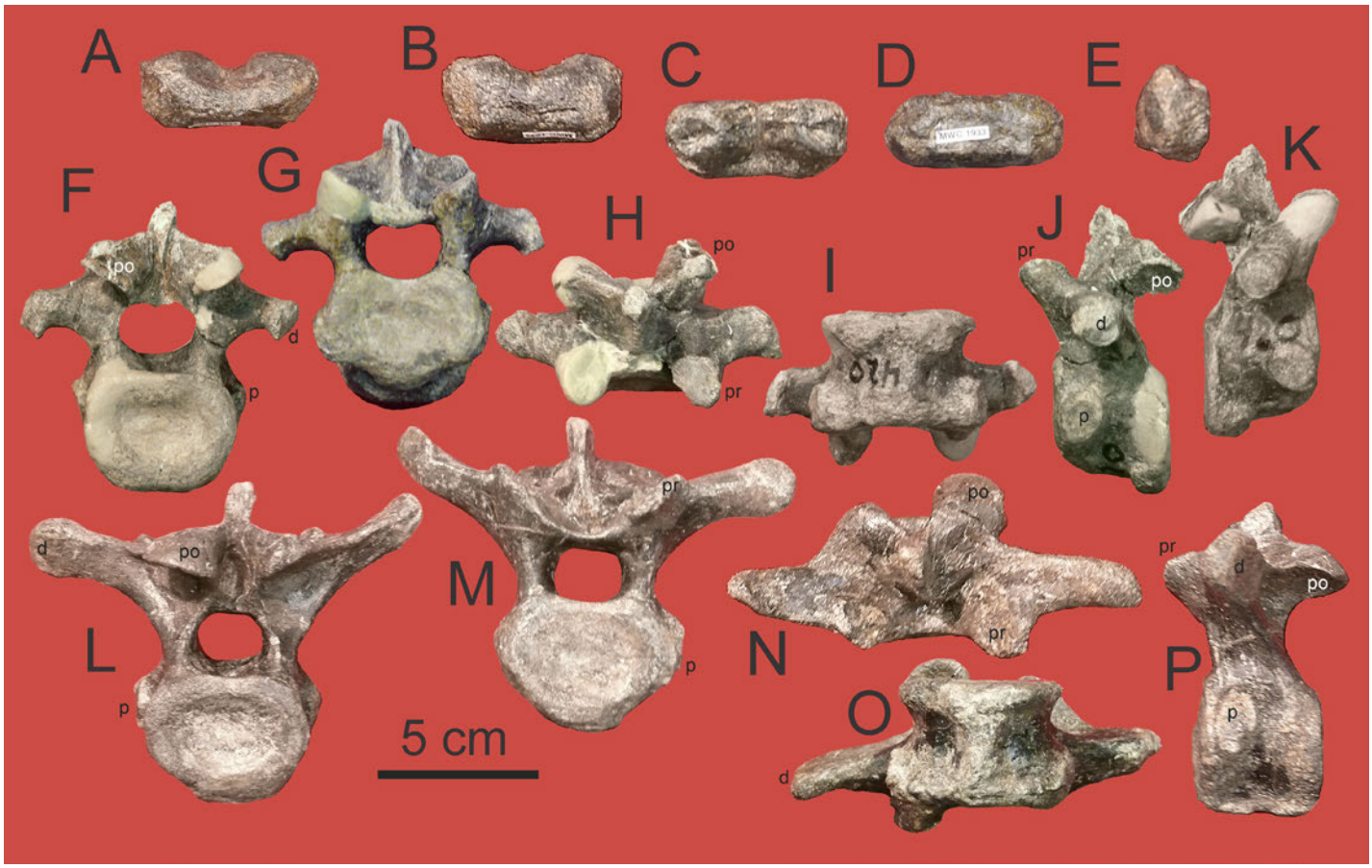

Figure 14. Cervical vertebrae from the revised hypodigm of *Mymoorapelta*. Atlas MWC 1933 in (A) cranial, (B) caudal, (C) dorsal, (D) ventral, and (E) right lateral views. Mid-cervical vertebra MWC 6738 in (F) cranial, (G) caudal, (H) dorsal, (I) ventral, (J) right lateral, and (K) left lateral views. Posterior cervical MWC 6737 in (L) cranial, (M) caudal, (N) dorsal, (O) ventral, and (P) right lateral views. Abbreviations: d = diapophysis, p = parapophysis, po = post zygopophysis, pr = prezygopophysis.

low, posteriorly inclined neural spine. Posteriorly, there is a fossa in the neural arch below the neural spine. On the anterior sides of the centrum, the parapophyses distinctly raised pads to articulate with the head of the cervical ribs. The transverse processes are subtriangular in cross section and angle upward to the diapophyses, which in turn are angled somewhat dorsally at approximately 20˚ and face posteriorly for the tuberculum of the cervical rib. The prezygapophyses angle 96˚ toward each other, whereas the postzygapophyses are angled at 136˚ away from each other. A wide depression is below each prezygapophysis to receive the preceding postzygapophysis. A ventrally bowed lamina connects the postzygapophyses. MWC 6737 does not possess a tapering ridge between postzygapophyses as seen in MWC 6738. A dorsoventrally ovate posterior fossa in neural arch is below the neural spine, and anteriorly below the neural spine there is a shallow depression that is wider than tall between prezygapophyses. MWC 1913 is a poorly preserved medial cervical centrum similar to that of MWC 6737.

Neither of *Mymoorapelta*'s cervical vertebrae exhibit the paired fossae dominating the ventral surface of the centra exhibited by the Lower Cretaceous nodosaurids *Texasites*, *Animantarx*, and *Europelta* (Carpenter and Kirkland, 1998; Carpenter et al., 1999; Kirkland et al., 2013).

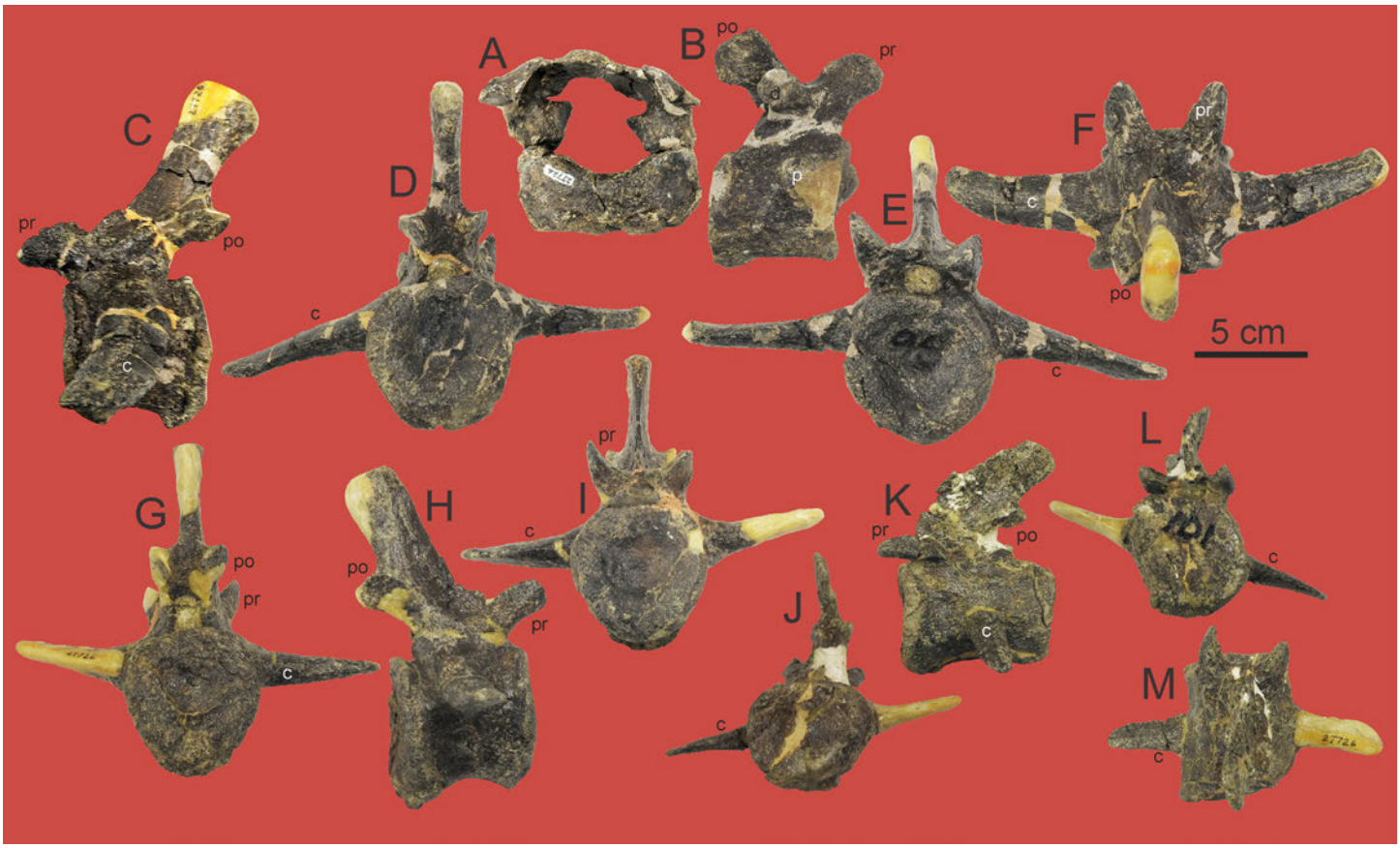

Figure 15. Vertebrae from holotype of *Gargoyleosaurus parkpinorum* DMNH 27726. Atlas (A) in posterior view. Third cervical vertebra in (B) lateral view. Anterior medial caudal vertebrae in (C) lateral, (D) posterior, (E) anterior, and (F) dorsal views. Posterior medial dorsal vertebra in: (G) posterior, (H) lateral and (I) anterior views. More distal vertebra in (J) posterior, (K) lateral, (L) anterior, and (M) dorsal views. Abbreviations: c = caudal ribs, d = diapophysis, p = parapophysis, po = post zygopophysis, pr = prezygopophysis.

Dorsal Vertebrae

Four dorsal vertebrae can be assigned to the expanded hypodigm of *Mymoorapelta* (Figures 16A through 16S). Of these, only the most anterior dorsal vertebra (MWC 1800) still retains the transverse processes and neural spines. This pervasive damage may be a result of predation or scavenging as suggested by the numerous tooth marks on the dorsal surface of the ilium. Therefore, it is impossible to determine their morphology. All dorsal centra exhibit a well-developed basivertebral venous fossa in the centrum below the neural canal. The centra are amphiplatyan with a tendency for the anterior margin to be more cupped than the posterior margin. The sides of the centra are smooth and depressed laterally and ventrally.

Dorsal vertebrae are considered to be anterior if the centrum is relatively short and the diapophysis is not exclusively on the neural spine. Medial dorsal vertebrae are interpreted to possess a dorsoventrally ovate neural canal with a relatively taller neural arch, whereas the most posterior dorsal vertebrae have more elongate centra and possess a circular neural canal with a relatively shorter neural arch by comparison with *Ankylosaurus* (Carpenter, 2004). The pedicel of the neural arch arises from the anterior part of the centrum and there are depressions below the postzygapophyses (best seen in lateral view) extending forward to the transverse processes. Thus, the neural arch appears to be angled anteriorly. However, the neural spine is posteriorly placed

Figure 16. Dorsal vertebrae of *Mymoorapelta* from Mygatt-Moore Quarry. First dorsal assigned to the revised hypodigm MWC 1800 in (A) cranial, (B) caudal, (C) dorsal (D) ventral, and (E) right lateral views. Medial dorsal vertebra assigned to the revised hypodigm MWC 1803 in (F) cranial, (G) right lateral, and (H) left lateral views. Second medial dorsal vertebra assigned to the revised MWC 1802 in (I) cranial, (J) caudal, (K) ventral, (L) right lateral, and (M) left lateral views. Referred dorsal vertebra MWC 1801 in (N) cranial, (O) caudal, (P) dorsal, (Q) ventral, (R) right lateral, and (S) left lateral views. Referred anterior dorsal vertebra MWC 5705 in (T) caudal, (U) dorsal, and (V) left lateral views. Referred dorsal vertebra MWC 6737 in (W) cranial, (X) ventral, and (Y) right lateral views. Paratype dorsal vertebra MWC 6733 in (Z) right lateral view. Dorsal vertebra MWC 6735 in (AA) cranial, (BB) caudal, (CC) dorsal, (DD) ventral, (EE) right lateral, and (FF) left lateral views. Abbreviations: d = diapophysis, p = parapophysis, po = post zygopophysis, pr = prezygopophysis.

on all the vertebrae. Its anterior margin arises at the front of the parapophyses with the base extending back to above or just posterior to the posterior margin of the centrum between the postzygapophyses. Although breakage makes the neural spine appear to be reclined, it was probably fully erect. There is only a narrow gap between the prezygapophyses, and the postzygapophyses are adjoined with a lamina extending at their base to the top of the neural canal. Thus, the medial and dorsal vertebrae have nearly the same tongue and groove articulation, which limits the mobility of the dorsal vertebrae as in ankylosaurids (Brown, 1908; Maleev, 1954; Carpenter, 2004). The parapophyses form raised circular to ovate pads on pedicels adjoining the base of the transverse processes. They have depressed centers and flaring rims to encompass the capitulum of the rib. There is no evidence of fusion of the ribs with any vertebrae.

MWC 1800 is identified as the first dorsal vertebrae (Figures 16A through 16E). The centrum is nearly circular in cross section as is the overlying the circular neural canal. The neural arch is relatively tall and arises from the anterior two-thirds of the centrum. The neural spine is erect and blade-like with the top of neural spine broken off such that it is impossible to determine if the neural spine is expanded dorsally as in many other ankylosaurs (Ostrom, 1970; Arbour and Currie, 2013a; Park, 2022). There is a subtriangular fossa 0.5 mm deep and 7 mm wide below the neural arch anteriorly, and slightly above to either side there are elongate shallow fossae approximately 18 mm wide, which would have received adjoining postzygapophyses allowing for increased lateral maneuverability. A vascular canal 2.6 mm in diameter is present on the medial side of both fossae. A ventrally bowed lamina connects the postzygapophyses below the medial triangular fossa. Posteriorly the postzygapophyses are separated below the neural spine. The prezygapophyses face inwards at an angle of 147˚, postzygapophyses are 148˚, indicating the potential for a great deal of lateral flexure. The postzygapophyses are slightly cupped to overlap prezygapophyses. The transverse process is T-shaped in cross section as is characteristic of ankylosaur transverse processes. The parapophyses face ventrolaterally from lateral ends of transverse processes and the diapophyses are at the base of the neural spine on the suture between the neural spine and centrum. Carpenter (2004; Carpenter et al., 2011) noted that in ankylosaurids the parapophysis shifts upward such that it lies completely on the lateral surface of the neural arch by the third dorsal vertebra.

MWC 1803 is a medial dorsal vertebra distinguished by its tall neural canal (Figures 16F through 16H). The faces of centrum are shallowly excavated. The neural arch is inclined anteriorly. It is not well preserved but the most striking feature is how anteriorly inclined the neural arch appears relative to the centrum.

MWC 1802 is a more posterior dorsal vertebra (Figures 16I through 16M). Although too damaged to measure, the angles between faces of the zygapophyses form a more acute angle than in MWC 1803. The centrum is more elongated in length than in width (Table 2). The neural spine is broken off near base, less teardrop-shaped in cross section, and the base is approximately 50 mm long with a max width of 8 mm. Parapophyses are below the transverse processes and well above suture between the neural spine and centrum.

MWC 1801 is a posterior dorsal vertebra (Figures 16N through 16S). Faces of the centrum are shallowly excavated. The centrum is longer than wide and the neural spine flat and blade like (Table 2). The parapophysis is situated under the transverse process. Even though poorly preserved, the faces of the prezygapophyses appear to form a more acute angle. The neural spine, although not complete, is more complete than the other dorsal vertebrae, with a length of approximately 50 mm and width of 5 mm. Zygapophyses on this specimen are the best preserved of those of any of the posterior dorsal vertebrae, the prezygapophysial facets angle toward each other at of 97˚, and the post-zygapophysial facets angle away from each other at 108˚. There are also four larger, poorly preserved, dorsal vertebrae from the referred individual (Figures 16T through 16FF) that are approximately 25% larger (Table 2), although they are not described in detail.

MWC 5705 is a large anterior dorsal vertebra, suspected to be from the larger animal (Figures 16T through 16V). The parapophysis is positioned on the suture between the neural spine and centrum. Faces of amphiplatyan centra are shallowly excavated and the

centrum is slightly medially constricted with a well-developed basivertebral venous fossa. The lateral margins are damaged around both anterior and posterior faces of the centrum, so it is difficult to determine the original shape. Although damaged, the prezygapophyses appear to form a relatively obtuse angle of 137˚ as in MWC 1800. A rugose depression extends down the posterior side of the neural arch between postzygapophyses to the top of the neural canal and there is a large pit on the side of the neural arch anterior to the transverse process. The neural spine is broken off just above the zygapophyses, and in cross section it widens from 5 mm anterior to 13 mm near the posterior margin and is somewhat teardrop shaped in cross section. At the base of the neural spine, anteriorly, is an elongate slot-shaped fossa, which extends at angles 45˚ posteroventral above the neural canal.

MWC 6734 is a large, poorly preserved dorsal vertebra (Figures 16W through 16Y) with well-developed basivertebral venous fossa. There is no excavation below the neural spine anteriorly. A ridge extends down the posterior side of the neural arch from below the prezygapophyses extending back to top of the neural canal. Parapophysis is well-developed immediately below the transverse process and the ventral margin of the centrum is rounded. Faces of the centra are shallowly excavated. The neural arch appears to incline anteriorly.

MWC 6733 is a large, more poorly preserved dorsal vertebra (Figure 16Z) that appears to have been damaged and weathered prior to burial. The pedicel appears shorter than that of MWC 6734 and this vertebra is considered to be more posterior. It also displays no fossa below the neural spine anteriorly. A ridge also extends down the posterior side of the neural arch from below the postzygapophyses to the top of the neural canal.

MWC 6735 is a large posterior dorsal vertebra from the referred material and, although not well preserved, it is the best-preserved dorsal vertebra represented by the referred material (Figures 16AA through 16FF). This vertebra exhibits the shortest pedicel for any known vertebrae assigned to *Mymoorapelta* and is interpreted to represent an extremely posterior dorsal vertebra, perhaps positioned in the range of the dorsosacrals of *Gargoyleosaurus* (Carpenter et al., 2013) and *Gastonia* (Kirkland, 1998). There is no fossa below the neural spine. A keel extends anteriorly down the posterior side of the neural arch below the prezygapophyses to the top of the neural canal. The diapophysis are well developed immediately below the transverse process, and the ventral margin of the centrum is rounded. The length of neural spine is about 70 mm and the width is 6 mm.

No dorsal vertebrae are recognized in the holotype of *Gargoyleosaurus* (Kilbourne and Carpenter, 2005). Three dorsal vertebrae (Figure 17) were collected with the Movie Valley Ankylosaur BYU 773-9430. They cannot be assigned with any certainty to either *Mymoorapelta* or *Gargoyleosaurus*. The most complete example (Figures 17F through 17I) preserves a complete neural spine with transverse processes that angle upward at about 30˚ to near the top of the neural spine, which is unexpanded unlike nodosaurids (e.g., Ostrom, 1970; Kirkland et al., 2013) and ankylosaurids (e.g., Vickaryous et al., 2004; Park, 2022). Ribs have not been observed to be fused to the free dorsal vertebrae in any Jurassic ankylosaurs.

Sacral Vertebrae

Mymoorapelta sacra from the Mygatt-Moore Quarry are fragmentary and represent portions of the sacra from at least three individuals (Figure 18). MWC 3613 is interpreted to be a sacral centrum from the revised hypodigm of *Mymoorapelta* (Figure 18A). It is approximately 20% to 25% smaller than those assigned to the referred specimens. As with the dorsal and cervical vertebrae, a well-developed basivertebral venous fossa extends down into the centrum from the center of the neural canal. The centrum was too damaged and abraded to yield meaningful measurements but was wider than tall. It appears not to have been fused to with adjoining centra and may represent a caudal sacral or perhaps a dorsosacral. There are two quite deep, circular pits or excavations on the posterior half of the centrum, below and on either side of the neural arch. These pits characterized the better-preserved sacral vertebra of the referred specimen described below.

MWC 6736 may be a caudosacral from the revised hypodigm of *Mymoorapelta* (Figure 18B). It is not very well preserved. The anterior face of the centrum is com-

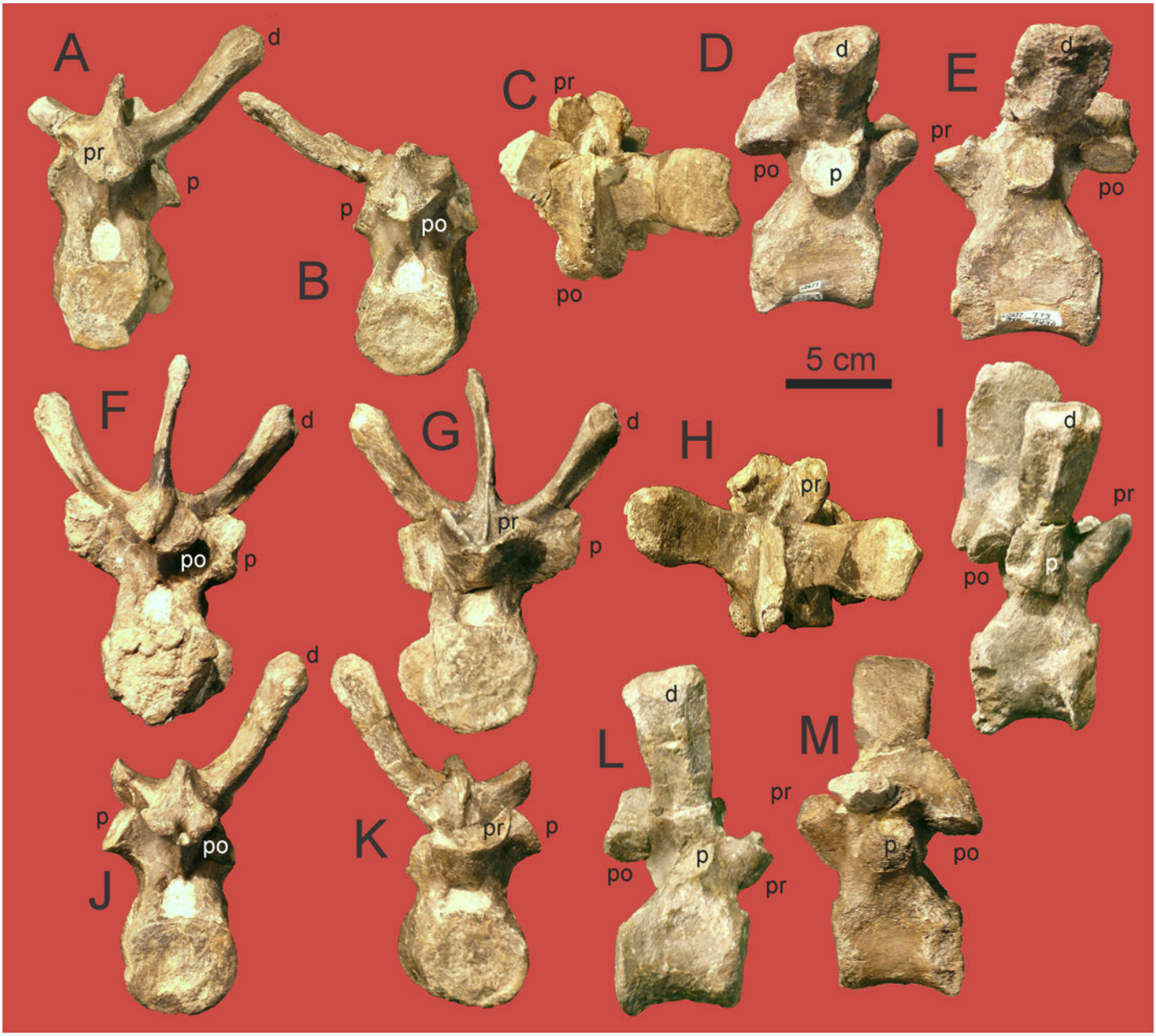

Figure 17. Dorsal vertebrae from Movie Valley Ankylosaur BYU 773-9430. Dorsal vertebra in (A) cranial, (B) caudal, (C) dorsal, (D) right lateral, and (E) left lateral views. Posteriorordsal vertebra in (F) cranial, (G) caudal, (H) dorsal, and (I) right lateral views and (J) cranial, (K) caudal, (L) right lateral, and (M) left lateral views. Abbreviations: d = diapophysis, p = parapophysis, po = post zygopophysis, pr = prezygopophysis.

pletely broken away and the neural arch is broken off above the neural canal. A well-developed basivertebral venous fossa extends down into the centrum from the center of the neural canal. The posterior face of the centrum is depressed and displaced ventrally about half the height of the centrum. The caudal ribs extend directly laterally as preserved and appear to be more massive than those on MWC 1804 or the other anterior caudal vertebrae from the revised hypodigm.

Portions of a larger sacrum have been recovered that are interpreted to pertain to the larger referred individual. The central portion is represented by two large fused

Figure 18. Sacral vertebrae from revised hypodigm and referred specimens of *Mymoorapelta*. Holotype abraded sacral centra MWC 5104 in (A) dorsal view. Holotype partial caudosacral vertebra MWC 6736 in (B) caudal view. Paratype partial sacrum preserving two plus centra MWC 6932 in (C) left lateral, (D) left lateral (E) ventral, (F) dorsal, and views. Paratype caudosacral centra MWC 3613 in (G) ventral, (H) anterior, (I) dorsal, (J) posterior, (K) right lateral, and (L) left lateral views. Paratype partial sacrum MWC 10347 in (M) ventral, N, anterior, (O) left lateral, (P) dorsal, and (Q) posterior views.

sacral vertebrae (MWC 6932) with what is interpreted to be just the poster margin of a third vertebra fused on anteriorly (Figures 18C through 18F). Most notably there is a ventral depression, whereas there is a keel on the underside of the sacrum from the Simon Quarry assigned to *Gargoyleosaurus* (Figure 19) by Carpenter et al. (2013). Traces of sutures between centra indicate the length of each centra is 56.5 mm, and medially at the narrowest point the posterior centum is 55.8 mm wide and the more anterior centrum is 58.7 mm wide. Each centrum includes a well-developed basivertebral venous fossa extending down into the centrum from the neural canal. The neural spines are broken off at the neural canal, which has considerable abrasion along the break.

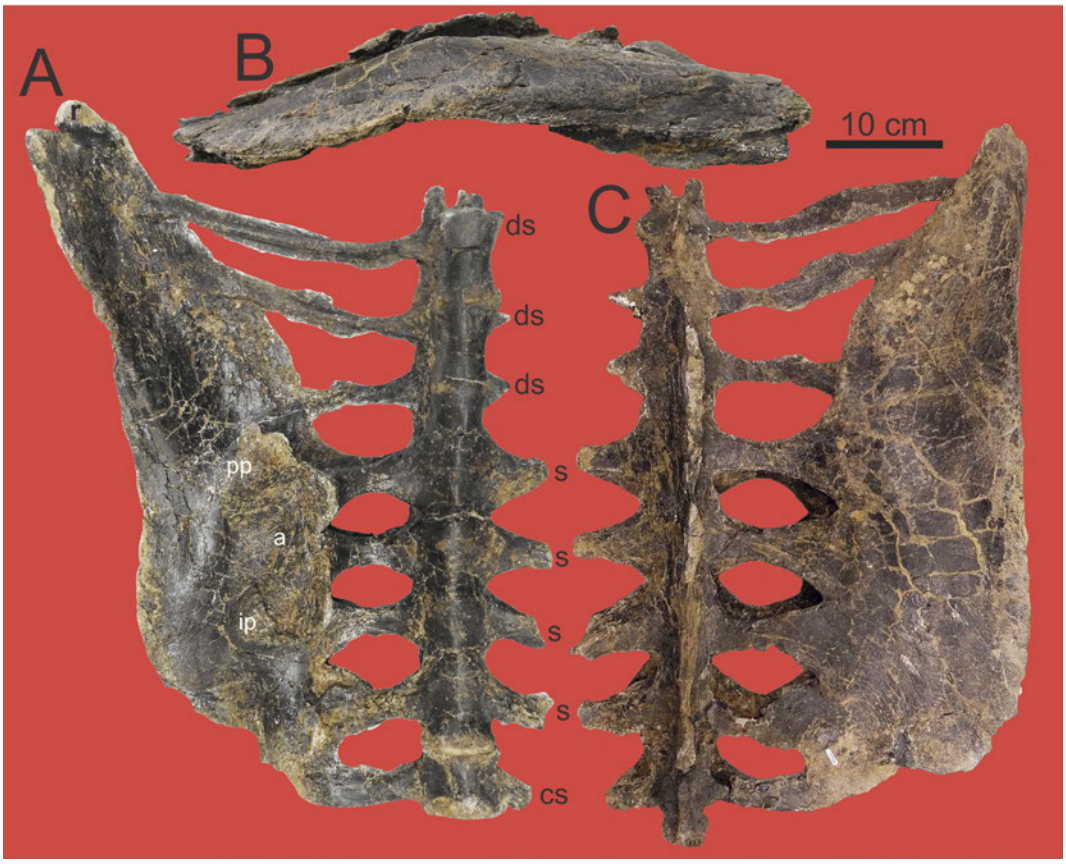

Figure 19. *Gargoyleosaurus* sacrum from Simon Quarry, northern Wyoming. DMNH 58831 in (A) ventral, (B) lateral, and (C) dorsal views.

The sacral ribs were broken off and abraded nearly flush with the sides of the centra posteriorly. The neural canal at the widest visible point measures about 29 mm.

There is a third sacral vertebra of comparable size (MWC 3613). The centrum is clearly wider than tall, and there is considerable abrasion around margins of faces of centrum and where the neural spine has broken away from centrum (Figures 18G through 18L). It appears that the centrum was not fused to the sacrum. The depressed ventral margin of the centrum is gently convex with no ventral depression. This centrum may represent a caudal sacral. Two pits/excavations are on the posterior half of the centrum, below and on either side of the neural arch. Although damaged it appears the anterior face of centrum was wider than the posterior face. This position as a sacral caudal is determined by comparison with MWC1804, which appears to be a damaged first caudal vertebrae from the revised hypodigm that shows similar but more shallow pits in this position.

A partial, fully fused anterior sacrum (MWC 10347) was recovered from the basal "pebble" bed (Chin and Kirkland, 1998) in 2022 indicating the presence of a minimum of three individuals of *Mymoorapelta* at the Mygatt-Moore Quarry. Although broken prior to burial, the specimen is the most complete portion of a sacrum recovered from the site (Figures 18M through 18Q). As preserved, the fossil has a maximum length of 209.75 mm and a maximum height toward the posterior end of 96.4 mm. It consists of four fused vertebrae broken where the ribs meet the transverse processes on the left side and through the base of the transverse processes on the right side. The neural spines are broken off above the neural arch, which fully obscures the neural canal. The anterior-most vertebra is damaged, but largely the anterior break appears to coincide with the anterior face of this vertebra (Figure 18N). This face is somewhat heart-shaped, narrowing ventrally, with a round neural canal estimated at 19.8 mm wide and 17.1 mm tall. The vertebrae increase in size posteriorly. The posterior-most preserved vertebra is highly damaged posteriorly and ventrally such that it cannot be determined

if it had a ventral depression. The centrum appears to be wider than tall, with a neural canal estimated to be 27.4 mm wide and 17.4 mm tall comparing well to that of the sacral neural canal in MWC 3613 (Figure 18P). We propose that MWC 10357 consists of two sacral vertebra and two dorsal vertebra forming part of the anterior synsacrum. The bases of the transverse processes of the anterior-most sacral and posterior-most dorsal synsacral vertebrae extend for approximately the length of the vertebrae and only extend laterally to the ribs at the anterior end.

The LACM sacrum (LACM.154873) has been identified as that of *Mymoorapelta* based on the distinct groove along the ventral surface of the sacral centra as in the holotype material (Figure 20B). It consists of three sacral vertebrae and one caudosacral vertebra. The sacral ribs are fused together distally to form a yoke to attach to the ilia. The specimen lacks any fused dorsosacral vertebra to form a synsacrum.

The initial discovery of the Cactus Park *Mymoorapelta* (MWC 2610) included several large sandstone blocks preserving external molds of portions of the sacrum. One block (Figure 21C) preserves the three sacral ribs (Kirkland, 1998; Carpenter et al., 2013). An external mold of the ventral portion of the anterior synsacrum with the associated ribs is joined to the preacetabular portion of the ilium (Figure 21A). Vertebrae associated with this block (not figured) are represented by slightly constricted cylindrical centra that were not fused together. An overlying sandstone block preserves ossified tendons that would have been placed along each side of these neural spines (Figure 21B).

It is estimated that a fully developed sacrum of *Mymoorapelta* would consist of one caudosacral vertebra, three sacral vertebrae, and four dorsosacral vertebrae fused into the synsacrum. In addition to lacking a ventral groove on the sacrum (Carpenter et al., 2013), *Gargoyleosaurus* differs in possessing four sacral vertebra (Figure 19). The ventral groove of the sacrum is present on most other sacra assigned to polacanthines (Blows, 2015; Kinneer et al., 2016; Raven et al., 2020) and nodosaurids (Carpenter et al., 1995; Burns, 2015; Lull, 1921). It is noteworthy that the sacrum of the new specimen of the Late Jurassic ankylosaur *Dracopelta* (NOVA-FCT-DCT-5556) from Portugal has the same sacral formula as the Simon Quarry specimen of *Gargoyleosaurus* and also lacks the ventral groove (Russo, 2024). The presence of a ventral sacral groove in *Mymoorapelta*, polacanthines, and in North America's nodosaurids appears to be a derived character as it is not present in *Scelidosaurus* (Norman, 2020b). It is also absent in the Middle Jurassic Chinese ankylosaur *Tianchisaurus* (Dong, 1993), ankylosaurids (Penkalski and Blows, 2013; Park et al., 2021), and Europe's struthiosaurids (Garcia and Pereda–Suberbiola, 2003; Kirkland et al., 2013; Ősi et al., 2019).

Caudal Vertebrae

Numerous caudal vertebrae are preserved with revised hypodigm and referred specimens of Mymoorapelta at the Mygatt-Moore Quarry (Figures 22 and 23). MWC 1804 had been interpreted as a caudosacral centrum (Kirkland and Carpenter, 1994; Kirkland et al., 1998), but it may instead represent the first caudal (Figures 22B through 22E). It is tentatively interpreted as belonging to the holotype individual because of its size but was reportedly collected as a float specimen by Pete Mygatt soon after the locality was discovered (P. Mygatt, Museum of Western Colorado volunteer, verbal communication,1982). It is somewhat wedge-shaped in lateral view such that the ventral length of the centrum may have been slightly shorter than the dorsal length. It also appears to have a narrower, flattened ventral margin of the centrum than the other anterior caudal vertebrae. The caudal ribs and the neural spine are broken off. The base of the neural spine is subtriangular in cross section at the neural canal and is widest anteriorly, narrowing posteriorly (Figure 22D).

MWC 1806 and 1805 (Figures 22F through 22O) are adjoining proximal caudal vertebrae that were described previously (Kirkland and Carpenter, 1994; Kirkland et al., 1998). Both neural spines expand upwards towards the dorsal terminus. MWC 1806 expands more than MWC 1805 and thus is interpreted to be the more anterior of the two. The neural spine in MWC 1806 is more erect than MWC 1805, which is angled slightly more posteriorly. The sutural contacts of the neural spines with the centra narrow anteriorly as in *Pola-*

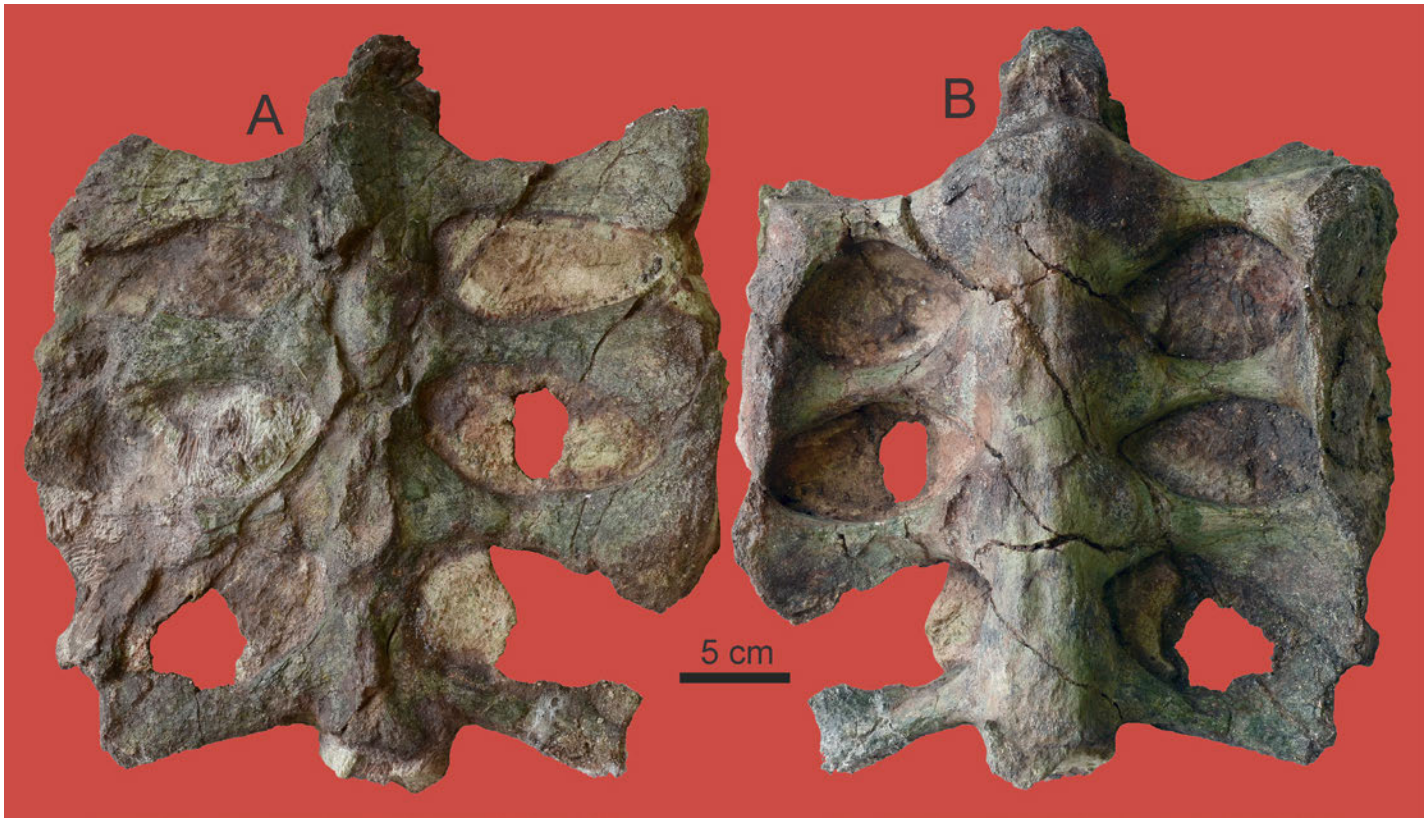

Figure 20. Complete *Mymoorapelta* sacrum from southeastern Utah. LACM.154873 in (A) dorsal and (B) ventral views.

canthus. The ventral sides of both centra are narrowly rounded and both possess a faint keel. A well-developed basivertebral venous fossa extends down into the centra from the center of the neural canals. The notochordal prominence is present on the posterior face of both caudal centra. Faces of centra have a more ovate or kidney bean shape in anterior view whereas they become more strongly heart shaped with a more pronounced chevron facet on the posterior face. Posterior chevron facets narrow anteriorly. The development of the chevron facet occurs at about the third caudal vertebra (Pereda-Suberbiola, 1994). Viewed dorsally, the prezygapophyses are widely separated and angle away from each other at about 60˚; however, they form a very obtuse angle of approximately 150˚ in a vertical plane. This feature is not preserved in MWC 1806, which was reconstructed to match MWC 1805. Postzygapophyses angle away from each other at approximately 105˚ vertically. Disparity between angles suggests fair amount of cartilage between zygopophyses, which may not be to the same degree in the dorsal vertebrae, allowing for increased maneuverability in the tail. The caudal ribs of both vertebrae extend horizontally flexing ventrally to about an angle of about 45˚ as in the Compton Bay polacanthid NHMUK R9293 (Blows, 1987, 2015), whereas they tend to angle more abruptly downward from the centrum on *Gastonia* (Kirkland, 1998; Kinneer et al., 2016) and the correlative Bexhill polacanthid (Blows and Honeysett, 2014b, Figures 5A and 5B; Blows, 2015). They are ovate in cross section, being about twice as long as tall and taper distally with no terminal expiation as in some ankylosaurids (Ostrom, 1970). In dorsal view the left caudal rib of MWC 1805 appears to turn slightly posteriorly and the right appears to turn slightly anteriorly. In MWC 1806 both are turned slightly anteriorly, suggesting the posterior turn on the left of MWC 1805 is either distortion or an ontogenetic abnormality. The neural spines are inclined posteriorly from 10˚ to 15˚ and have an expanded dorsal terminus as in *Gastonia, Polacanthus*, and *Sauropelta* (Ostrom, 1970; Kirkland

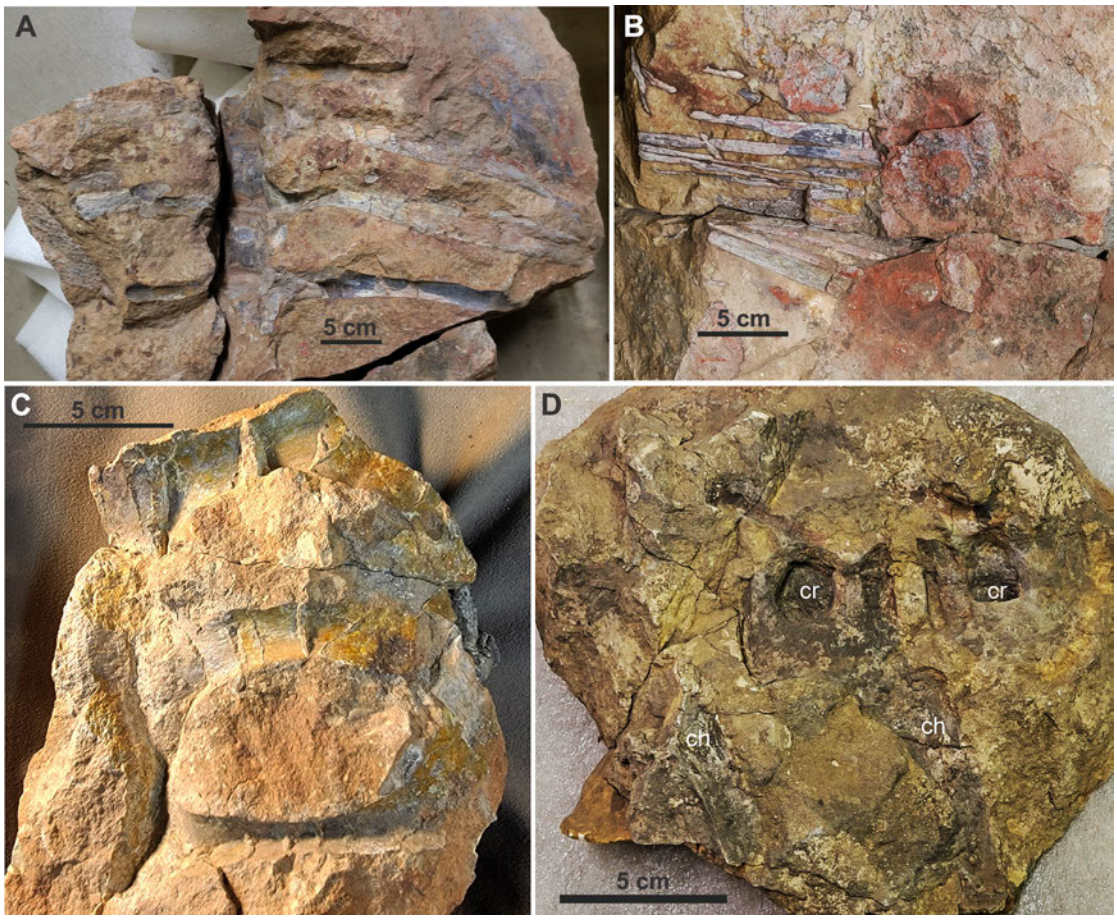

Figure 21. Axial skeletal molds from pelvic area of the Cactus Park *Mymoorapelta*, MWC 2610. (A) Ventral mold of the synsacral area with dorsal ribs. (B) Ossified tendons from along synsacral vertebral neural spines. (C) Ventral mold of a portion of the right side of sacrum. (D) Right lateral mold of proximal caudal vertebrae. Abbreviations: cr = impression of base of caudal ribs, ch = impressions of chevrons.

1998; Blows, 2015; Kinneer et al., 2016). In posterior view, the neural spine of MWC 1805 expands from 13 mm to at least 25 mm at dorsal terminus. However, the lateral margins of the terminus are worn. The neural spine maintains a consistent anterior to posterior length of 22 mm from the prezygapophyses to its dorsal termination. The proximal caudal vertebra tentatively assigned to *Gargoyleosaurus* sp. (Figure 5A) from the Maelyn Quarry at the Eccles Dinosaur Park in Ogden, Utah (EDP-SM 2017.01.096). Although this specimen is poorly preserved and more lightly constructed it appears to compare well with those of *Mymoorapelta*.

A partial proximal haemal arch or chevron (MWC 1912) from about this position on the tail of the holotype individual has been identified (Figures 22P through 22R). The left side bounding the haemal canal is broken and the distal end is incomplete. However, it appears to have been approximately as long as the neural proximal neural spines and caudal ribs of those of the proximal caudal vertebrae (MWC 1805, 1805). The flattened right articular surface is oval, and although it is flaring, it appears to have been separate from the left articular surface. Its anterior posterior length is consistent from the articular surface to its distal end, and it is lensoidal in cross section. In lateral view, it curves uniformly posteriorly. Those preserved in the Cactus Park *Mymoorapelta* (Figure 21D) are similar in morphology, but appear to be proportionally longer, perhaps repre-

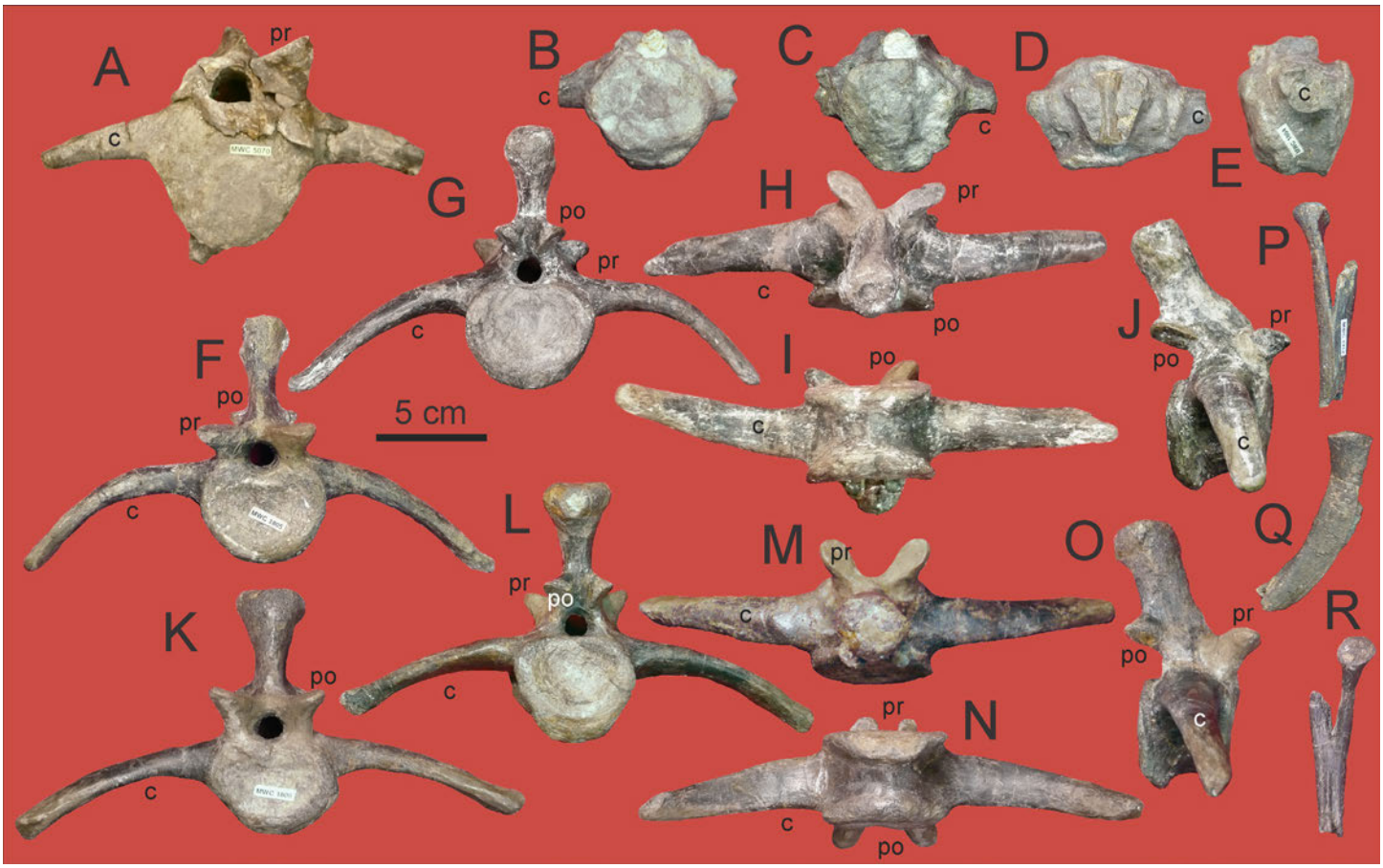

Figure 22. Proximal caudal vertebrae from revised hypodigm and referred specimens of *Mymoorapelta*. Partial proximal caudal vertebra from paratype MWC 5878 in (A) cranial view. Partial first caudal vertebra from revised hypodigm MWC 1804 in (B) cranial, (C) posterior, (D) dorsal, and (E) left lateral views. Second caudal vertebra from revised hypodigm MWC 1805 in (F) cranial, (G) posterior, (H) dorsal, (I) ventral, and (J) right lateral views. Third caudal vertebra from revised hypodigm MWC 1806 in (K) cranial, (L) posterior, (M) dorsal, (N) ventral, and (O) right lateral views. Proximal chevron from revised hypodigm MWC 1912 in (P) cranial, (Q) right lateral, and (R) posterior views. Abbreviations: c = caudal ribs, po = post zygopophysis, pr = prezygopophysis.

senting a more anterior position below the tail. Unlike the haemal arches in proximal polacanthid and nodosaurid tails, the haemel arches in ankylosaurds are typically fused to the centra (Arbour et al., 2009; Thompson et al., 2011; Arbour and Currie, 2016).

MWC 1807 is a well-preserved, small medial caudal vertebra from the revised hypodigm (Figures 23N through 23R) that may represent about the same position in the tail as MWC 3651 from the paratype individual. The top of the neural spine is slightly but distinctly expanded. It has an anterior notochordal bump just above the middle of centrum on the anterior face. The centrum is about as long as it is wide (Table 2). The ventral sides of the centra are flattened with a central depression. Both anterior and posterior chevron facets are developed, but the poster facets are much more strongly expressed. In dorsal view, the right caudal rib is inclined posteriorly, and the left is inclined anteriorly. In lateral view the caudal ribs extend nearly horizontally; an apparent downward flexion consists mainly of thinning of the rib laterally from the dorsal side. The notochordal prominence is well developed on the central face anteriorly and is recognizable on the centrum face posteriorly. Ventral chevron facets are developed

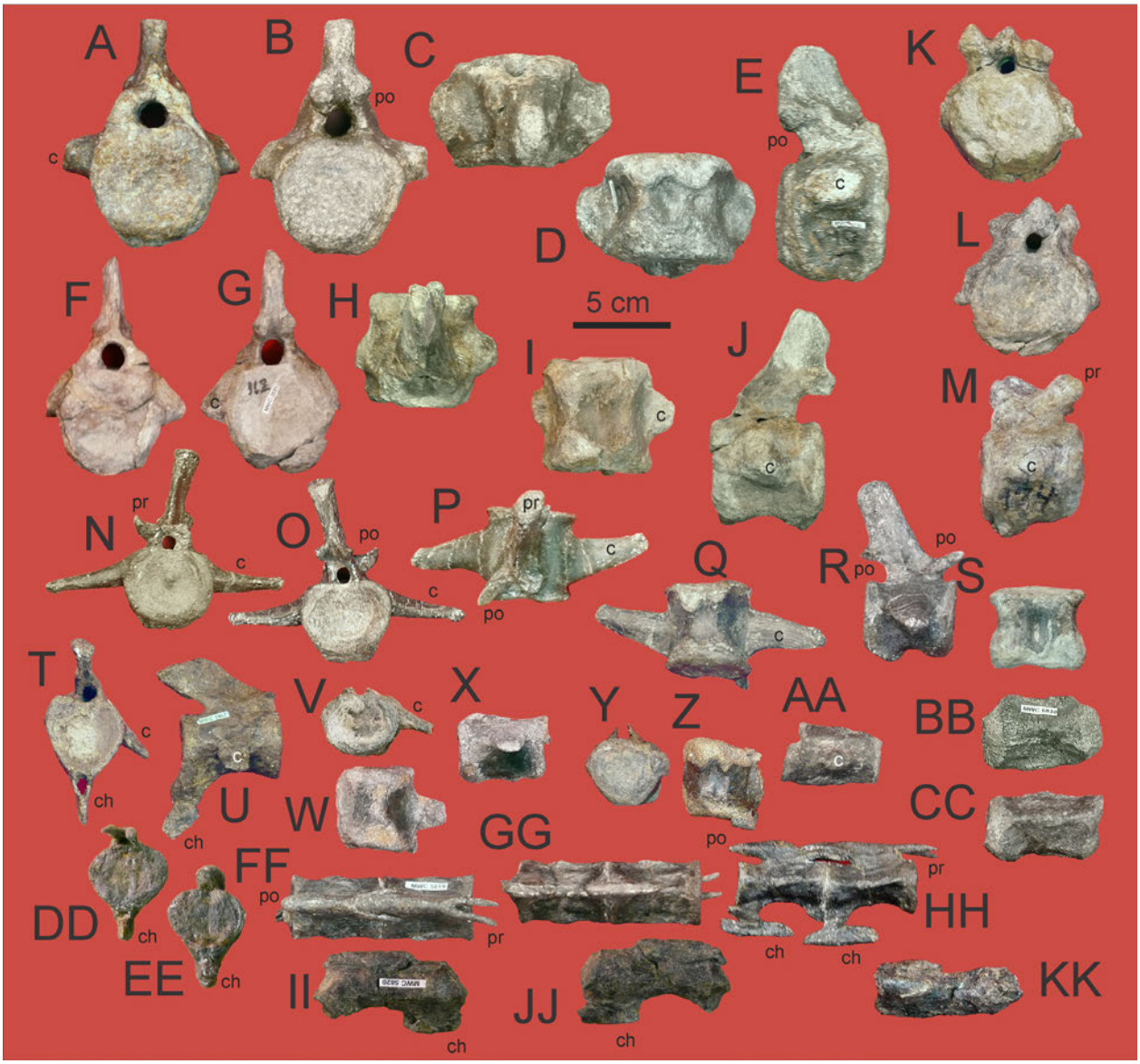

Figure 23. Medial to distal caudal vertebrae from revised hypodigm and referred specimen of *Mymoorapelta*. Medial caudal vertebra from referred specimen MWC 4036 in (A) cranial, (B) posterior, (C) dorsal, (D) ventral, and (E) right lateral views. Medial caudal vertebra from paratype MWC 3651 in (F) cranial, (G) posterior, (H) dorsal, (I) ventral, and (J) left lateral views. Partial medial caudal vertebra from referred specimen MWC 6732 in (K) cranial, (L) posterior, and (M) right lateral views. Medial caudal vertebra from revised hypodigm MWC 1807 in (N) cranial, (O) posterior, (P) dorsal, (Q) ventral, and (R) right lateral views. Medial caudal vertebral centra from revised hypodigm MWC 1913 in (S) dorsal view. Medial caudal vertebra with fused chevron from revised hypodigm MWC 1907 in (T) posterior and (U) right lateral views. Partial medial caudal vertebra from revised hypodigm MWC 5012 in (V) cranial, (W) ventral, and (X) left lateral views. Medial caudal vertebra from revised hypodigm MWC 6739 in (Y) cranial and (Z) ventral views. Partial distal caudal vertebra from revised hypodigm MWC 1808 in (AA) right lateral view. Distal caudal vertebral centra from revised hypodigm MWC 5830 in (BB) ventral and (CC) right lateral views. Pair of fused distal vertebra with fused chevrons from revised hypodigm MWC 1839 in (DD) cranial, (EE) posterior, (FF) dorsal, (GG) ventral, and (HH) right lateral views. Partial pair of fused distal vertebra with fused chevron from revised hypodigm MWC 5820 in (II) left lateral and (JJ) right lateral views. Pair of fused distal vertebral centra from revised hypodigm MWC 5818 in (KK) left lateral view. Abbreviations: c = caudal ribs, ch = chevron, po = post zygopophysis, pr = prezygopophysis.

anteriorly and posteriorly but are more prominent posteriorly. The underside of the centrum is flattened and appears to be depressed due to the prominence of the facets for the chevrons. The prezygapophyses rise from above the neural canal almost horizontal to each other and flex upward laterally producing a curved articular surface angling from 180˚ to 100˚ as they flex along their length. The postzygapophyses are deflected away from each other forming an angle of 80˚ and face laterally. The neural spine is slightly expanded dorsally from the zygapophyses giving a posterior width of 8 mm expanding to 12 mm at the dorsal termination. In lateral view the neural spine tapers very little and is approximately 14 mm long. It is angled 30˚ posteriorly.

The holotype of *Gargoyleosaurus* preserves three medial caudal vertebrae. Kilbourne and Carpenter (2005) describe the most anterior of these (Figures 15C through 15F), as a proximal caudal vertebra and propose that its differences from the proximal caudal vertebrae of *Mymoorapelta* as representing diagnostic differences between these two taxa. We note that this vertebra compares well with MWC 1807 as a medial caudal vertebra and given the scarcity of caudal vertebral remains from *Gargoyleosaurus* in general, it is impossible to distinguish these taxa based on caudal vertebra.

MWC 6739 is a small, poorly preserved mid-caudal centra 43.9 mm long with a distinct ventral groove that appears to have been slightly longer than wide and is 34.4 mm at its tallest point (Figure 23S). Medial caudal vertebra in in *Mymoorapelta* and perhaps polacanthines in general have centra whose width, length, and height are subequal with more distal centra becoming more elongate.

MWC 1907 is a bit more posterior caudal vertebra in which the zygapophyses were largely obliterated in preparation and bases smoothed over and filled to the extent which no sign of them remains (Figures 23T and 23U). The neural spine is fairly short and angles posteriorly beyond centrum at 56˚ and is slightly expanded distally. The transverse processes are short and straight and extend 18 mm downward at about 45˚. Its straight chevron is about the length of the neural spine, inclined posteriorly past centrum at about 25˚, and is fully fused to the posterior end of the centrum. It is slightly anteroposterior expanded just below the haemal arch. The ventral margin is rounded.

MWC 5019 may be a more anterior element than MWC 1907 (Figures 23V through 23X). Fragments of the neural spine are present but cannot be attached to the centrum. The caudal ribs appear to have been longer and less ventrally inclined. The anterior face of the centrum appears to be only slightly depressed relative to the posterior face. MWC 6739 is another poorly preserved medial caudal vertebra about as long as wide with a rounded ventral surface (Figures 23Y and 23Z).

MWC 1808 is a poorly preserved distal caudal centra that is 51.8 mm long with a distinct caudal rib preserved as a round bump about 5 mm high on the flank of the centrum (Figure 23AA). MWC 5830 is a large distal caudal centra with the characteristic lateral ridge along the side of centrum that reflect the caudal ribs on all of the most distal centra. The ventral margin of the centra is sharply rounded.

The six most distal caudal vertebrae (Figures 23DD through 23KK) of *Mymoorapelta* are fused together as are those of the struthiosaurine nodosaurid *Europelta* (Kirkland et al., 2013). This may also be the case with the "incipient" tail club in the holotype of *Polacanthus foxi* NHMUK R175 noted by Blows (1987) and reinterpreted by Carpenter and Kirkland (1998; Blows, 2015). Whether this is a natural character or rather the result of a pathology is unknown; however, we propose it is a result of relying on swinging the tail in defense (Arbour and Snively, 2009; Arbour and Zanno, 2018, 2020). MWC 1839 is a well-preserved pair of distal caudal attached to each other by their mutual fusion with the intervening chevron (Figures 23DD through 23HH). The faces of the centra are flat. The neural arches are low without neural spines. The prezygapophyses are fused together and extend back over the tiny pair of postzygapophyses much as in the handle of a derived ankylosaurid (Arbour and Snively, 2009; Arbour et al., 2009). The caudal ribs form a slight expansion of a distinctive ridge that extends down the side of the centra. The ventral side of the centra has a distinct keel that extends between the fused centra. The chevrons are skid-shaped, extending farther anteriorly than posteriorly, but do not touch. Their ventral margins are flattened. The haemael

canal is round in cross section and is about 5 mm in diameter. MWC 5820 (Figures 23II and 23JJ) is a more distal pair of fully fused vertebrae. Their preserved neural arch is fully fused such that it is difficult to interpret. The neural canal can barely be discerned but appears to be only a few mm across. Laterally, the centra are swollen broadly. The preserved chevron is skid-shaped but damaged anteriorly and posteriorly. Its ventral margin is flattened. The haemael canal is round in cross section and is about 4 mm in diameter. Both the anterior and posterior ends are broken off suggesting that they had adjoining vertebrae fused to these in life. MWC 5818 (Figure 23KK) is an even more distal pair of fused vertebral centra from the expanded hypodigm that are difficult describe morphologically as there are no distinct neural spines or chevrons. These may represent the distal end of the tail.

Four caudal vertebrae are interpreted to represent the larger referred individual from the southwest pit. All possess a well-developed basivertebral venous fossa that extends down into the centra from the center of the neural canals. MWC 5070 is a large proximal caudal (Figure 22A) from the referred individual. Although it looks like it may have been weathered prior to burial, considerable damage appears to have been caused during collection. It might represent the same position as MWC 1805 or a bit more posterior as there is a slight depression on the ventral side of the centrum. MWC 4036, 6732, and 3651 are large, proximal to medial caudal vertebrae (Figures 23A through 23M). All appear to have been weathered prior to burial. The ventral sides of the centra are flattened with a central depression. Both anterior and posterior chevron facets are developed, but the posterior facets are much more strongly expressed. They are superficially like MWC 1807 except for their larger size (Table 2).

Ribs

Several ribs and partial ribs have been recovered (Figure 24). In general, they are typical for ankylosaurs, except for the more medial ribs being more triangular in cross section versus more T-shaped as is typical in more derived ankylosaurs (Vickaryous et al., 2004).

MWC 3747 (Figures 24A through 24C) is the proximal end of anterior dorsal rib. As with other anterior dorsal ribs it is L-shaped in cross section just distal to the tuberculum, where it measures 19.3 mm across and 24.1 mm deep. MWC 5061 is a large anterior dorsal rib from the southwestern part of the quarry, as with other anterior dorsal ribs it is L-shaped in cross section just distal to the tuberculum where it measures 31.3 mm across and 38.2 mm deep just distal to the tuberculum. MWC 5094 is a small anterior dorsal rib as with other anterior dorsal ribs it is L-shaped in cross section just distal to the tuberculum where it measures 16.0 mm across and 28.9 mm deep.

MWC 1810 (Figures 24D through 24F) is a long T-shaped rib 23.7 mm wide and 19.0 mm deep just distal to the tuberculum. This rib expresses how wide *Mymoorapelta* would be in life. MWC 3763 (Figures 24G through 24I) is a large more T-shaped rib section 29.6 mm wide and 25.5 mm deep just distal to the tuberculum. MWC 4329 (Figures 24J through 24L) is a damaged T-shaped rib more than 26 mm wide and 29.5 mm deep just distal to the tuberculum. MWC 1811 (Figures 24M through 24O) is a posterior T-shaped rib 21.7 mm wide and 18.4 mm deep to the tuberculum,

MWC 1840 (Figures 24P and 24Q) is a dorsal-sacral rib only moderately swollen medially and is 28.0 mm wide and 15.8 deep just distal to the tuberculum. It would have extended from the anterior synsacrum to join with the preacetabular process of the ilium. It compares well with those preserved with the Cactus Park *Mymoorapelta* (Figure 21A).

Pectoral Girdle

A worn distal end of a right scapula MWC 6743 has been recovered from the Mygatt-Moore Quarry (Figures 25A through 25C). The distal end of scapula is broken off across the acromion process extending to its lower margin where it would be in contact with the coracoid. By comparison, the coracoid is fused to the scapula (Figures 25H through 25J) on the larger Dry Mesa scapula-coracoid (BYU 725-12963). The acromion process rises from the entire lateral margin of MWC 6743, as preserved, tapering along the posterior margin towards its distal, broken end. The depth of this scapula, including the acromion process is 49.7 mm (mediolat-

Figure 24. Dorsal ribs from revised hypodigm of *Mymoorapelta*. Left anterior dorsal rib head MWC 3747 in (A) medial, (B) posterior, and (C) anterior views. Left anterior medial dorsal rib MWC 1810 in (D) medial, (E) posterior, and (F) anterior views. Right medial dorsal rib MWC 3763 in (G) anterior, (H) medial, and (I) posterior views. Right medial dorsal rib head MWC 4329 in (J) anterior, (K) medial, and (L) posterior views. Left posterior dorsal rib MWC 1811 in (M) posterior, (N) medial, and (O) anterior views. Left posterior dorsal rib MWC 1840 in (P) posterior, (Q) medial, and (R) anterior views.

eral thickness at the acromion). At this point it is 61.7 mm wide, anteroposterior. Between the acromion process the glenoid is smoothly concave. The area of the glenoid is thickened and smoothly concave. It faces laterally at an angle of about 45˚. The width of the scapula at the glenoid (anteroposterior) is 96.1 mm. The glenoid itself on the scapula is 45.0 mm (mediolaterally). The glenoid is more laterally oriented in the MWC specimen than it is in the isolated fused scapula from the Dry Mesa Quarry.

The Dry Mesa scapula-coracoid is well preserved and undistorted although there is some damage to the posterior margin of the coracoid (Figures 25H through 25J). It was originally described as Ankylosauria indeterminant (Kirkland et al., 1998) but is herein considered to represent a fused scapulocoracoid of *Gargoyleosaurus*, if not *Gargoyleosaurus parkpinorum*, as determined by the morphology of the co-occurring caudal plates (Figure 4). It does not appear as robust as MWC 6743. It is strongly bowed through an arc of approximately 135°, indicating that it came from an animal with a body rounded in cross section. The maximum length of the scapulocoracoid is 414 mm (453 mm along the lateral surface); nearly one-third of the length is made up of the coracoid as observed in *Sauropelta* (Ostrom, 1970; Coombs, 1978a). Both the extreme ends are pitted and rugose indicating both a cartilaginous scapular extension distally and a cartilaginous contact with the sternals proximally.

The scapula is proportionally more slender than that of any known ankylosaur. It has a maximum width of 97.8 mm proximally and a minimum width of the blade of 67.9 mm. It thins from 43.5 mm at the base of the acromion process to 15.1 mm distally. The scapula seems to lack any synapomorphic features of the Nodosauridae. It has

Figure 25. Scapula-coracoids. Partial right distal scapula from revised hypodigm of *Mymoorapelta* MWC 6743 in (A) lateral, (B) cranial, and (C) medial views. Proximal right scapula blade of holotype of *Gargoyleosaurus* DMNH 27726 in (D) lateral and (E) medial views. Proximal right scapula blade of holotype of *Gargoyleosaurus* DMNH 27726 in (F) lateral and (G) medial views. Fused right scapula-coracoid from *Gargoyleosaurus*, Dry Mesa Quarry BYU 725-12963 in (H) lateral, (I) medial, and (J) cranial views. Partial distal scapula from holotype of *Mymoorapelta* MWC 6743 in (D) lateral, (E) cranial, and (F) medial views. Abbreviations: ap = acromium process, cf = corocoid foramen, cvp = cranioventral process, g = glenoid, scs = scapula-corocoid suture.

a low acromian process, 43.3 cm high along the anterior margin of the scapula opposite the glenoid reminiscent of the primitive condition observed in *Mymoorapelta* (Figure 25A) and the Ankylosauridae (Coombs, 1978a; Coombs, and Maryańska, 1990; Vickaryous et al., 2004; Parish, 2005). The glenoid measures 60.0 mm wide across its inner surface.

The coracoid is 154.6 mm long by 119.6 mm wide at the distal margin of the glenoid. The coracoid foramina extends laterally from about 1 cm behind the glenoid just below the suture with the scapula on the medial surface of the coracoid. It is interesting that the more elongate coracoid appears more similar to that of Nodosauridae and the scapula compares best with an ankylosaurid (Coombs, 1978a; Sereno, 1986). However, the coracoids are proportionally much more elongate in nodosaurids *Texasites* (=*Pawpawsaurus*) and *Animantarx* (Coombs, 1995; Carpenter and Kirkland, 1998; Carpenter et al., 1999). A cranioventral process is well developed and is separated from glenoid by a broad subglenoid notch. Although rarely noted, this character is present in *Gastonia* (Kirkland, 1998) and many ankylosaurids, but is largely ab-

sent in nodosaurids (Coombs, 1978a; Coombs and Maryańska, 1990; Vickaryous et al., 2004; Parrish, 2005).

The holotype of *Gargoyleosaurus* preserves the proximal and distal portions of the fused scapulocoracoid (Figures 25D through 25G). The proximal end of the scapula is more expanded than that of the Dry Mesa scapula and was measured at 157 mm wide by Kilbourne and Carpenter (2005). They also measured the coracoid as 154.6 mm long. The cranioventral process is not well developed if the shallow subglenoid notch is restricted to just ventral to the glenoid. Overall, this portion of the coracoid appears to be more like that of the nodosaurid *Sauropelta* (Coombs, 1978a). When viewed together, these differences add support to our idea that the Dry Mesa ankylosaur elements may represent a different species than *Gargoyleosaurus parkpinorum*.

Forelimb

Humerus: The revised hypodigm includes a well-preserved, undistorted right humerus (MWC 6745) that measures 263.5 mm in total length (Figures 26A through 26F). There is some bone missing on the articular surfaces. The humeral head is missing less than 5 mm of bone as can be determined by the unabraded medial portion, which is deeply pitted for the cartilaginous cap. Therefore, the total length of the humerus would be closer to 270 mm if perfectly preserved. Even less bone is missing on the margins of the articular surfaces on the distal end. Coombs (1978b) provides the most comprehensive description of ankylosaur forelimb morphology. Many of the muscle origin and insertion scars are well expressed forming major landmarks in describing the morphology of the bone. There are tooth marks on the bone best exemplified by a series of seven on echelon cuts, 6 to 8 mm long and 3 to 6 mm apart on the posterior surface of the bone below the neck of the shaft.

The proximal margin of the deltopectoral crest is well below the level of the humeral head and is lower than the internal process as in other polacanthids for which the humerus is known; *Polacanthus* NHMUK R1106 (Pereda-Suberbiola, 1994; Blows, 2015) and *Gastonia* BYUVP 14549 (listed as BYU vp136 in Kirkland, 1998, Figure 6F). Thus, the mediolateral width of the proximal end (96. 8 mm) is measured from the lateral margin of the humeral head to the internal process. The head of the humerus measures 73.1 mm across (mediolaterally) and anterior-posteriorly 43.6 mm. The humeral head is in line with the long axis of the humerus as in ankylosaurids, whereas it is inclined more medially in nodosaurids like *Sauropelta* (Coombs, 1978b). It is almost exclusively on the posterior and proximal surface and is scarcely visible anteriorly unlike the well-preserved *Gastonia* humerus from the Dalton Wells Quarry (Figures 27C through 27H). The internal process forms a triangular, medial expansion of the humerus that is separated from the humeral head by a shallow trough sloping down the posterior surface such that it is not visible as a distinct notch in anterior view. This is the opposite case with *Gastonia*.

The maximum mediolateral width of the proximal end of the humerus from the proximal end of the deltopectoral crest to the position of the internal process is 137.5 mm. However, the lateral margin of the deltopectoral crest expands away from the shaft of the humerus, unlike that of *Polacanthus* (Pereda-Suberbiola, 1994; and Blows, 2015) and *Gastonia* (Kirkland, 1998) where it is nearly parallel to the long axis of the humerus. The deltopectoral crest is flexed anteriorly at about 80˚ relative to the long axis of the humeral head as in other polacanthids and nodosaurids, unlike struthiosaurids, ankylosaurids, and stegosaurs (Thompson et al., 2011; Kirkland et al., 2013). The anterior surface on the proximal end of the deltopectoral crest has a deep circular pit about 8 mm across on the anterior margin of the expanded insertion scar for the *scapular* deltoid muscle. The insertion for the *pectoralis* muscle forms a thickened elevated scar on the anterior surface on the distal end of the deltopectoral crest about 18 mm across. Nearly opposite and more medial to this on the posterior surface of the deltopectoral crest is an even greater roughed expansion of more than 20 mm across that marks the insertion for the *scapulohumeralis anterior* muscle. Thus, the distal end of the deltopectoral crest is markedly thicker at as much as 40 mm. A roughen attachment area separates the lower half of the

Figure 26. Forelimb bones from revised hypodigm of *Mymoorapelta*. Right humerus MWC 6745 in (A) cranial, (B) lateral, (C) caudal, (D) medial, (E) proximal, and (F) distal views. Right ulna MWC 1814 in (G) cranial, (H) lateral, (I) proximal, (J) medial, (K) caudal, and (L) distal views. Left ulna MWC 1814 in (M) cranial, (N) lateral, (O) caudal, (P) medial, (Q) proximal, and (R) distal views. Left ulna MWC 5643 and left radius MWC 5643 in articulation in (S) cranial view. Left radius MWC 5438 in (T) cranial, (U) lateral, (V) caudal, (W) medial, (X) proximal, and (Y) distal views. Abbreviations: dp = deltopectoral process, hh = humeral head, lc = lateral condyle, mc = medial condyle, o = olecranon, s = sigmoid notch.

deltopectoral crest from the shaft of the humerus on the posterior side of the humerus instead of the proximally tapering ridge marking this boundary in *Gastonia* and *Polacanthus*. The distal end of the deltopectoral crest extends distally approximately 50% the total length of the humerus.

The shaft of the humerus is waisted between the base of the deltopectoral crest and the distal condyles. At its narrowest, the shaft is 32.9 mm wide (mediolaterally) and is 35.2 mm wide (anteroposteriorly), with a circumference of 111.4 mm. A distinct ridge extends obliquely across its anterior surface from the deltopectoral crest to the margin of the radial condyles as in *Gastonia*, but unlike *Polacanthus* (Blows, 2015; Kinneer et al., 2016). The distal end of the humerus is 112.1 mm (mediolaterally). The lateral (radial) condyle is slightly smaller than the medial condyle and is nearly even with it distally. Although separated by broad depressions anteriorly and posteriorly, no distinct notch separates the distal condyles as in *Polacanthus*, whereas a shallow notch is present in *Gastonia*. Additionally, the medial condyle in *Gastonia* is proportionally much narrower than in *Mymoorapelta*. Lateral to the radial condyle there is an expansion on the lower surface of the humerus for the lateral epicondyle. It is abraded, but clearly less expanded than in *Gastonia* or *Polacanthus*.

Coombs (1978a) noted ankylosaurid humeri could be distinguished from those of nodosaurids in having

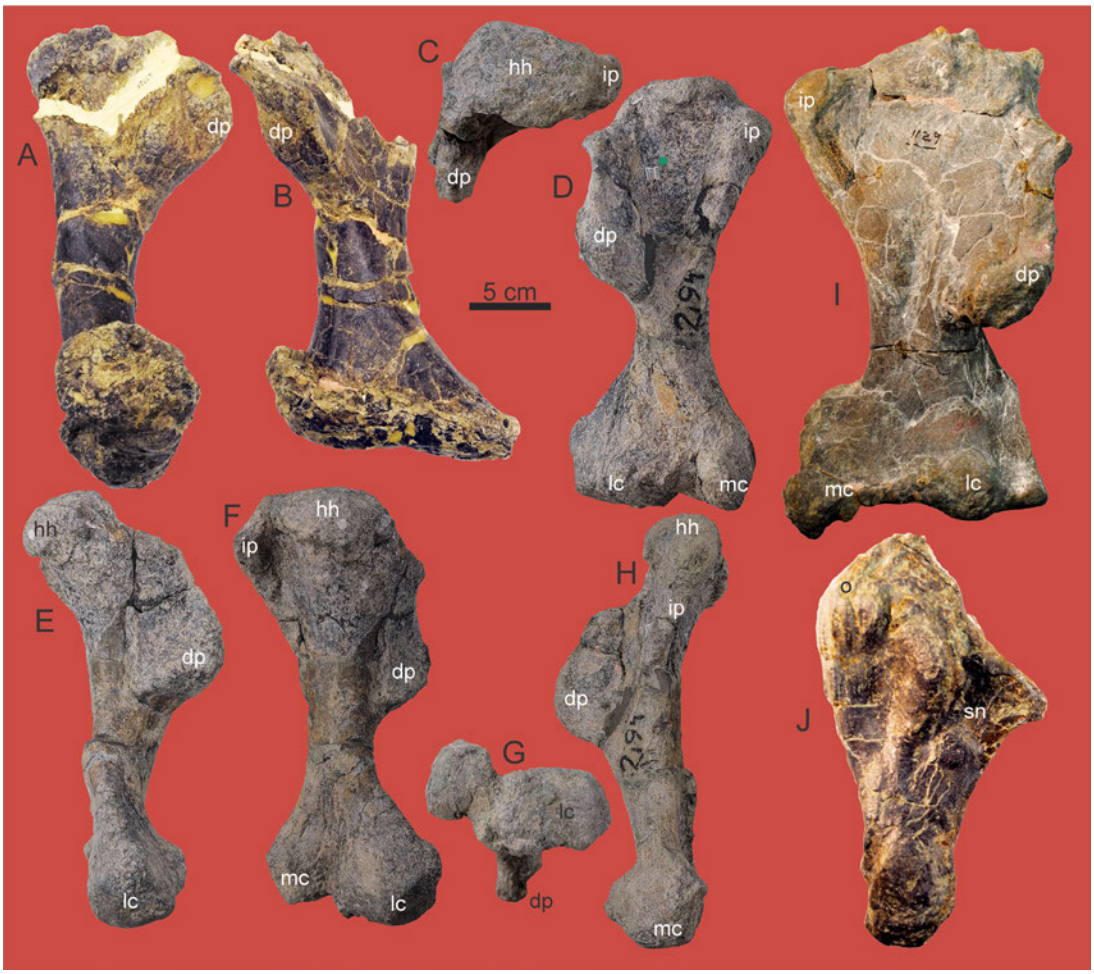

Figure 27. Forelimb of *Gargoyleosaurus* and *Gastonia*. Humerus of holotype of *Gargoyleosaurus* DMNH 27726 in (A) lateral and (B) anterior views. Subadult *Gastonia* right humerus from Dalton Wells Quarry at Utahraptor State Park, north of Moab, Utah, BYU 7510-14549 in (C) proximal, (D) cranial, (E) lateral, (F) caudal, (G) distal, and (H) medial views. *Gastonia* left humerus from Gaston Quarry CEUM 11205 in (I) cranial view. *Gastonia* left ulna CEUM 3565 in (J) lateral view. Abbreviations: dp = deltopectoral process, hh = humeral head, ip = internal process, lc = lateral condyle, mc = medial condyle. o = olecranon, sn = sigmoid notch.

deltopectoral crests extending for 50% of the total length of the humerus with a flattened ovate vs. spherical lateral (radial) condyle. In this, polacanthids, including *Mymoorapelta*, are like ankylosaurids in having a long deltopectoral crest with a flattened radial condyle (Figures 26F and 27G). The known complete polacanthid humeri are essentially identical except, as noted above, and the humeri for *Gastonia* and *Polacanthus* are more robust with more strongly developed muscle attachments suggesting more mature individuals. *Gastonia* (BYU VP 14549) has a minimum circumference of 149.6 mm with a length of 287.5 mm. It is worth noting that most bones in the Gaston Quarry, as exemplified by CEUM 11205 (Figure 27I), are extremely flattened due to compaction, but it is difficult to explain the extremely distal margin of its deltopectoral process purely by compaction. Perhaps this very ankylosaurid trait reflects ontogeny, as this is the largest known *Gastonia* humerus.

The partial humerus from the type specimen of *Gargoyleosaurus* (Figures 27A and 27B) is missing much of its proximal end and the distal end is distorted and, as noted by Kilbourne and Carpenter (2005), perhaps pathological. It is considerably more massively constructed with a minimum circumference of the shaft of 175 mm.

Ulnae: Both the right and the left ulnae are preserved with the expanded hypodigm from the Mygate-Moore Quarry (Figures 26G through 26S). The right ulna, MWC 1814 (Figures 26G through 26L), has a total length of 198.0 mm. It has been figured in previous descriptions of *Mymoorapelta* (Kirkland and Carpenter, 1994, Figure 6; Kirkland et al., 1998, Figures 4A and 4B). It has a massive olecranon. The lateral mar-

gin of the olecranon is slightly damaged, proximally and distally. The height of the olecranon from the base of the articular surface with the humerus is 65.5 mm. The shaft of the ulna is laterally compressed with a width of 18.9 mm, mediolaterally, and is anterolaterally narrowest just above the distal condyles at 25.3 mm. The anterior-lateral width of the ulna at the base of the proximal articular surface is 76.8 mm.

The left ulna, MWC 5438, is better preserved (Figures 26M through 26S) and has a total length of 198.4 mm. The articular surface from the top of the olecranon to the base of the sigmoid notch is 81.7 mm. The maximum width of the anterolateral face of the olecranon is 78.2 mm. The anterior-lateral width of the ulna at the base of the proximal articular surface is 83.9 mm. The distal end of the left ulna flexes slightly towards the radius, and measures 44.6 mm wide (mediolateraly) and is 28.8 mm wide (anterior-posteriorly). The shaft is flattened anterolaterally and measures at its narrowest 19.7 mm wide anteriolaterally by 24.1 mm across posteriolaterally with a minimum circumference of 82.4 mm just above the expansion for the distal condyle.

On both ulnae, the olecranon is highly rugose with a striated texture that strengthens proximally. On both, three well-developed foramina penetrate the bone in a line parallel and just medial to the distinct rim that separates the vertical articular surface with the humerus. The radial notch is open and angled somewhat laterally. A low, rounded ridge extends proximally up to the top of the olecranon lateral to the medial process separating the laterally facing articular surface for the articular condyles of the humerus above the position for the proximal articular surface of the radius. The medial and lateral processes form a broadly obtuse angle of approximately 130˚, with the margin for the radius a raised roughed ridge that would have anchored cartilage and connective tissue. About 20 mm below this boundary there is a raised roughened area possibly for connective tissue that would be opposed to a similar matching roughed area on the radius. Below this, the distal 30 mm is raised and roughened possibly for connective tissue that would be opposed to a similar matching roughed area on the distal end of the radius. The gap formed between these connective tissues between the ulna and radius can only be speculated upon, but the close correlation between these features suggests that there was little mobility between the ulna and radius. About 35 mm above the distal end of the ulna below the lateral process, a strongly developed but small tubercle extends out from the shaft. The margins of the distal end of the ulna are roughed for connective tissue. The distal end is flexed medially. The surface of the distal end is flattened with pitting for the attachment of cartilage.

The ulnae in *Gastonia* (Figure 27J) appear to be considerably more massive with a proportionally large olecranon (Kirkland, 1998; Kilbourne and Carpenter, 2005) as in *Cedarpelta* (Carpenter et al., 2008) and many ankylosaurs (Maryańska, 1977). The more elongate ulnae of *Mymoorapelta* are more similar to those found in *Peloroplites* (Carpenter et al., 2008) and other nodosaurids (Carpenter et al., 1999).

Radius: The well-preserved left radius, MWC 5438 (Figures 26S through 26Y), is 156 mm long. The proximal end is widest anteroposteriorly at 59 mm. In proximal view the flattened proximal end is grooved and pitted to hold the cartilaginous cap and forms an obtuse triangle, with the open angle fitting between the medial and lateral process of the ulna below the radial notch. The proximal end is 39 mm wide, and slopes downward laterally at about 70˚ relative to the shaft, forming a continuous, flat articular surface for the humerus with the top of the medial process of the ulna. About 20 to 25 mm below the obtuse angle formed by the proximal end articulation with the ulna, there is a slightly raised roughed area that may be for connective tissue with ulna, below which, near the distal end there is a second larger raised area for connective tissue matching that on the distal end of the ulna. About 30 mm above the distal end of the radius, below the contact with the end of the medial process of the ulna, there is a strongly developed but small tubercle extending out from the shaft. The shaft of the radius is slender, sub-cylindrical, and 22.5 mm in diameter with a minimum circumference of 67 mm. There is a distinct tuberosity on the lateral side of the radius about 25 mm above the distal condyle near the midpoint of the shaft. The distal end is nearly circular in cross section and

smoothly convex with weak pitting for the cartilaginous cap. It measures 45.4 mm anteriorly-posteriorly and 39.9 mm mediolaterally. The margins are both rugose for connective tissue. The distal end of the radius is angled medially at about 70˚ relative to the shaft, such that the entire radius appears to be skewed laterally. In articulation with the ulna (Figure 26S) and the humerus, the elbow was angled from the vertical by at least 20˚.

Manual elements: Three metacarpals have been identified from the Mygatt-Moore Quarry, two large examples (MWC 10638 and MWC 1816) and one smaller example (MWC 1908). The largest MWC 10638 (Figures 28A through 28G) is proximodistally 48.7 mm long and proximally anteroposteriorly longer (31.0 mm) than wide (25.6 mm). The distal end is twisted 103° relative to the long axis of the proximal end and is 27.4 mm mediolaterally across its articulation and 20.2 mm mediolaterally. The minimum width of the shaft is 13.4 mm. This metatarsal is interpreted to represent metacarpal III by comparison with ankylosaur manus models of Currie et al. (2011) and Senter (2011).

The slightly smaller MWC 1816 (Figures 28H through 28L) is 48.2 mm long, and proximally mediolaterally wider (32.8) mm than deep (19.8 mm). The distal end is twisted much less at about 10° to 15° relative to the proximal end; it is wider than long at 26.9 mm in mediolateral width and 16.2 mm depth. It may represent metacarpal II (Currie et al., 2011; Senter, 2011). The smaller MWC 1908 (Figures 28M through 28R), appears to be a more lateral, metacarpal only 29.9 mm long. Its proximal end is more symmetrical at 21.3 mm wide and 17.1 mm deep. The distal end is 17.8 mm wide and 12.3 mm deep. It may represent metacarpal V. (Currie et al., 2011; Senter, 2011).

There are two manual phalanges, MWC 1817 (Figures 28S through 28X) and 3613 (Figures 28Y through 28CC), identified. Most significantly are their extremely short lengths, less than a cm each, and near symmetrical convex distal and concave proximal ends. There is one possible manual ungual, MWC 939 (Figures 28TT through 28XX). Superficially it is similar to the pedal unguals. However, it is acutely pointed at its distal end (as opposed to rounded as in the pedal unguals) and it is asymmetric mediolateral. It is 39.6 mm long and 19.6 mm deep at its articulation.

Pelvic Girdle

Ilium: In the initial description of *Mymoorapelta maysi* (Kirkland and Carpenter, 1994), the ilium, MWC 1815 (Figures 29A through 29F), was designated the holotype specimen for the species. Even with the expanded hypodigm for the species presented here, this ilium is the most unique individual bone in *Mymoorapelta* with its near rectangular shape in dorsal view and its long ventrally enrolled preacetabular process. MWC 1815 has a total anteroposterior length of 530 mm and horizontal width of 127 mm, at the position of the acetabulum. Given the downward flexure of the preacetabular process, the ilium's width is nearly the same front and back. There is no evidence of any distortion in the preservation of this bone and the vertically enrolled preactetabular process appears to be unique among Ankylosauria.

Ventrally (Figure 29F), the length from the anterior margin of the pubic peduncle to the posterior margin of the ischial peduncle is 164 mm. The width of the acetabulum between these peduncles (as expressed on the ilium) is 115 mm. The length of the opening of the acetabulum is estimated at 59.5 mm. The mediolateral depth of the acetabulum is 53 mm. The post-pubic length of the ilium from the center of the acetabulum is 192.3 mm making the length of the post-acetabular about equal to that of the length of the acetabulum. The pre-acetabular length of the ilium from the center of the acetabulum is 347.5 mm. The post-acetabular portion of the ilium is decidedly thicker from the ischial peduncle to the posterior margin. It is about as long as the length of the acetabulum as in polacanthids and nodosaurids (Lull, 1921). The depth of the ilium at the pubic peduncle (from the top if the ilium) is 125.4 mm. The depth of the ilium at the ischial peduncle (from the top of the ilium) is 69.8 mm. The acetabulum was open unlike that of other ankylosaurs (Coombs, 1978a; Coombs, and Maryańska, 1990; Vickaryous et al., 2004; Parrish, 2005)

The length of attachment with the sacral yoke extends from near the posterior margin of the prepubic process, posteriorly for 209.5 mm. It is estimated that there were three sacral rib attachments and one caudal rib attachment in this sacral yoke. Looking anteriorly, there is no specific scar for the first dorsal-sacral rib.

Figure 28. Manual and pedal elements from revised hypodigm and referred specimens of *Mymoorapelta*. Metacarpal MWC 10638 in (A) dorsolateral, (B) dorsal, (C) medial, (D) ventral, (E) lateral, (F) dorsal, and (G) ventral views. Metacarpal MWC 1816 in (H) ventral, (I) lateral, (J) medial, (K) proximal, and (L) distal views. Metacarpal MWC 1908 in (M) ventral, (N) lateral, (O) medial, (P) dorsal, (Q) proximal, and (R) distal views. Possible manual phalanx MWC 1817 in (S) dorsal, (T) lateral, (U) proximal, (V) ventral, (W) medial, and (X) distal views. Possible manual phalanx MWC 3616 in (Y) medial, (Z) ventral, (AA) lateral, (BB) proximal, and (CC) distal views. Metatarsal possibly from right pes MWC 4028 in (DD) ventral, (EE) medial, (FF) lateral, (GG) proximal, and (HH) distal views. Pedal phalanx MWC 3615 in (II) dorsal, (JJ) ventral, (KK) lateral, (LL) medial, (MM) proximal, and (NN) distal views. Pedal phalanx MWC 1932 in (OO) ventral, (PP) lateral, (QQ) medial, (RR) proximal, and (SS) distal views. Possible manual ungual MWC 939 in (TT) dorsal, (UU) proximal, (VV) ventral, (WW) lateral, and (XX) other lateral views. Pedal ungual MWC 6728 in (YY) dorsal, (ZZ) proximal, (AAA) ventral, (BBB) lateral, and (CCC) other lateral views. Pedal ungual MWC 3752 in (DDD) dorsal, (EEE) proximal, (FFF) ventral, (GGG) lateral, and (HHH) other lateral views. Pedal ungual MWC 3714 in (III) dorsal, (JJJ) proximal, (KKK) ventral, (LLL) lateral, and (MMM) other lateral views. Pedal ungual MWC 8237 in (NNN) dorsal, (OOO) proximal, (PPP) ventral, (QQQ) lateral, and (RRR) other lateral views.

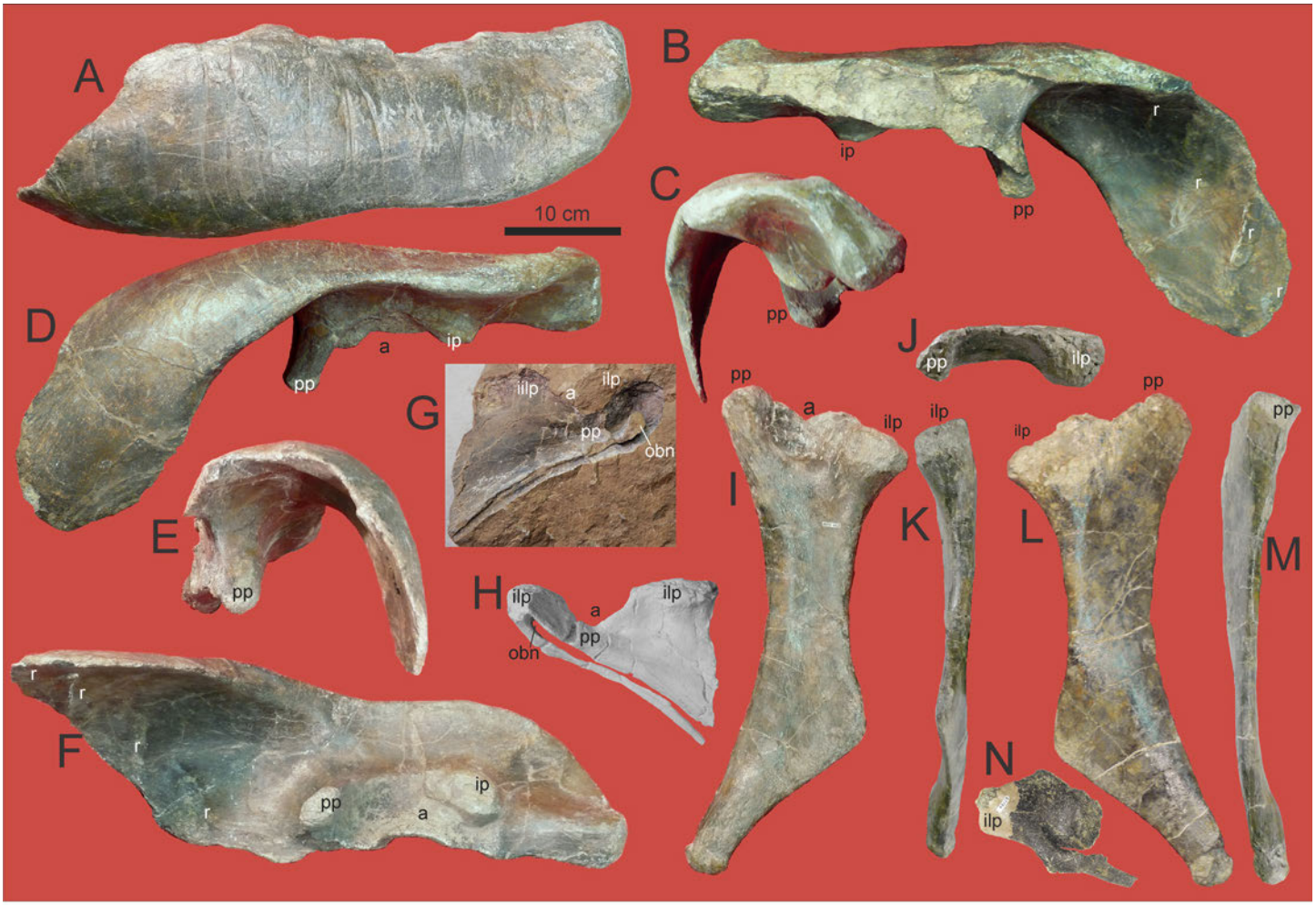

Figure 29. Pelvic girdles. Holotype *Mymoorapelta* right ilium MWC 1815 in (A) dorsal, (B) medial, (C) caudal, (D) lateral, (E) cranial, and (F) ventral views. Lateral side of articulated proximal ischium and pubis of Cactus Park *Mymoorapelta* MWC 2610 in (G) eternal mold and (H) latex peal. Referred right ischium MWC 4027 in (I) lateral, (J) proximal, (K) caudal, (L) medial, and (M) anterior views. Right pubis of holotype of *Gargoyleosaurus* DMNH 27726 in (N) lateral view. Abbreviations: a = acetabulum, iilp = ilial peduncle of ischium, ilp = ilialpeduncle of pubis, ip = ischial peduncle, obn = obturator notch, pp = pubic peduncle, r = rib scars on preacetabular portion of ilium by overlapping distal dorsal ribs.

However, anterior to this rib position, there is thickening of the ventral surface of the ilium and a scar for the attachment of each of the three more anterior ribs under this ventral side. The most anterior of these has the distal end of the rib still attached; these ribs are approximately 54 mm apart. Given that spacing, the next rib in the series would have been along the anterior margin of the ilium (Figures 29B and 29F).

The dorsal surface of the ilium (Figure 29A) is crossed by dozens of grooves interpreted as representing tooth marks of a predatory dinosaur, in keeping with the hypothesis that the neural spines of the dorsal vertebrae were bitten off (Kirkland and Carpenter, 1994; Kirkland et al., 1998). Similar grooves were noted on the dorsal surface of the Bexhill "*Polacanthus*," but were interpreted as representing a natural feature of unknown purpose but perhaps in relation to the overlying sacral shield in polacanthids (Blows and Honeysett, 2014b; Blows, 2015). Further study of these grooves is warranted.

Although no ilia were preserved with the type specimen of *Gargoyleosaurus parkpinorum*, a complete right ilium 559 mm long with attached synsacrum from

a larger individual (DMNH 58831) was assigned to *Gargoyleosaurus* based on comparison of its cervical ring (Carpenter et al., 2013). Several significant differences deserve to be pointed out. The preacetabular process is not nearly as enrolled laterally and angles away from the main axis of the ilium at about 30° (Figure 19). The post-acetabulum is proportionally shorter, such that the length of the post-acetabular is about one half the length of the acetabulum as in more derived ankylosaurids (Coombs, 1978b; Carpenter et al., 2013).

Ischium: A well-preserved left ischium, MWC 4027 (Figures 29I through 29M), was recovered with the type material, but its large size may indicate that it may pertain to the larger referred individual. The ischium has a total length of 404.5 mm. The width across the proximal end is 159.3 mm; between the peduncles, the slightly damaged opening of acetabulum measured approximately 72 mm. The pubic peduncle is smaller than the iliac peduncle and is somewhat subtriangular in shape. The pubic peduncle is flattened overall, somewhat trapezoidal in shape tapering to the edge of the open acetabulum.

The ischium has a distinct bend about two-thirds of its length down the shaft. The upper portion of the ischium above the bend narrows slightly to 67.7 mm, at the bend it has widened to 99.4 mm, and the bend is 250.7 mm below the proximal end along the posterior margin. The distal length of the posterior margin of the ischium below the bend is 176.2 mm, and the distal end of the ischium is slightly expanded and measures 37.1 mm anteroposteriorly and 24.3 mm mediolaterally.

The lateral margin above the distal end of the ischium is thickened and rugose, with an attachment area that extends all the way up along the medial posterior boundary to the bend in the ischium, which is expanded and rugose for the *rectus abdominis* and the *ischiocaudalis* (Coombs, 1979). The attachment scar for the *ischio-trochantericus* starts above the terminal expansion and runs proximally up the lateral side of the posterior margin, just to and just above the bend on the ischium. The scar for the *adductor femoris* is not as well marked but is found along the anterior margin extending from well above the bend in the ischium at approximately the narrowest part of the upper ischium and to within less than 100 mm of the pubic peduncle.

The expanded width of the ischium at the bend makes the overall ischium look less bent than is typical in nodosaurids (Coombs, 1978a). However, in nodosaurids, the ischium does not expand at the bend. This ischium is most similar to that of *Gastonia burgei* (Kirkland, 1998; Kinneer et al., 2016); however, it is narrower at the bend in *Gastonia*. Additionally, in *Gastonia lorriemcwhinneyae* the thinner ischium is smoothy curved as in nodosaurids (Kinneer et al., 2016). The angular bed in the ischium of *Mymoorapelta* and *Gastonia burgei* is reminiscent of that of many stegosaurs (Galton and Upchurch, 2004; Maidment et al., 2015) and may well be a shared character that documents this as the primitive character state in Ankylosauria with the straight ischium of ankylosaurids the derived character state (Kirkland, 1998; Kirkland et al., 2013).

There is a lateral mold of proximal portion of a right ischium in articulation with a right pubis preserved in a sandstone block (Gaston et al., 2001) from the Cactus Park *Mymoorapelta*, MWC 2610 (Figures 29G and 29H). Though adding little to the morphological description of the ischium, its articulation with its pubis lends considerable support to the documentation that *Mymoorapelta* maintained an open acetabulum.

Pubis: Although no pubis is preserved in the type material of *Mymoorapelta*, the lateral mold of the Cactus Park *Mymoorapelta*, MWC 2610 pubis (Figures 29G and 29H) provides valuable information as to the morphology of the pubis in *Mymoorapelta*. The right pubis is preserved with the holotype of *Gargoyleosaurus* (Figure 29I) and was described in detail by Kilbourne and Carpenter (2005). The pubis of *Mymoorapelta* and *Gargoyleosaurus* are morphologically similar to each other in that the main body is subrectangular and is smooth where it makes up a portion the acetabulum. The slender postpubic process extends from near the center of the main body in both, and both bear a small ventrally situated triangular flange. The post acetabulum is more complete in *Mymoorapelta* and extends ventrally along the length of the preserved portion of the ischium (Figures 29G and 29H). An elongate postpubic process is also recognized in *Kun-*

barrasaurus from the Lower Cretaceous of Australia, although it is highly reduced in most other ankylosaurs where known (Molnar, 1996; Vickaryous et al., 2004; Parrish, 2005; Raven, 2021; Raven et al., 2023).

Hindlimb

Femur: The hind limb is poorly known in *Mymoorapelta* and *Gargoyleosaurus*. Only the femur is known in the type material of *Gargoyleosaurus* (Kilbourne and Carpenter, 2005). At 465 mm long and with a shaft 193 mm in circumference, it is robustly constructed and primitive in maintaining a well-separated femoral head and anterior trochanter. It is refigured herein (Figures 30A through 30E) largely for completeness and to provide contrast to the smaller tibia and the type specimen of *Mymoorapelta*, MWC 6746 (Figures 30F through 30I). An unprepared femur is present with the Cactus Park *Mymoorapelta*, MWC 2610.

Tibia: A partial left tibia is preserved at the Mygatt Moore Quarry, MWC 6746 (Figures 30F through 30I). Overall, it compares well with the partial tibia DMNH 15162 (Figures 30J through 30M) from Garden Park, Colorado. It is 251.3 mm long and damaged both proximally and distally. The proximal end is damaged around the entire proximal margin and the proximal surface is flat (slightly convex) and slopes posterolateral. The distal end on the side medial to the contact with the astragalus is broken off. As with other ankylosaurs, the tibia is expanded on both ends, with the long axis of the distal articulation twisted about 70° laterally, relative to the proximal end. The shaft is narrow with a 36.2 mm mediolateral width, with the narrowest anterior-posterior width of 33.9 mm a bit lower on the shaft. A slight notch is on the lateral margin of the tibia distally for the articulation of the fibula. The astragalus is not fused to the tibia. In nearly all features this tibia compares well with an isolated tibia DMNS 15162 (Figures 30J through 30M) from Garden Park described in Kirkland et al. (1998).

Pes: One metatarsal, MWC 4028 (Figures 28DD through 28HH), was collected. It is tentatively identified as the third and is 90.1 mm long. Its proximal end is subrectangular, deeper at 54.6 mm tall, and 25.4 wide indicating that proximally, the metatarsals were closely appressed on either side. The posterior articulation slopes posteriorly. The distal end is asymmetric.

There are two proximal phalanges. MWC 3615 (Figures 28II through 28NN) is 31.8 mm in length and is asymmetric (anterior medially). MWC 1932 (Figures 28OO through 28SS) is 26.3 mm in length. It has a larger proximal articulation than MWC 3615 and is less mediolateral asymmetric.

There are four pedal unguals (Figures 28YY through 28RRR). They are wedge shaped in lateral view with evenly rounded termination. The largest of these, MWC 3714 (Figures 28III through 28MMM), has a maximum dorsal length of 48.3 mm, a proximal height of the articulation of 26.9 mm, and is damaged on both lateral margins. The best-preserved pedal ungual (MWC 3752) is only slightly smaller at 45.1 mm long (Figures 28DDD through 28HHH). The proximal articulation is 20.1 mm high and 24 mm wide. Its surface is fairly rugose, and in dorsal view has a blunt 'arrowhead' shape with strong vascular grooves on either side of the attachment point of the claw. The unguals are similar to those of nodosaurids such as *Sauropelta* (Ostrom, 1970) and *Niobrarasaurus* (Carpenter et al., 1995), and are proportionally longer than those of ankylosaurids such as *Dyoplosaurus* (Arbour et al., 2009) and *Pinacosaurus* (Currie et al., 2011). The partial manus reported for the type specimen of *Dracopelta* from the Upper Jurassic of Portugal (Pereda-Suberbiola et al., 2004) has been reinterpreted as a pes based on its short blunt unguals, phalangeal formulas, and the presence of other right hindlimb elements, namely a partial femur, and tibia and fibula (Russo and Mateus, 2021; Russo, 2024).

There is a partial articulated pes from the Cactus Park *Mymoorapelta* MWC 2610 (Figure 31). It is interpreted to represent a right pes prepared in dorsal view on the sandstone block in which it is preserved. Metatarsal one is considered to missing with the preserved metatarsal tentatively identified as representing two through five. A single tarsal is preserved and overlaps the proximal articular surfaces of metatarsals two and three. As with the preserved third metatarsal of the type specimen MWC 4028 the proximal end of metatarsal three is narrow. The numbers of pedal digits in ankylo-

Figure 30. Hindlimb bones. Holotype femur of *Gargoyleosaurus* DMNH 27726 in (A) proximal, (B) anterior, (C) lateral, (D) posterior, and (E) posterior views. *Mymoorapelta* revised hypodigm partial left tibia MWC 6746 in (F) anterior, (G) lateral, (H) medial, and (I) posterior views. Distal right tibia from Garden Park DMNH 15162 in (J) anterior, (K) lateral, and (L) posterior views, and MWC 6746 (M) distal view. Abbreviations: 4th = Fourth trochanter, a = depression for astragulas, at = anterior trochanter, cn = cnemial crest, h = femoral head, lc = lateral condylus, mc = medial condylus.

saurids are only known for a few taxa and vary between and within species (Currie et al., 2011) and as such is a difficult character to utilize in phylogenetics.

Dermal Skeleton

All thyreophorans are characterized by an extensive covering of large scales underlain by dermal bone (osteoderms) forming transverse bands that are commonly recovered in the fossil record (Brown, 1908; Coombs, 1971, 1978a; Martill et al., 2000; Arbour et al., 2014; Arbour and Evans, 2017; Brown, 2017; Brown et al., 2017; Norman, 2020c). However, although we are confident that the overall pattern of scales is present

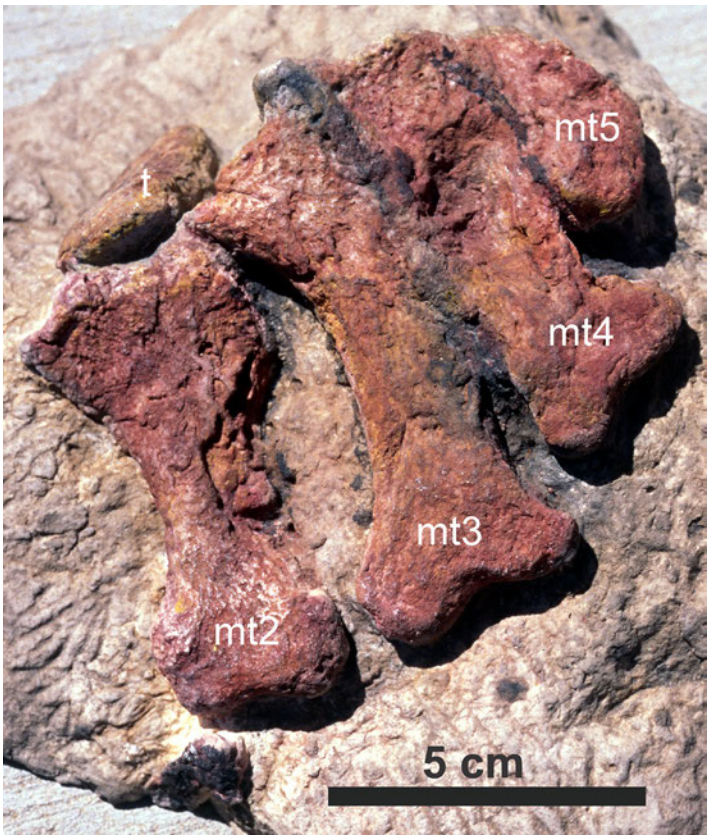

Figure 31. Cactus Park *Mymoorapelta* partial left pes MWC 2610 in dorsal view. Abbriviations: mt2 = second metatarsal, mt3 = third metatarsal, mt4 = fourth metatarsal, mt5 = fifth metatarsal, t = tarsal.

when the young thyreophoran first hatches from its egg (Stanford et al., 2011), the overall ontogenetic history of thyreophoran osteoderms beyond the early ossification of the cervical rings in the ankylosaur *Pinacosaurus* (Hill et al., 2003; Burns et al., 2011, Burns, 2015) is unknown. In most ankylosaurs, there are no midline osteoderms, and the transverse bands (rows) are formed of flat or low keeled elements along each side of the midline, which become more spinose or plate-like laterally. Large, erect, dorsal spines are an exception and are only known in a few taxa such as the derived Polacanthinae *Polacanthus* (ex. Blows, 2015) and *Gastonia* (Kirkland, 1998; Kinneer et al., 2016), and the European Struthiosaurinae Nodosauridae, *Struthiosaurus* (Nopcsa, 1929; Ösi and Pereda-Suberbiola, 2017) and *Hungarosaurus* (Ösi and Makádi, 2009; Ösi and Pereda-Suberbiola, 2017).

Superficially basal thyreophoran osteoderms in *Scutellosaurus* are smooth with fine pits and short irregular grooves on the order of a mm across (Main et al., 2005). A similar appearance is characteristic of *Mymoorapelta* osteoderms (Kirkland and Carpenter, 1994; Kirkland et al., 1998). Although it has been noted that the surface of polacanthid ankylosaurs is smooth, the fine pitting and grooving on the surface of *Mymoorapelta* osteoderms has not been noted. However, in *Gargoyleosaurus* (Kilbourne and Carpenter, 2005), *Gastonia* (Kirkland, 1998; Blows, 2015; Kinneer et al., 2016), and *Hoplitosaurus* (Bodily, 1969) the surface of the osteoderms is considerably smoother. Blows (1987, 2015) considered *Polacanthus* osteoderms to have an overall coarser surface texture than any of the other polacanthid.

Structurally, Polacanthid osteoderms are closer to basal thyreophoran osteoderms like those of *Scutellosaurus* and *Scelidosaururs* in having a well-developed external and internal cortex with structural fibers surrounding a remodeled trabecular core that may be from 50% to 80% of the total thickness of the osteoderm (Scheyer and Sanders, 2004; Burns, 2010; Burns and Currie, 2014). Nodosaurids differ in having a very thin or no internal cortex, whereas ankylosaurids have proportionally thinned the entire osteoderm retaining both external and internal cortex with some including Haversian bone in their cores (Scheyer and Sander, 2004; Burns and Currie, 2014). Both *Gargoyleosaurus* (Hayashi et al., 2010) and *Mymoorapelta* (Burns and Currie, 2014) fit this model well (Figure 32). As with basal thyreophorans, both *Gargoyleosaurus* and *Mymoorapelta* have concave bases (Scheyer and Sanders, 2004; Hayashi et al., 2010; Burns and Currie, 2014), However most ankylosaurs assigned to the Polacanthinae have flatter, less concave bases (Blows, 2015). A very large polacanthine from the Poison Strip Member of the Lower Cretaceous Cedar Mountain Formation of Utah has thickened dorsal osteoderms with decidedly convex bases (Bodily, 1969). Similar massive dorsal osteoderms with convex bases are also present in *Hoplitosaurus marshi* from the Lower Cretaceous Lakota Formation of South Dakota (Gilmore, 1914, Figure 70).

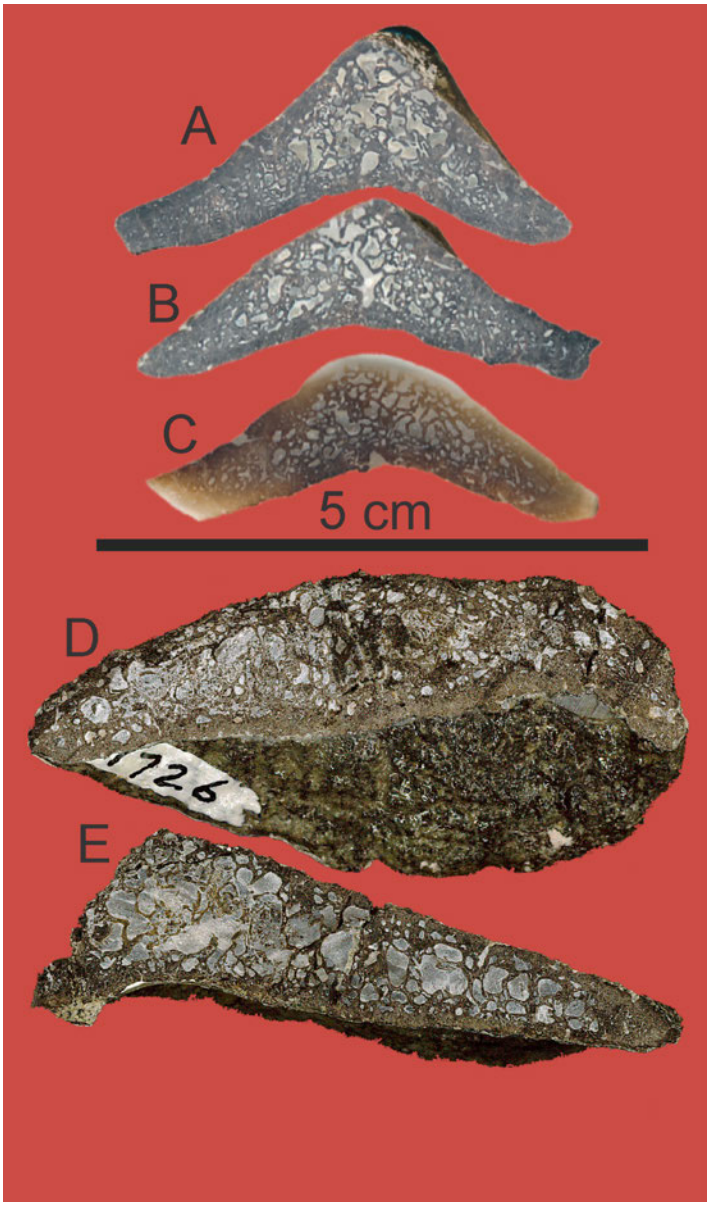

Figure 32. Osteoderm histology. *Mymoorapelta* dorsal osteoderm MWC 7064 (A and C) part and counterpart of cut osteoderm. (B) Thin section. *Gargoyleosaurus* dorsal osteoderm DMNH 27726 (D and E) part and counterpart of cut osteoderm.

Osteoderm is used in reference to nearly all dermal elements of the fossils described herein, with the term ossicle for simple ovoid dermal bones of approximately 1 cm or less in diameter following (Burns and Currie, 2014). Cervical half rings may be fused or unfused for Jurassic polacanthids. Dorsal armor is ventrally concave with larger crested subrectangular- to teardrop-shaped elements interpreted to be situated anteriorly, with smaller, more posterior dorsal osteoderms more circular in outline with low crest or low apical prominence. The larger osteoderms in the sacral region are also round with low apical prominences surrounded by fused ossicles. Simple elongate crested osteoderms are considered to be situated on the legs, along the tail, and/or on the lateral margins of the body posterior to the posteriorly grooved shoulder spines and anterior to the sacral-caudal plates. The bases of the grooved shoulder spines and sacral caudal plates are deeply excavated with medial vascular openings a few mm in diameter (Kirkland et al., 1998).

Generally, the form and arrangement of osteoderm are assumed to be of taxonomic significance (e.g., Coombs, 1978a; Ford, 2000; Burns, 2008), but they have rarely and only recently been applied to phylogenetics (Vickaryous et al., 2004; Arbour and Currie, 2016; Raven, 2021; Raven et al., 2023; Russo, 2024).

Cervical ring elements: Several osteoderms from the cervical rings of *Mymoorapelta* have been recovered from the Mygatt-Moore Quarry (Figure 33). To properly describe the cervical armor of *Mymoorapelta,* it is important to consider the morphology of basal ankylosaur cervical armor in a phylogenetic sense. Ankylosaurs cervical rings are made up of three pairs of cervical osteoderms fused to a band of underlying dermal bone in adult animals. Ankylosaurids possess two full cervical rings and nodosaurids possess three cervical rings divided at the midline (Penkalski, 2001; Vickaryous et al., 2004). *Scelidosaurus* primitively has five to six cervical rings consisting of three pairs of osteoderms with deeply interdigitating sutures based on examining the cast of David Sole's (amateur British collector) specimen exhibited in St. George, Utah SGDS 1311 described by Norman (2020c). The fused cervical rings in derived ankylosaurs consist of cervical osteoderms fused to a band formed of subdermal connective tissue (Arbour and Currie, 2013a, 2016). Osteoderms pertaining to the cervical rings of *Mymoorapelta* are recognized by the presence of ossified connective tissues attached to the base of these osteoderms (Figure 33) with that of the lateral spines orig-

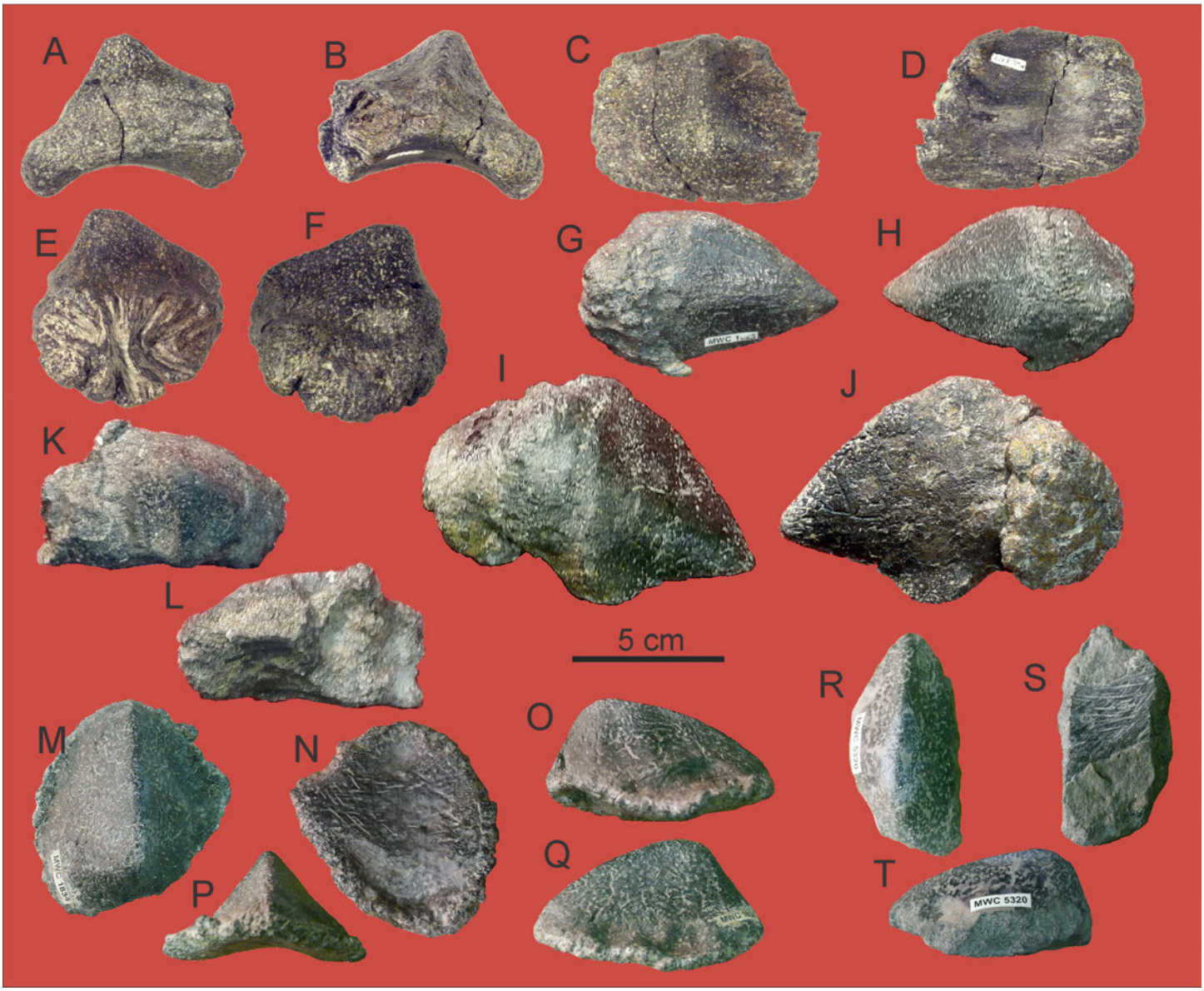

Figure 33. Cervical osteoderms from revised hypodigm of *Mymoorapelta*. Possible first cervical half ring section MWC 6977 in (A) posterior, (B) anterior, (C) dorsal, (D) ventral, (E) lateral, and (F) medial views. Possible second cervical spine MWC 1825 in dorsal (G) and (H) ventral views. Possible third cervical spine MWC 6752 in (I) dorsal and (J) ventral views. Anterior medial cervical half ring fragment MWC 3744 in (K) dorsal and (L) ventral views. Cervical or perhaps anterior dorsal osteoderm MWC 1834 in (M) dorsal, (N) ventral, (O) lateral, (P) posterior, and (Q) other lateral views. Cervical ring fragment MWC 5320 in (R) dorsal, (S) ventral, and (T) lateral views.

inating from the base of spines (Figures 33G through 33J) as in *Gastonia* (Figures 34I, 34K, and 34L).

Gargoyleosaurus was found with parts of two cervical rings (Figures 34A through 34D) that are more completely preserved than those of *Mymoorapelta*. The articulated skeleton of *Dracopelta* from the Upper Jurassic of Portugal has three cervical rings (Russo, 2024). Given the general incompleteness of the type specimen of *Gargoyleosaurus*, it cannot be discounted that a third ring is missing in this specimen. Kilbourne and Carpenter's (2005) interpretation that the first cervical ring of *Gargoyleosaurus* included a single, medial

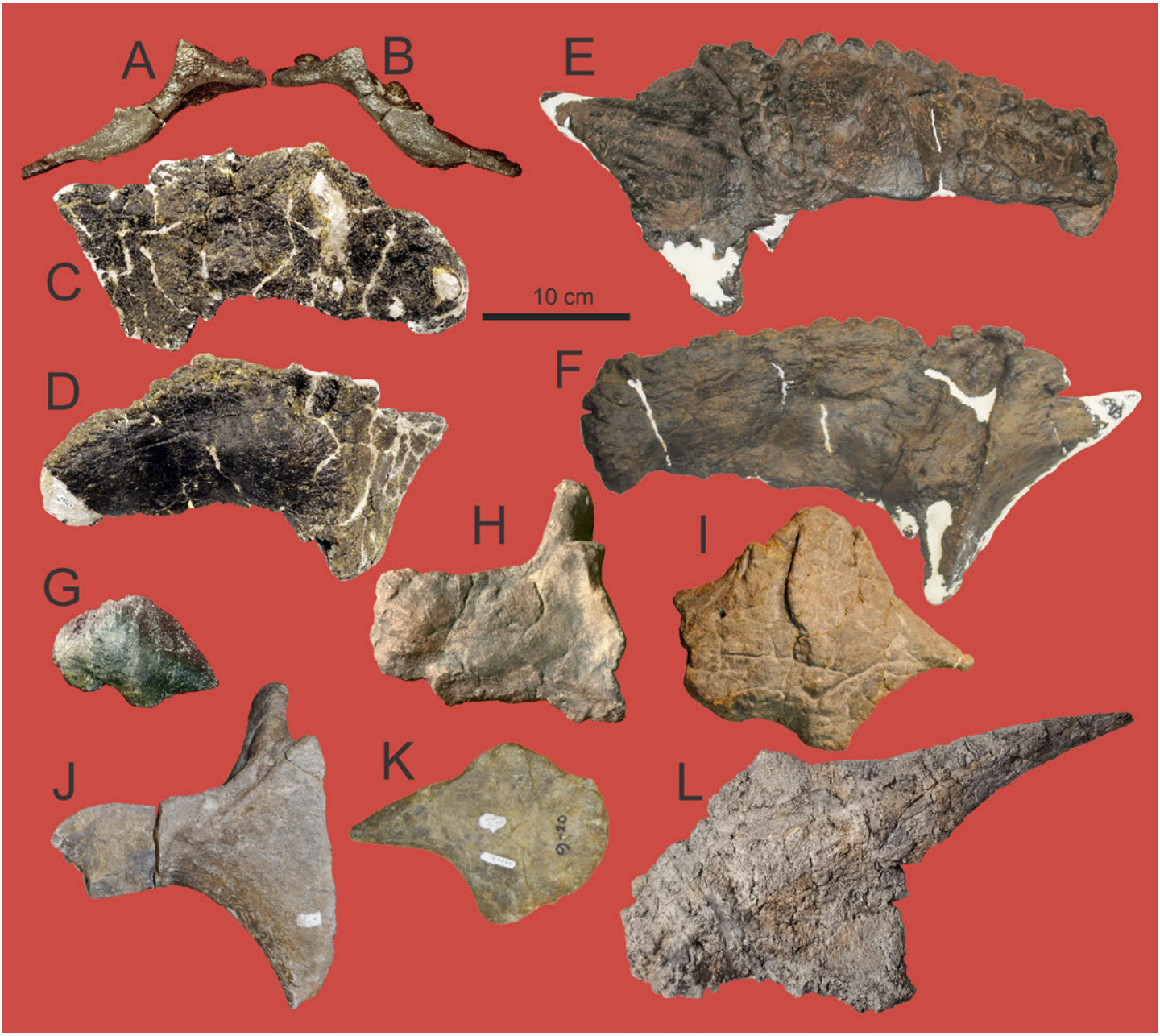

Figure 34. Comparison of cervical osteoderms. (A through D) *Gargoyleosaurus* DMNH 27726. Part and counterpart of cut first right quarter ring, (A and B) and right second quarter ring in (C) dorsal and (D) ventral views. Second right quarter ring of *Gargoyleosaurus* from Simon Quarry DMNH 58831 in (E) dorsal and (F) ventral views. *Mymoorapelta* second lateral cervical spine MWC 6753 in (G) dorsal view. *Gastonia burgei* first cervical ring CEUM 1212 in (H) dorsal view. *Gastonia burgei* second or possibly third lateral cervical spine CEUM 1215 in (I) dorsal view. *Gastonia lorriemcwhinneyae* large first cervical ring DMNS 45665 in (J) dorsal view. *Gastonia lorriemcwhinneyae* second lateral cervical spine DMNS 49698 in (K) ventral view. *Gastonia lorriemcwhinneyae* third lateral cervical spine, "splate" DMNS 57635 in (L) ventral view.

osteoderm unlike any previously described ankylosaur has been substantiated by the identification of a similar midline osteoderm on the midline of the first cervical ring of *Dracopelta* (Russo, 2024). Unfortunately, no lateral spines are preserved with the cervical rings of *Dracopelta*.

Based on this interpretation, *Gargoyleosaurus* had a minimum of two cervical rings as in ankylosaurids but not joined at the midline as in a nodosaurids. Each half ring was ventrally concave to conform to the neck and was thickest where each major osteoderm came together. The larger half ring (Figure 34C) from the midline out was formed of the small scute with a central apex followed by a keeled scute two to three times larger, and a triangular plate sticking out laterally from the neck and, although forming a nearly equilateral triangle, was recurved anteriorly. Small ossicles are fused to the dorsal surface of the ring on the margins and intermediate to these larger elements in the larger second ring from the Simon Quarry (Figures 34E and 34F). Note, that the cervical ring section figured for *Tianchisaurus nedegoapeferima* from the Middle Jurassic of Northwestern China is superficially like those of *Gargoyleosaurus* (Dong, 1993). In *Mymoorapelta*, the cervical rings may represent a less mature stage of development as the major elements are not fused together. However, it is important to recognize that fully fused cervical rings are not known for any polacanthine taxon (e.g., *Gastonia* [Kirkland, 1998; Blows, 2015; Kinneer et al., 2016]).

The extensive collection of *Gastonia lorriemcwhinneyae* from the type locality at the DMNH includes multiple examples of each of three types of lateral cervical spines (Kinneer et al., 2016).

1. A somewhat triangular spine attached to a curved basal ring of connective tissue that would have wrapped around the neck just posterior to the back of the skull (Figure 34J). This spine is interpreted as lining up with the postorbital boss at the back of the skull. The spine would angle anteriodorsally, whereas the same spine in *Gastonia burgei* (Figure 34H) would angle out more horizontally. These are interpreted as representing lateral spines of the first cervical ring.
2. A broad spine (Figure 34K) with a moderately elongate tip that appears to be longer than those identified as comparable in *Gastonia burgei* (Figure 34I). Ossified connective tissue extends out of the base of these spines and are considered to be analogous to the lateral spines preserved in the half rings of *Gargoyleosaurus*. These spines are interpreted as representing the lateral spines of the second cervical ring.
3. A narrow, elongated spine with a broad base (Figure 34L) matches the morphology of the splates (spine-plates) in *Polacanthus* and *Hoplitosaurus* (Gilmore, 1914, Plate 28; Blows, 1987, 2001, 2015; Pereda-Suberbiola, 1993, 1994; Blows and Honeysett, 2014b). This cervical spine morphology is not recognized in *Gastonia burgei*. Blows (2015) interpreted these as being from the shoulder region, but herein, we propose that these as representing the lateral spines of the third cervical ring.

It is not possible to assign the dorsal osteoderms to specific cervical rings in *Mymoorapelta*, but we can propose the placement of the lateral cervical elements to specific rings. Kilbourne and Carpenter (2005) mistakenly interpreted that the solid blade-like plates (spines) of *Mymoorapelta* as not represented in *Gargoyleosaurus*; however, we recognize them as representing the unfused lateral plates of *Mymoorapelta*'s cervical rings (Blows, 2015). These cervical spines are similar to those of the second ring in *Gastonia* (Kirkland, 1998, Figures 7A through 7D) (Figures 34I, 34K, and 34L). Their dorsal surfaces and thus orientation are recognized by the presence of small ossicles fused to their bases on their dorsal side as in *Gargoyleosaurus*.

The first cervical ring in *Mymoorapelta* may be represented by MWC 6977 (Figures 33A through 33F) and the second cervical ring is 56.0 mm wide anterioposteriorly at the apex of the scute and about 47 mm thick. The line marking a separation between the keratin-covered external portion of the scute and the internal ring of bone is best developed along the posterior margin. The medial of element, where it would articulate with the next more lateral scute, has a deep and complexly fluted surface similar to that observed between adjoining cervical elements in the *Scelidosaurus*, SGDS 1311.

The small biconvex cervical plate, MWC 1825 (Figures 33G and 33H), is interpreted as possibly representing the lateral spine of a right cervical half ring.

The anterior edge is longer and more convexly arcuate. Weak ridges about 0.5 cm apart extend from the base of the dorsal surface and toward the apex. One small ossicle fused to the posterior margin of the base appears as a small subsidiary spine. This cervical plate is 51.1 mm wide at its exposed base, 27.9 mm thick, and extended outward 59.4 mm. Blows (2001) speculated that this plate may represent one of the spines (his "tricorn") from immediately behind the skull in *Scelidosaurus* (Norman, 2020c).

The larger cervical spine (MWC 6752) is interpreted to represent the lateral spine of the third cervical half ring. This cervical spine is 76.6 mm wide anteroposteriorly at its exposed base, 34.4 mm thick, and extended outward 76.0 mm and, thus, while thicker, it is similar in size (Figure 34G) to the lateral spine on the smaller (Figures 4A and 4B) versus the larger cervical ring (Figures 34C and 34D) of the *Gargoyleosaurus* type specimen (Kilbourne and Carpenter, 2005). The plate is nearly flat on the dorsal surface and convex on the ventral surface and is convexly arcuate anteriorly and slightly concave posteriorly. Very weak ridges nearly 1 cm apart extend from the exposed base toward the apex of the plate on its dorsal surface. Similar ridges are more strongly expressed in the lateral cervical spine of the largest cervical half ring of *Gargoyleosaurus* from the Simon Quarry (Figures 34E and 34F) and are not expressed at all in *Gastonia*.

Blows (2015, Figure 7.10) suggested that elongate ridged spines attached a basal plate of connective tissue from the Compton Bay *Polacanthus* (NHMUK PV R9293) and represent upright cervical spines oriented at 90° to the interpreted orientation of the cervical spines discussed here. Laterally oriented cervical spines such as described here for *Mymoorapelta*, *Gargoyleosaurus*, and *Gastonia*, differ strongly from the cylindrical, upright cervical spines that occur in *Struthiosaurus* (Seeley, 1881) and *Hungarosaurus* (Ösi et al., 2019).

It is assumed that the more medial dorsal cervical osteoderms are oriented, so the "medial" ridge or keel (Burns, 2008) is more laterally positioned with its apex positioned posteriorly (Figures 33M through 33T). The smaller of the cervical osteoderms (MWC 3744) is ventrally broken along its posterior and lateral side. However, the separation between the keratin-covered external portion of the scute and the internal ring of bone is apparent anteriorly. Medially, small intermediate ossicles are present along the broken margin. It is 44.8 mm wide anteroposteriorly at the apex of the scute and 46.3 mm thick.

We hypothesize that the initial origin of the cervical bands in ankylosaurids would have been from the ossification of the connective tissues originating from the base of the lateral cervical spines of primitive ankylosaurs like *Mymoorapelta*. Cervical rings with spinose lateral plates are not characteristic of ankylosaurids (Coombs, 1978a; Coombs and Maryańska, 1990; Vickaryous et al., 2004; Parrish, 2005) and some nodosaurids such as *Stegopelta* (Carpenter and Kirkland, 1998), *Silivaurus* (Eaton, 1960; Carpenter and Kirkland, 1998), and *Panoplosaurus* (Carpenter, 1990), whereas they characterize many nodosaurids such as *Sauropelta* (Carpenter, 1984; Carpenter and Kirkland, 1998), *Edmontonia* (Carpenter, 1990), and *Borealopelta* (Brown, 2017; Brown et al., 2017) and struthiosaurids such as *Struthiosaurus* (Seeley, 1881; Nopcsa, 1929; Pereda-Suberbiola and Galton, 2001) and *Hungarosaurus* (Ösi, 2005; Ösi et al., 2019).

Dorsal osteoderms: The first fossils of *Mymoorapelta* recognized at the Mygatt-Moore Quarry as an ankylosaur from the Morrison Formation were three dorsal osteoderms recovered in August of 1989 (Figures 35N, 35O, and 35DD through 35GG). Subsequently, many osteoderms attributed to the dorsal surface of *Mymoorapelta* have been recovered from the site for which the 36 best-preserved examples are figured here to show the breadth of anatomy displayed by these osteoderms (Figure 35). Largely, dorsal osteoderms are identified as having a base length longer than the height of the osteoderm. Whereas most of these osteoderms are attributed to the back of *Mymoorapelta* overlying the ribs, some may have been from tail and the legs.

Some large subrectangular to ovate osteoderms are interpreted to be from the shoulder region (Figures 35A through 35M) like those in many nodosaurids (Lambe, 1919; Russell, 1940; Carpenter, 1990; Brown, 2017; Brown et al., 2017), struthiosaurids (Ösi, 2005; Kirk-

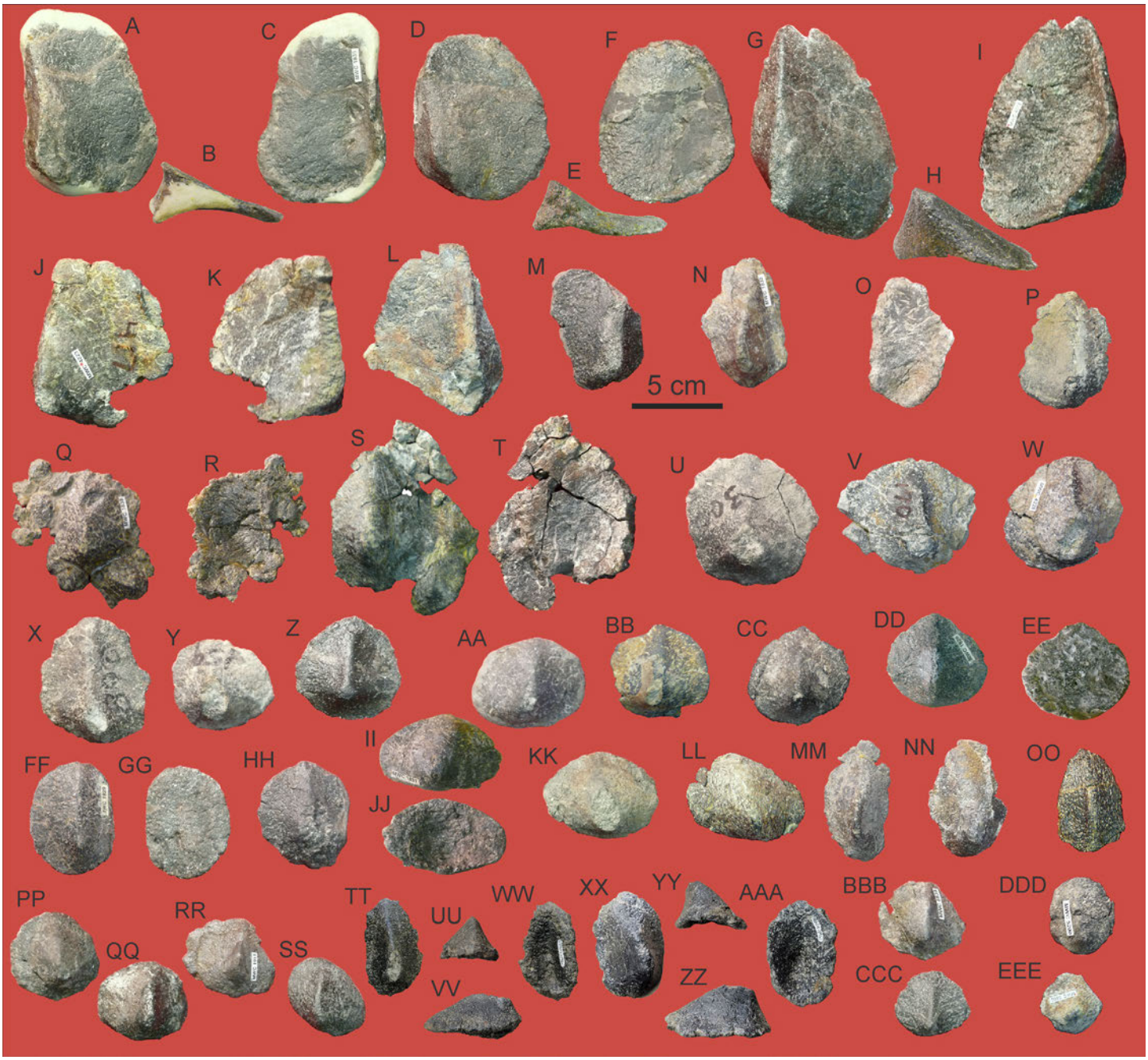

Figure 35. Caption is on the following page.

land et al., 2013; Ösi et al., 2019) and at least some ankylosaurids (Carpenter, 2004; Arbour and Currie, 2013b, Arbour and Mallon, 2017). Large, subrectangular osteoderms are not present in the shoulder region of *Dracopelta* (Russo and Mateus, 2021; Russo, 2024). The hypothetical orientation on *Mymoorapelt*a's dorsal shoulder osteoderms is based on the orientation of osteoderms on the backs of other ankylosaurs where they are preserved in situ such as *Edmontonia* (Matthews, 1922) and *Borealopelta* (Brown, 2017; Brown et al., 2017). These osteoderms are somewhat longer anteroposteriorly than wide and narrow anteriorly with

Figure 35 is on the revious page. Dorsal osteoderms from revised hypodigm of *Mymoorapelta*. Anterior dorsal osteoderm MWC 1835 in (A) dorsal, (B) caudal, and (C) ventral views. Anterior dorsal osteoderm MWC 1836 in (D) dorsal, (E) caudal, and (F) ventral views. Anterior dorsal osteoderm MWC 4018 in (G) dorsal, (H) caudal, and (I) ventral views. Anterior dorsal osteoderm MWC 4223 in (J) dorsal and (K) ventral views. Anterior dorsal osteoderm MWC 4030 in (L) dorsal view. Smaller possible anterior dorsal osteoderm MWC 6761 in (M) dorsal view. Smaller possible anterior dorsal osteoderm MWC 1832 in (N) dorsal and (O) ventral views. Smaller possible anterior dorsal osteoderm MWC 6753 in (P) dorsal view. Section of fused sacral shield MWC 1838 in (Q) dorsal and (R) ventral views. Section of fused sacral shield MWC 6751 in (S) dorsal and (T) ventral views. Dorsal osteoderm MWC 6762 in (U) dorsal view. Dorsal osteoderm MWC 6755 in (V) dorsal view. Dorsal osteoderm MWC 4228 in (W) dorsal view. Dorsal osteoderm MWC 6768 in (X) dorsal view. Dorsal osteoderm MWC 6767 in (Y) dorsal view. Dorsal osteoderm MWC 6769 in (Z) dorsal view. Dorsal osteoderm MWC 6763 in (AA) dorsal view. Dorsal osteoderm MWC 4029 in (BB) dorsal view. Dorsal osteoderm MWC 5016 in (CC) dorsal view. Dorsal osteoderm MWC 1826 in (DD) dorsal and (EE) ventral views. Dorsal osteoderm MWC 1829 in (FF) dorsal and (GG) ventral views. Dorsal osteoderm MWC 6766 in (HH) dorsal view. Dorsal osteoderm MWC 1831 in (II) dorsal and (JJ) ventral views. Dorsal osteoderm MWC 6759 in (KK) dorsal view. Dorsal osteoderm MWC 6764 in (LL) dorsal view. Elongate dorsal osteoderm MWC 6754 in (MM) dorsal view. Elongate dorsal osteoderm MWC 4196 in (NN) dorsal view. Elongate dorsal osteoderm MWC 6765 in (OO) dorsal view. Dorsal osteoderm MWC 6760 in (PP) dorsal view. Dorsal scute MWC 6757 in (QQ) dorsal view. Dorsal osteoderm MWC 1911 in (RR) dorsal view. Dorsal osteoderm MWC 6756 in (SS) dorsal view. Elongate "hollow" osteoderm MWC 10487 in (TT) dorsal, (UU) anterior, (VV) lateral, and (WW) ventral views. Elongate "hollow" osteoderm MWC 10486 in (XX) dorsal, (YY) anterior, (ZZ) lateral, and (AAA) ventral views. Dorsal osteoderm MWC 5838 in (BBB) dorsal view. Dorsal osteoderm MWC 6758 in (CCC) dorsal view. Dorsal osteoderm MWC 5200 in (DDD) dorsal view. Small dorsal osteoderm MWC 3860 in (EEE) dorsal view.

a laterally situated keel that comes to a low apex at the posterior margin of the osteoderm. The base of these osteoderms are deeply excavated under the posterior apex of this keel. Many of the larger dorsal osteoderms of nodosaurids are distinctly different, having tear-drop or comma shapes with the posteroventral depression extending beyond the ventral margin of the osteoderm into the overhanging apex of the medial keel (Lambe, 1919; Burns, 2008).

Smaller oval to nearly circular osteoderms are typically about 50 mm or less in diameter and are more abundantly associated with the holotype of *Mymoorapelta* (Figures 35U through 35EE). In these, the crest with its posterior apex is more medially oriented. These are interpreted to form rows on the back of *Mymoorapelta* anterior to the sacrum. It is possible that some of the more anteroposteriorly elongate forms were situated on the dorsal surface of the tail (Figures 35MM through 35OO and 35TT through 35AAA). There is no evidence for the abundant interstitial ossicles characteristic of the polacanthine ankylosaurs from the Cedar Mountain Formation (Kirkland, 1998; Kinneer, et al., 2016; Kirkland et al., 2016).

Although there were fewer curated examples, a similar array of dorsal osteoderms (Figure 36) are documented for the holotype of *Gargoyleosaurus.* Similar large osteoderms from the shoulder region (Figures 36A through 36L) are present as are smaller osteoderms (Figures 36Q through 36AA) that would have formed rows farther back dorsally on the type specimen of *Gargoyleosaurus* (Kilbourne and Carpenter, 2005).

Large (2023) identified the ankylosaur specimen from the Hanksville-Burpee Quarry (Figure 1) as *Gargoyleosaurus* based on a distinct depression of the dorsal osteoderms lateral to the medial keel. This depression is apparent on the larger dorsal osteoderms, but not so much on the smaller, more posterior osteoderms (Figure 36), so we consider this identification tentative, basically considering the limited diagnostic skeletal material associated with this specimen to date. However, we do agree that dorsal osteoderms, particularly when examined in a large population of elements, may well be of taxonomic importance. The many dorsal osteoderms from the Compton Bay *Polacanthus*, NHMUK PV R9293 (Blows, 1987, 2015), appear to be diagnostic in

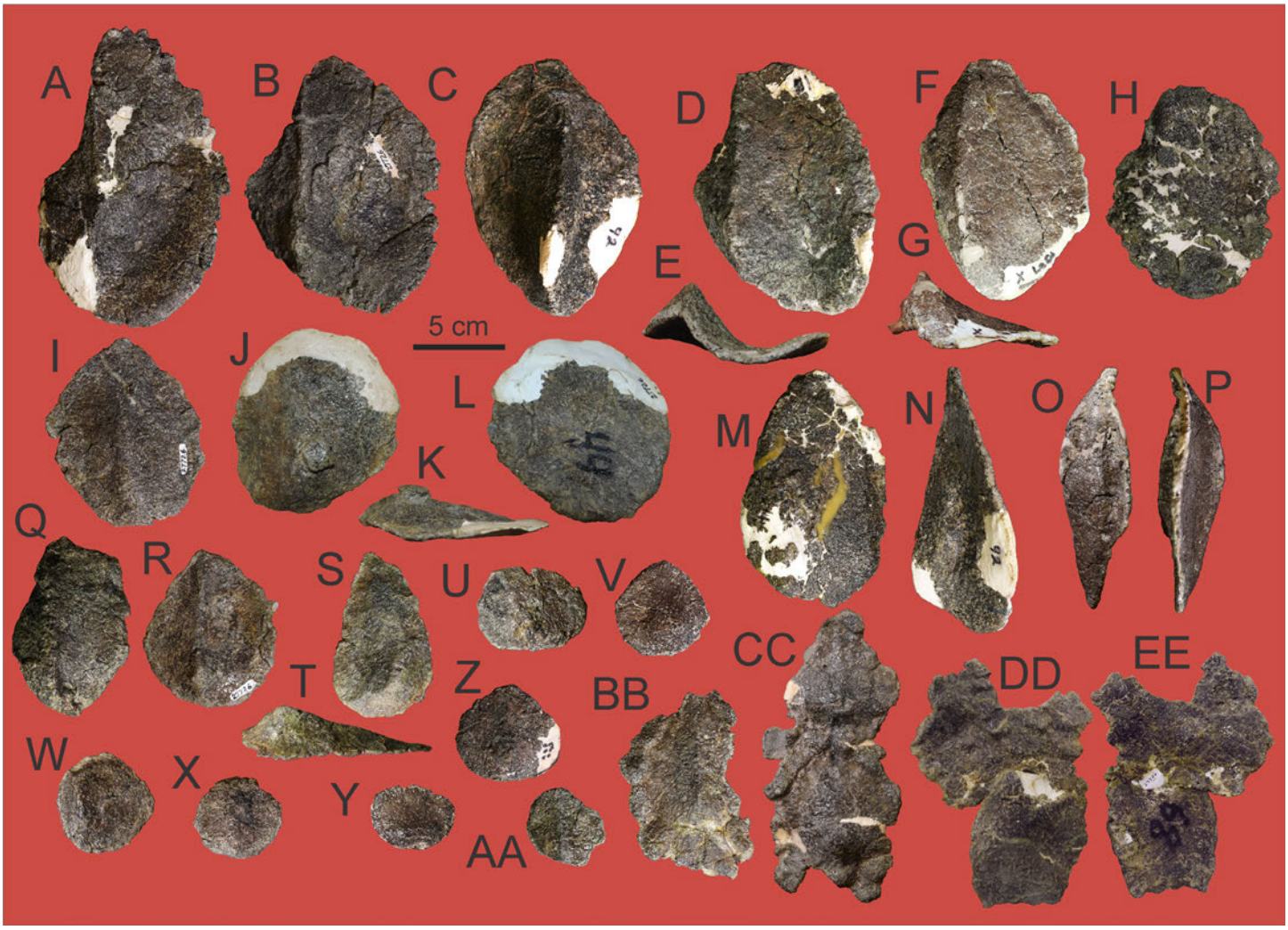

Figure 36. Dorsal osteoderms from holotype of *Gargoyleosaurus parkpinorum*. Large dorsal osteoderms from shoulder region in dorsal views (A through C). Large dorsal osteoderm from shoulder region in (D) dorsal and (E) posterior views. Large dorsal osteoderm from shoulder region in (F) dorsal and (G) posterior views. Large dorsal osteoderms in dorsal view (H and I). Large dorsal osteoderm in (J) dorsal, (K) lateral, and (L) ventral views. Elongate osteoderms (M through P). Dorsal osteoderms in dorsal views (Q, R, and U through AA). Dorsal osteoderms in (S) dorsal and (T) lateral views. Fragments of sacral shield in dorsal view (BB and CC). Portion of sacral shield in (DD) dorsal and (EE) ventral views.

also having a depression lateral to the keel and having a distinct ridge around the margin of the osteoderm. These features are not present in the holotype of *Polacanthus foxi*, NHMUK PV R175 (Blows, 2015), supporting the separation of these specimens proposed by Raven et al. (2020). Likewise, the bases of the larger dorsal osteoderms (including dorsal spines) are surrounded by a circumference marked by radial ridges and grooves in *Gastonia burgei* that are not present in *Gastonia lorriemcwhinneyae* (Kirkland, 1998; Kinneer et al., 2016).

There are no examples of massive dorsal spines in *Mymoorapelta*, *Gargoyleosaurus* (Kilbourne and Carpenter, 2005), and *Dracopelta* (Russo, 2024) as have been documented in derived polacanthids such as *Gastonia*, *Hoplitosaurus*, and *Polacanthus* (Gilmore 1914; Blows, 1987, 2015; Pereda-Suberbiola, 1993, 1994; Kirkland, 1998; Kinneer et al., 2016) and possibly in *Nodosaurus* (Lull, 1921).

Sacral shield: A sacral shield of fused osteoderms across the pelvic area was once thought to be a unique characteristic of polacanthine ankylosaurs (Blows, 1987; Pereda-Suberbiola, 1994; Kirkland, 1998; Ösi and Pereda-Suberbiola, 2017; Carpenter, 2001) but is now acknowledged to be widespread across various ankylosaur clades (Arbour et al., 2011, 2014; Raven, 2021; Raven et al., 2023). Arbour et al. (2011) defined a sacral or pelvic shield as a continuous carapace of osteoderms, not forming transverse bands, extending across the ilia and sacrum of an ankylosaur and noted that they were represented by three distinct morphologies:

1. unfused osteoderms in the form of rosettes but not coossified,
2. fused osteoderm rosettes, and
3. coossified polygonal osteoderms of fairly uniform size.

Rosettes are defined by larger osteoderms isolated from each other by bands of smaller ossicles. Type 2 sacral shields appear to be restricted to polacanthid ankylosaurs, whereas the other sacral shield types are found in both ankylosaurid and nodosaurid clades (Arbour et al., 2011).

Both the type specimen of *Mymoorapelta* (Figures 35Q through 35T) and the type specimen of *Gargoyleosaurus* (Figures 36BB through 36EE) only preserve portions of what can best be described as partial rosettes of incompletely fused sacral shields (Kirkland et al., 1998; Kilbourne and Carpenter, 2005). It would be a logical conclusion to assume that these taxa did not process fully formed sacral shields, particularly as no fully formed sacral shields have yet been recognized for either species of *Gastonia* (Kirkland, 1998; Kinneer et al., 2016). However, a fully formed sacral shield is preserved in sandstone blocks associated with the pelvic region of the Cactus Park *Mymoorapelta* specimen (Figure 37). Although, mostly represented by external molds, the fossils seem to indicate that the sacral shield was constructed of large osteoderms like the isolated presacral osteoderms from the holotype of *Mymoorapelta* arranged in anteroposterior directed rows surrounded by small ossicles (Kirkland, 1999; Blows, 2015). Larger osteoderms may have been arranged along the lateral margins (Figure 37A). The specimens suggest that a fully fused sacral shield was developed in mature or even gerontic individuals of both *Mymoorapelta*, *Gargoyleosaurus*, and *Gastonia*. It is worth noting that *Dracopelta* also processed a fully developed sacral shield (Russo, 2024).

The sacral shield of *Polacanthus foxii* had a more irregular arrangement of larger osteoderms across the center of the shield although clearly laterally large, slightly elongate osteoderms ran along its lateral and posterior margins (Hulke, 1888; Pereda-Suberbiola, 1994; Blows, 2015; Raven et al., 2020). The larger osteoderms on the sacral shield sections of *Gastonia burgei* are distinctive in that, like its larger dorsal osteoderms, they are surrounded by a circumference marked by radial ridges and grooves that are absent in *Gastonia lorriemcwhinneyae* (Kirkland, 1998; Kinneer et al., 2016).

Shoulder spine: A single beautifully preserved left shoulder spine, MWC 1816 (Figures 38A through 38D), is known from the type material of *Mymoorapelta*; it was described and figured in Kirkland and Carpenter (1994) and Kirkland et al. (1998). Its anterior length is 284.6 mm, and its posterior length is 219.1 mm. As in *Gargoyleosaurus*, *Gastonia*, *Polacanthus*, and *Hoplitosaurus,* it has a wide posterior groove 10 to 15 mm deep that extends from the apex to the base of the spine, giving the spine a triangular cross section unlike any of the plates described below. The spine is 57.1 mm wide below the posterior groove. The excavated attachment area extends up the spine posteriorly such that the spine is interpreted to be reclined at an angle of about 45˚ relative to the base length (135.5 mm) of the attachment area. About the first 40 mm of the anterior edge is more vertically oriented before inclining posteriorly. As with the majority of the caudal plates there are weak ridges 12 to 14 mm apart on the dorsal face of the spine that extend from the base distally before fading away about halfway to the apex of the spine. The ridges do not converge on the apex of the spine but maintain their spacing such that they would intersect with the ante-

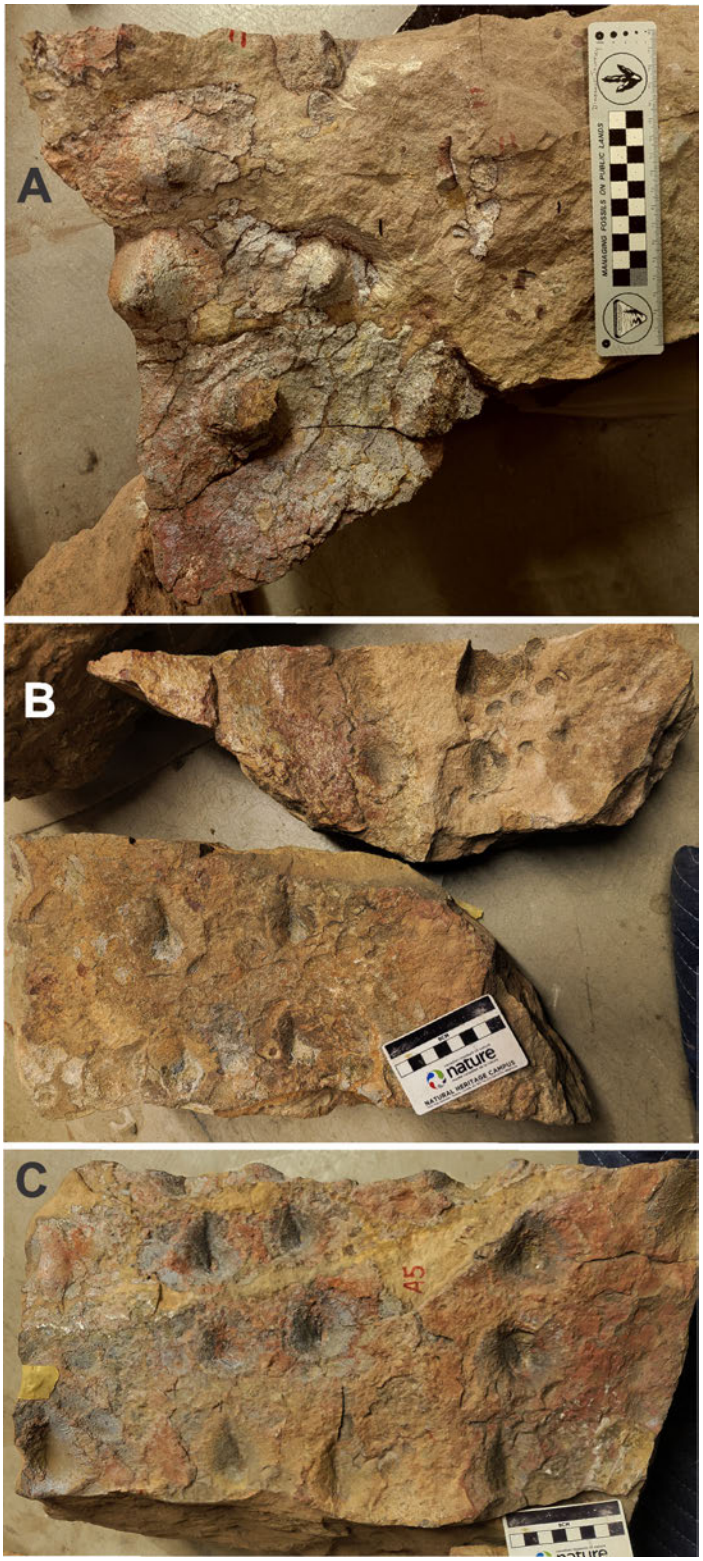

Figure 37. Cactus Park *Mymoorapelta* sacral shield sections MWC 2610. (A) Lateral portion of sacral shield. (B and C) Sandstone blocks preserving external molds of the dorsal sacral shield.

rior margin of the spine if they did not vanish on the surface first. The ridges are best developed posteriorly.

Two grooved shoulder spines (Figures 38E through 38H) are present among the elements preserved with the type specimen of *Gargoyleosaurus* (DMNH 27726) (Kilbourne and Carpenter, 2005). Although both are more reclined with a narrower posterior groove and lack dorsal ridges, their general morphology is strikingly similar to that of the *Mymoorapelta* shoulder spine. Both were initially described as right shoulder spines as they appeared to be articulated (Kilbourne and Carpenter, 2005), but we interpret only the longer, more erect spine (Figures 38E and 38F) as being from the right side, whereas the lower, even more reclined spine (Figures 38G and 38H) as being from the left side of the animal. We are in agreement that there was a minimum of two pairs of posteriorly grooved shoulder spines in *Gargoyleosaurus*. The question remains as to whether there was a more erect shoulder spine like that preserved in *Mymoorapelta* situated more anteriorly and is missing in the type material of *Gargoyleosaurus*. Certainly, it is likely that there was more than one pair of shoulder spines of this morphology in *Mymoorapelta*. The possible *Gargoyleosaurus* material from the Dry Mesa Quarry includes a posteriorly grooved shoulder spine, BYU 725-17351 (Figures 38I and 38J). Although not so well preserved, this spine compares well with the longer, more erect of the two spines from the type specimen of *Gargoyleosaurus*.

Grooved shoulder spines are not known from the type specimen of *Polacanthus foxii* (Hulke, 1882; Pereda-Suberbiola, 1993, 1994; Raven et al., 2000; Blows, 2015), the Compton Bay *Polacanthus* (Blows, 1987, 2015), or *Hylaeosaurus* (Blows, 2015; Raven et al., 2020). However, two isolated grooved shoulder spines have been recovered from the Lower Cretaceous Wessex Formation on the Isle of Wight, England (Delair, 1982; Blows, 2015). The type material of *Hoplitosaurus marshi* from the Lakota Formation includes a well-preserved right grooved shoulder spine 330 mm long (Gilmore, 1914, Plate 29). It is more erect like MWC 1816, has a broken off apex, and is more massive. Grooved shoulder spines are well represented in *Gastonia* with at least ten from *Gastonia lorriemcwhinneyae*

Figure 38. Grooved shoulder spines. Left lateral grooved shoulder spine from revised hypodigm of *Mymoorapelta maysi* MWC 1818 in (A) caudal, (B) dorsal, (C) medial, and (D) ventral views. *Gargoyleosaurus parkpinorum* holotype grooved shoulder spines DMNH 27726. Right shoulder spine in (E) dorsal and (F) ventral views. Left shoulder spine in (G) dorsal and (H) ventral views. Dry Mesa *Gargoyleosaurus* right lateral grooved shoulder spine BYU 725-17351 in (I) caudal, (J) ventral, and (K) dorsal views.

in the collections of the DMNH ranging from somewhat erect to recumbent (Kirkland, 1998; Kinneer et al., 2016), suggesting that a minimum of three pairs of this spine form in the shoulder region of at least North America's polacanthids.

Caudosacral plates: There are at least 17 dorsoventrally thin, hollow-based, recurved, asymmetrical, triangular plates (Figure 39, Table 3). As with the large grooved shoulder spine, it is assumed that the point of the triangle recurved posteriorly. These plates are similar in appearance to those in *Polacanthus* (Hulke, 1882; Blows, 1987, 2015; Pereda-Suberbiola, 1993, 1994; Gasulla et al., 2011; Raven et at., 2020). Similar plates are present in *Gargoyleosaurus* (Kilbourne and Carpenter, 2005) and *Gastonia* (Kirkland, 1998; Kinneer et al., 2016), and are believed to be mostly lateral caudal plates. Lateral caudal plates are widely distributed in the Ankylosauria (Seeley, 1881; Ostrom, 1970; Arbour et al., 2009, 2013; Kirkland et al., 2013; Arbour and Currie, 2016; Arbour and Evans, 2017; Norman, 2020c). All caudal plates are biconvex in cross section, although the dorsal side is more so than the ventral side. The biconvexity of the spines results in sharp anterior and posterior margins.

There are nine complete "typical" inclined caudal plates (Figures 39A through 39S). In addition, there are three specimens (MWC 6747, 6748, and 6750) that were not figured as they were only represented by the distal 100 to 120 mm apical portion of the plate. As with *Polacanthus,* the larger plates are assumed to be positioned more proximally along the tail. In dorsal profile, the anterior edge of the plate is convex and is longer than the posterior concave edge. The result is that the apex of the plates overhangs the posterior margin of the base. The bases of the plates are hollow, and the rims are asymmetrical, similar to those of the neck spine. In all but one plate, the most proximal point of the basal rim of the fluted side is more posterior than that of the rim of the other side; this gives the plate its asymmetrical appearance. The base length of the caudal plates (Table 3) would appear to overlap with approximately two caudal vertebrae. As in the cervical spine, the caudal plates also have several nutrient foramina 3 to 4 mm across along the midline of the deeply hollow base (e.g., Figure 39H). On the most convex (dorsal) side, there is faint, parallel fluting 1 to 1.5 cm apart with the ridge in the position of 4th to 6th from the posterior margin curving back to the apex of the plate. As the ridges are parallel with each other, anterior ridges would impinge on the anterior edge of the plate and more posterior ridges would impinge on the posterior edge. However, these ridges vanish before reaching the margin of the plate. Three smaller plates (Figures 39Z through 39EE) with longer base lengths (Table 3) are assumed to be caudal plates from the more distal tail.

Two plates, MWC 1824 and 2677 (Figures 39V through 39Y), appear to represent a matched pair of plates. They are in the same size range as the laterally inclined caudal plates (Figures 39A through 39S) but have a proportionally longer base length relative to the height of the plate (Table 3). Otherwise, they are nearly morphologically identical to the inclined caudal plates of *Mymoorapelta* (Kirkland et al., 1998). It is hypothesized that this pair of plates was situated laterally along the posterior margin of the sacral shield area. Similar plates have been identified in several ankylosaurids (Arbour, 2009; Arbour et al., 2009, 2013; Carpenter et al., 2011; Park et al., 2021) and possible in *Sauropelta* (Carpenter and Kirkland, 1998).

One plate fragment, MWC 2868 (Figures 39T and 39U), has the base broken away and a relatively broad symmetrical apex. The dorsal surface appears fairly convex and the basal surface is flat. It is relatively smooth and unornamented. Although assumed to be situated laterally on *Mymoorapelta*, there is no evidence as to where such a plate would be situated.

Proximal caudal plates appear to have taxonomic potential (Morgan et al., 2016); as in a population of specimens the plates have distinctively different shapes in dorsal view (Figure 40). The external molds of the caudal plates from the Cactus Park ankylosaur (Figure 40) compare well with those of *Mymoorapelta* (Figure 39). Along these lines, the caudal plates from the type specimen of *Gargoyleosaurus* (Figures 41A through 41P) are clearly distinct from those of the type material of *Mymoorapelta* (Kilbourne and Carpenter, 2005), in that, the apexes of the plates are only slightly posterior to the posterior margin of the plate or even anterior to it.

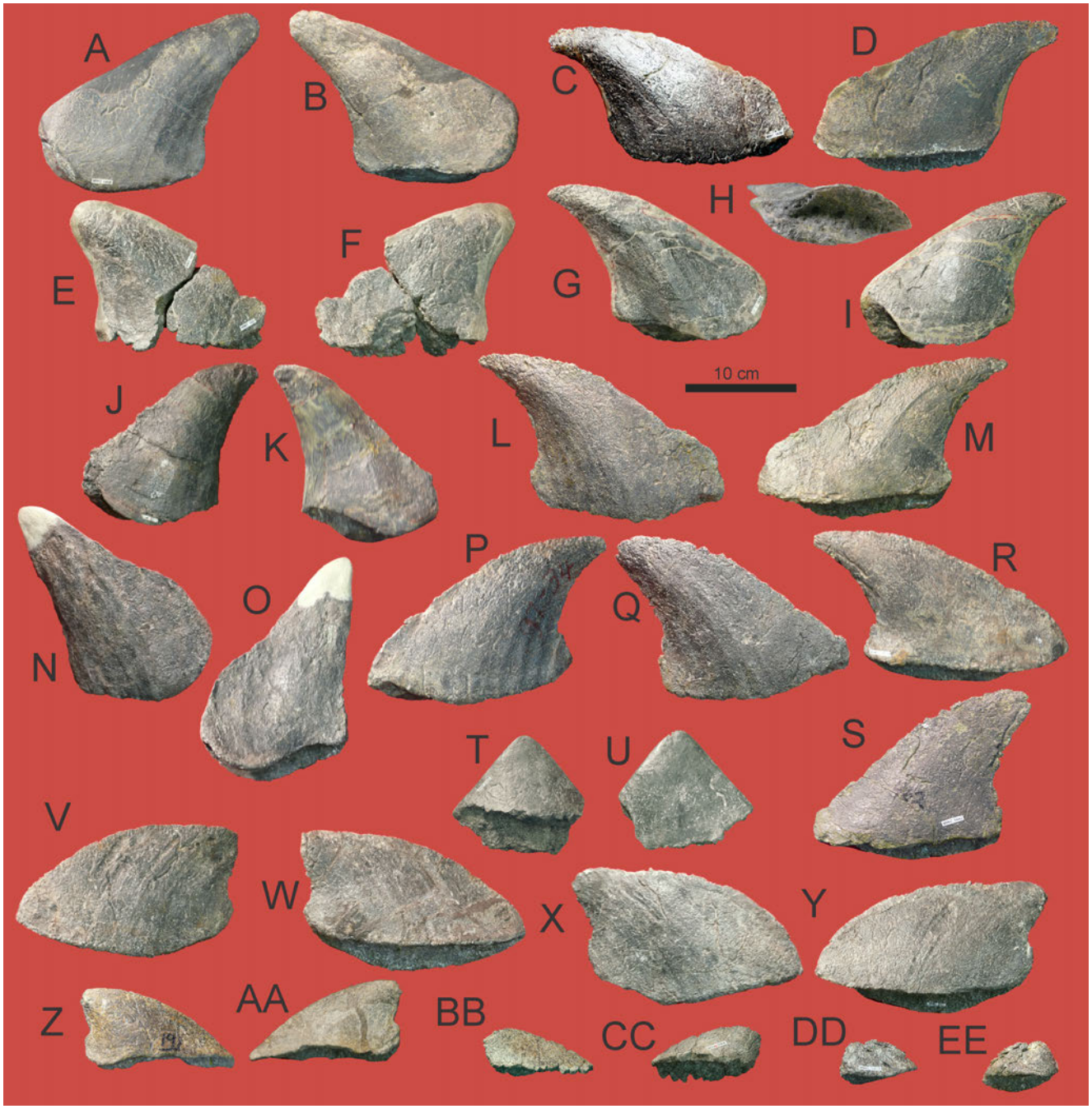

Figure 39. Caudal plates from revised hypodigm of *Mymoorapelta*. Left upper caudal plate MWC 1819 in (A) dorsal and (B) ventral views. Right upper caudal plate MWC 1820 in (C) dorsal and (D) ventral views. Right upper caudal plate MWC 1821 in (E) dorsal and (F) ventral views. Right upper caudal plate MWC 1822 in (G) dorsal, (H) basal, and (I) ventral views. Left upper caudal plate MWC 1823 in (J) dorsal and (K) ventral views. Right upper caudal plate MWC 2678 in (L) dorsal and (M) ventral views. Right upper caudal plate MWC 2867 in (N) dorsal and (O) ventral views. Left upper caudal plate MWC 5148 in (P) dorsal and (Q) ventral views. Right upper caudal plate MWC 5642 in (R) dorsal and (S) ventral views. Possible sacral plate MWC 2868 in (T) dorsal and (U) ventral views. Left sacro-caudal plate MWC 1824 in (V) dorsal and (W) ventral views. Right sacro-caudal plate MWC 2677 in (X) dorsal and (Y) ventral views. Possible distal caudal plate MWC 6747 in (Z) dorsal and (AA) ventral views. Distal lower caudal plate MWC 4226 in (BB) dorsal and (CC) ventral views. Distal right upper caudal plate MWC 5479 in (DD) dorsal and (EE) ventral views.

Table 3. Measurements (in mm) of lateral shoulder spine and lateral caudal plates *Mymoorapelta* material from the Mygatt-Moore Quarry.

Mymoorapelta Spines and Plates								
		Anterior length	**Anterior straight segment to flexture above base**	**Posterior length**	**Base length**	**Maximum thickness**	**Angle of apex in degrees**	**Dorsal ridges present?**
MWC 1818	shoulder spine	284.8	43.6	219.1	135.5	57.1	18	yes
MWC 1819	caudal plate	228.2	14.7	158.3	151.9	34	43.5	yes
MWC 1820	caudal plate	241.4	52.5	136.2	162.2	37.5	29	yes
MWC 5148	caudal plate	253.7	16.6	123.8	188.2	31.6	24	yes
MWC 5642	caudal plate	231.7	29.1	138.6	165.3	33.3	39	yes
MWC 2678	caudal plate	253.7	45.4	122.8	171.9	35.6	26	yes
MWC 2867	caudal plate		77.2		131.3	47.2	60	yes
MWC 1823	caudal plate	195.7	34.9	136.2	118.7	36.7	40	weak
MWC 1822	caudal plate	212.2	0	133.2	139.2	49.2	36.5	yes
MWC 1821	caudal plate					42.9	36	yes
MWC 1824	caudal plate	220.2	15.2	91.4	220.1	51.3	16	yes
MWC 2677	caudal plate	225.3	16.6	104.9	193.1	44.3	17	yes
MWC 6747	caudal plate	154.8	0	68	135.2	32.6	19	no
MWC 4226	distal caudal plate				92			no
MWC 5479	distal caudal plate					30.4		no

This results in the posterior side of the plate being nearly vertical or sloping anteriorly. Thus, the caudal plates of *Mymoorapelta* and *Gargoyleosaurus* have a very different morphology in dorsal view. These differences are distinct enough, such that, although only three caudal plates (Figures 41Q through 41V) have been recovered from the Dry Mesa Quarry in western Colorado, it is apparent that ankylosaur represents *Gargoyleosaurus*.

The ankylosaur fossils from the Meilyn Quarry near the base of Morrison Formation in southern Wyoming (Figures 1 and 3) include several long, low caudal plates (Figures 5C through 5E) of a morphology most similar to *Gargoyleosaurus* but more recurved like *Mymoorapelta*. Taken together with their caudal vertebrae (Figures 5A and 5B), they might have been diagnostic as a distinct new species of Morrison ankylosaur. Sadly, these unique fossils have been dispersed mostly into private collections, where the specimens are not available for study. Perhaps future collections from this locality will provide material to more fully characterize this taxon.

CONCLUSIONS

There are two well-documented ankylosaur genera within the Morrison Formation distinguished primarily on differences in their basicrania, pelvic regions, and osteoderms. Both share characteristics that have been used to differentiate the Polacanthidae from the rest of Ankylosauria, including a triangular skull in dorsal view, similar forelimbs and pectoral girdles, and a similar pattern of osteoderms. Superficially, *Mymoorapelta* and *Gargoyleosaurus* mounted skeletons appear very similar (Figure 42) as the animals are similar in size and elements from both taxa have been used in the development of these mounted skeletons. Future generations of mounted skeletons and carefully researched paleoart should be able to better differentiate these taxa.

Whereas the type specimen of *Gargoyleosaurus* has a well-preserved skull and cervical rings, the material of *Mymoorapelta* from the Mygatt-Moore Quarry more completely reflects the genus. Overlapping skeletal el-

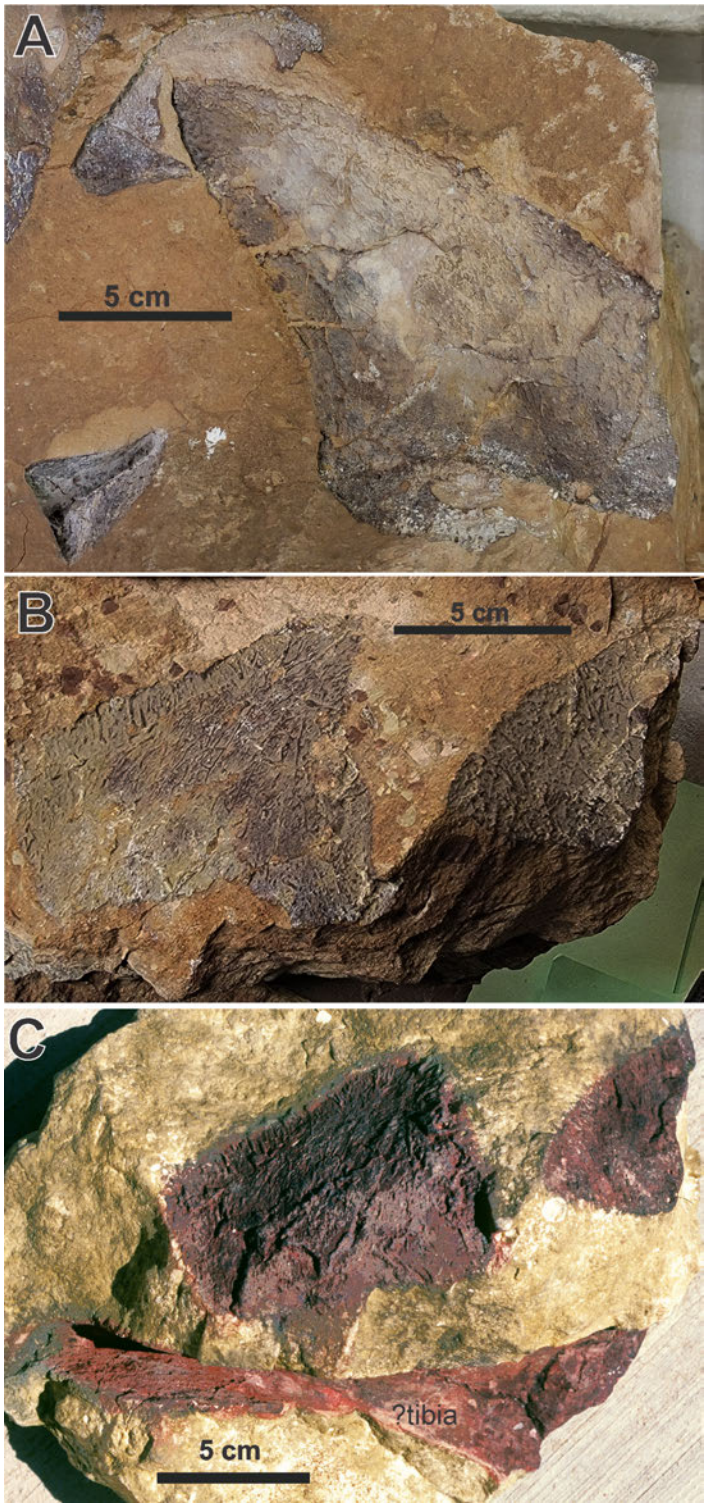

Figure 40. Cactus Park *Mymoorapelta* caudal plates MWC 2610. (A) External mold of dorsal surface caudal plate. (B) External molds of adjoining caudal plates. (C) External molds of a second pair of adjoining caudal plates with a possible tibia fragment.

ements from various sites that have yielded ankylosaur material from throughout the Morrison Formation have added considerably to our knowledge of each genus. *Mymoorapelta maysi* is only known from the upper Morrison, whereas *Gargoyleosaurus* appears to occur throughout the Morrison and may be represented by more than one species. Neither genus is known from strata younger than Kimmeridgian (Turner and Peterson, 1999; Trujillo and Kowallis, 2015).

Given that these dinosaurs represent an entire order unknown in the Morrison Formation prior to 1990 and now documented at 12 localities spanning 4 states, it is clear that additional paleontological field work in even the best studied formations may yield significant results.

ACKNOWLEDGMENTS

Don DeBlieux (Utah Geological Survey [UGS]) assisted in the photography of the braincase of *Mymoorapelta*. All paleontological excavations on public lands done under permits issued by Bureau of Land Management or the State of Utah. Ken Carpenter (Museum of Natural History, University of Colorado) is thanked for providing a cast of the holotype skull and cervical rings of *Gargoyleosaurus* that were essential in carrying out this project, as were our many discussions about ankylosaur systematics. Don Burge former director of the Utah State University Eastern's Prehistoric Museum provided casts of *Gastonia*, *Animantarx*, *Peleroplites*, and *Cedarpelta*. Bill Blows (retired Department of Applied Biological Sciences, City University, London) and Jim Madsen (deceased DinoLab, Salt Lake City and first Utah State Paleontologist) provided us with casts of *Polacanthus* material. Rob Gaston (GastonDesign, Inc.) is thanked for providing several casts of ankylosaur skulls that were critical to this research. Photographs of the Meilyn ankylosaur specimens were provided by Jason Cooper (Dinosaurs of America LLC.). Discussions on vertebral anatomy with Larry Witmer (Witmer Lab, Ohio University) and Matt Wedell (Western University of Health Sciences) are appreciated. Kelli Trujillo (University of Wyoming) is thanked for her help working out the stratigraphy of

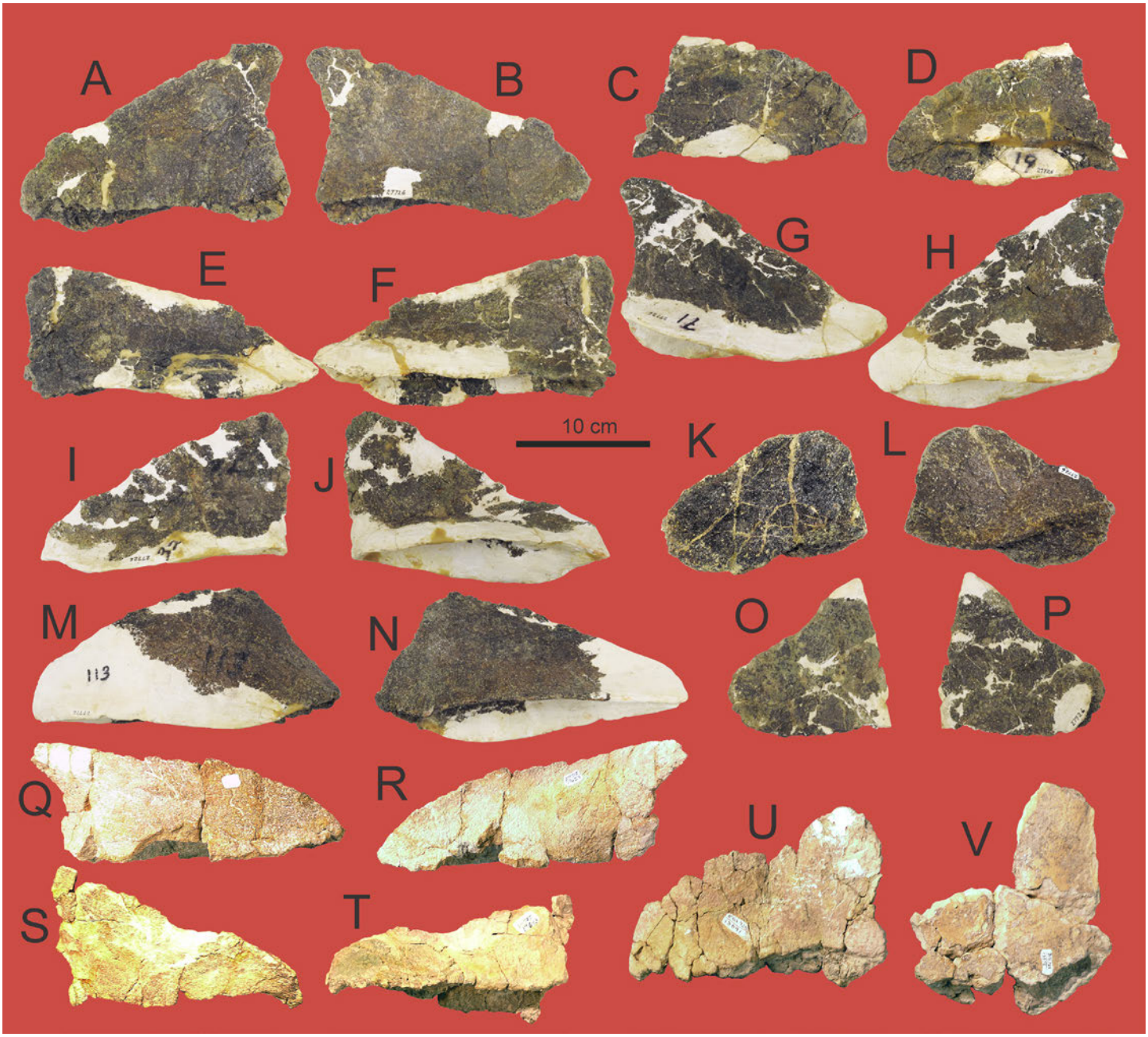

Figure 41. Caudal plates from *Gargoyleosaurus*. Caudal plates from holotype of *Gargoyleosaurus* DMNH 27726. Well-preserved proximal plates in (A) dorsal and (B) ventral views. Left caudal plate in (C) dorsal and (D) ventral views. Right caudal plate in (E) dorsal and (F) ventral views. Right caudal plate in (G) dorsal and (H) ventral views. Left caudal plate in (I) dorsal and (J) ventral views. Smaller left caudal plate in (K) dorsal and (L) ventral views. Right caudal plate in (M) dorsal and (N) ventral views. Smaller right caudal plate in (O) dorsal and (P) ventral views. Caudal plates of *Gargoyleosaurus* from Dry Mesa Quarry. Left caudal plate BYU 725-17643 in (Q) dorsal and (R) ventral views. Left caudal plate BYU 725-17623 in (S) dorsal and (T) ventral views. Partial left caudal plate BYU 725-13891 in (U) ventral view. Partial left caudal plate BYU 725-13975 in (V) ventral view.

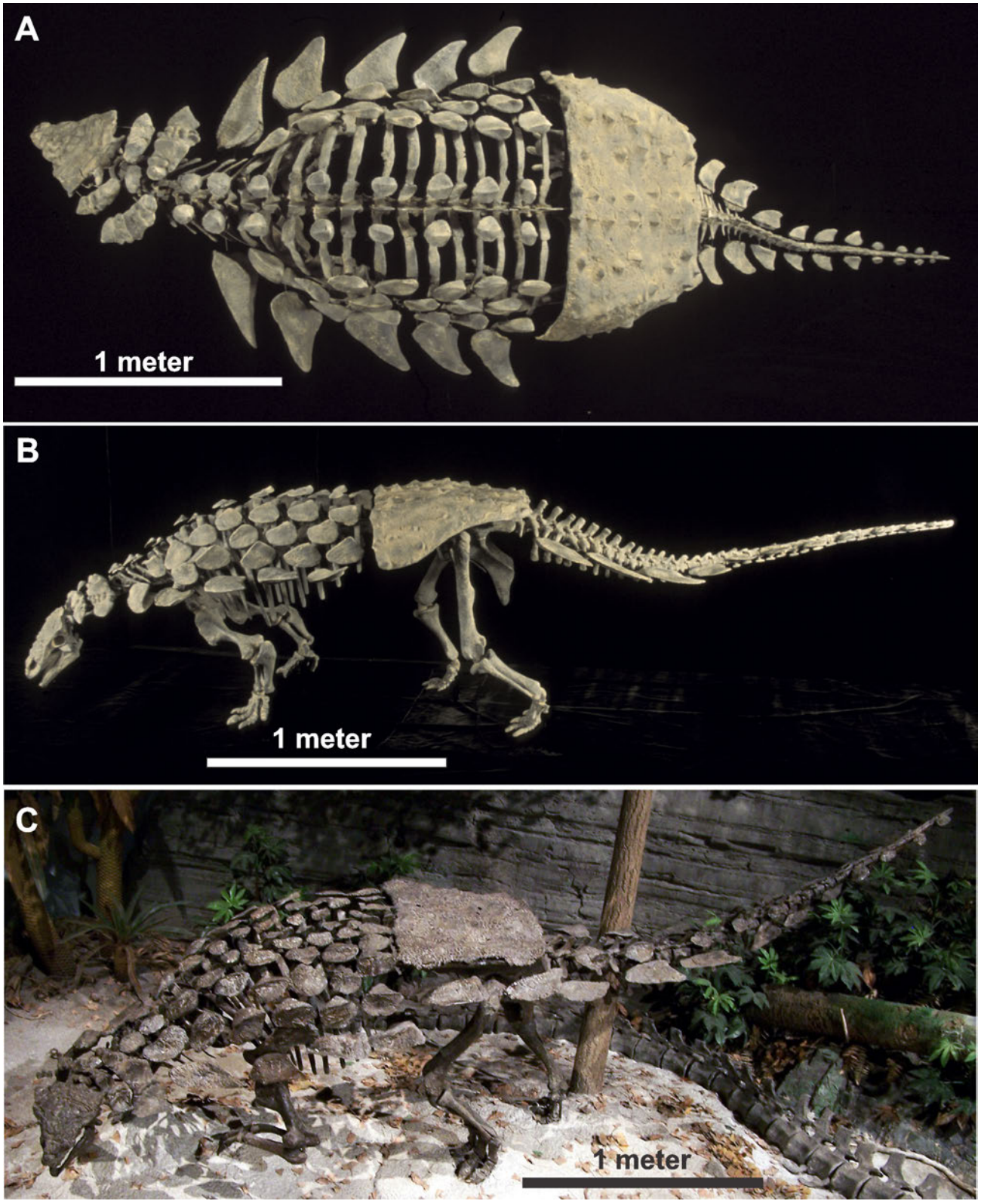

Figure 42. Skeletal mounts of ankylosaurs from the Morrison Formation. Reconstructed skeleton of *Mymoorapelta* by Gastondesign.com (about 2010) in (A) anteriodorsal and (B) in lateral views. Reconstructed skeleton of *Gargoyleosaurus* at Museum of Ancient Life at Thanksgiving Point, Lehi, Utah, in (C) dorsolateral view.

the Morrison Formation in central Wyoming. Joshua Lively (Utah State University Eastern Prehistoric Museum) is thanked for photographing the dorsal osteoderms of *Gargoyleosaurus*. Carolyn Staehle (independent paleoartist) is gratefully acknowledged for her drawings of the *Gargoyleosaurus* skull. Ethan Cowgill is thanked for exposing the basicranium in the Cactus Park specimen. We also thank the many scientists and curators that made access to specimens in their collections possible, Kevin Seymour (Royal Ontario Museum), Kieran Sheppard (deceased, Canadian Museum of Nature), Andrew Newman (Royal Tyrrell Museum of Paleontology), Phil Currie (University of Alberta), Mark Loewen (Utah Museum of Natural History), Malcolm McKenna (deceased, American Museum of Natural History), Mark Norrell (deceased, American Museum of Natural History), Rinchen Barsbold (Mongolian Institute of Geology, Ulaanbaatar), Don Burge (former director of the Prehistoric Museum), John Bird (retired, Utah State University Eastern Prehistoric Museum), Ken Carpenter (Museum of Natural History, University of Colorado), Joshua Lively (Utah State University Eastern Prehistoric Museum), Rod Scheetz (Brigham Young University [BYU] Museum of Paleontology), Joe Sertich (Smithsonian Tropical Research Institute and the Colorado State University), Ken Stadtman (retired, BYU Museum of Paleontology), Angela Milner (deceased, Natural History Museum of London), Dong Zhiming (Institute of Vertebrate Paleontology and Paleoanthropology [IVPP], Chinese Academy of Sciences), Xu Xing (IVPP), Hailu You (IVPP), and Luis Alcalá (Dinopolis Foundation, Tyrell, Spain). Technical reviews by Don DeBlieux, Stefan Kirby, and Stephanie Carney (all UGS) are appreciated. Peer reviews by Ken Carpenter (Museum of Natural History, University of Colorado) and Bill Blows (retired, Department of Applied Biological Sciences, City University, London) resulted in improving the manuscript.

REFERENCES

Arbour, V.M., 2009, Estimating impact forces of tail club strikes by Ankylosaurid dinosaurs: PLoS ONE, v., e6738, https://doi.org/10.1371/journal.pone.0006738.

Arbour, V.M., Burns, M.E., Bell, P.R., and Currie, P.J., 2014, Epidermal and dermal integumentary structures of Ankylosaurian dinosaurs: Journal of Morphology v. 275, no. 1, p. 39–50, https://doi.org/10.1002/jmor.20194.

Arbour, V.M., Burns, M.E., and Currie, P.J., 2011, A review of pelvic shield morphology in ankylosaurs (Dinosauria, Ornithischia): Journal of Vertebrate Paleontology, v. 85, p. 298–302.

Arbour V.M., Burns M.E., and Sissons R.L., 2009, A redescription of the ankylosaurid dinosaur *Dyoplosaurus acutosquameus* Parks 1924 (Ornithischia: Ankylosauria) and a revision of the genus: Journal of Vertebrate Palaeontology, v. 29, p. 1117–1135.

Arbour, V.M., and Currie P.J., 2013a, *Euoplocephalus tutus* and the diversity of ankylosaurid dinosaurs in the Late Cretaceous of Alberta, Canada, and Montana, USA: PLoS ONE, v. 8, no. 5, e62421, https://doi.org/10.1371/journal.pone.0062421.

Arbour, V.M, and Currie, P.J., 2013b, The taxonomic identity of a nearly complete ankylosaurid dinosaur skeleton from the Gobi Desert of Mongolia: Cretaceous Research, v. 46, p. 24–30.

Arbour, V.M., and Currie P.J., 2016, Systematics, phylogeny and palaeobiogeography of the ankylosaurid dinosaurs: Journal of Systematic Palaeontology, v. 14, p. 385–444, https://doi.org/10.1080/14772019.2015.1059985.

Arbour, V.M., and Evans, D.C., 2017, A new ankylosaurine dinosaur from the Judith River Formation of Montana, USA, based on an exceptional skeleton with soft tissue preservation: Royal Society, Open Science, http://dx.doi.org/10.1098/rsos.161086.

Arbour, V.M., Lech-Hernes, N.L., Guldberg, T.E., Harum, J.H., and Currie, P.J., 2013, An ankylosaur dinosaur from Mongolia with in situ armour and keratinous scale impressions: Acta Paleontologica Polonica, v. 58, p. 55–64, https://www.app.pan.pl/archive/published/app58/app20110081.pdf.

Arbour, V.M., and Mallon, J.C., 2017, Unusual cranial and postcranial anatomy in the archetypal ankylosaur *Ankylosaurus magniventris*: Facets, v. 2, p. 764–794, http://www.facetsjournal.com/doi/10.1139/facets-2017-0063.

Arbour, V.M., and Snively, E., 2009, Finite element analyses of ankylosaurid dinosaur tail club impacts: The Anatomical Record, v. 292, p. 1412–1426, https://anatomypubs.onlinelibrary.wiley.com/doi/10.1002/ar.20987.

Arbour, V.M., and Zanno, L.E., 2018, The evolution of tail weaponization in amniotes: Proceedings Royal Society B, v. 285, http://dx.doi.org/10.1098/rspb.2017.2299.

Arbour, V.M., and Zanno, L.E., 2020, Tail weaponry in ankylosaurs and glyptodonts—an example of a rare but strongly convergent phenotype: The Anatomical Record, v. 303, p. 988–998, https://anatomypubs.onlinelibrary.wiley.com/doi/10.1002/ar.24093.

Barrett, P.M., and Maidment, S.C.R., 2011, Wealden armoured dinosaurs, *in* Batten, D.J., editor, English Wealden fossils: London, Palaeontological Association, Field Guides to Fossils, v. 14, p. 391–406.

Blows, W.T., 1987, The armoured dinosaur *Polacanthus foxi* from the Lower Cretaceous of the Isle of Wight: Palaeontology, v. 30, p. 557–580.

Blows, W.T., 2001, Dermal armor of the polacanthine dinosaurs, *in* Carpenter, K., editor, The armored dinosaurs: Bloomington, Indiana University Press, p. 363–385.

Blows, W.T., 2015, British Polacanthid dinosaurs: Manchester, Siri Scientific Press, Monograph Series, v. 7, 223 p., https://siriscientificpress.co.uk/products/british-polacanthid-dinosaurs.

Blows, W.T., and Honeysett, K., 2014a, New teeth of nodosaurid ankylosaurs from the Lower Cretaceous of Southern England: Acta Palaeontologica Polonica, v. 59, p. 835–841, https://www.app.pan.pl/archive/published/app59/app20120131.pdf.

Blows, W.T., and Honeysett, K., 2014b, First Valanginian *Polacanthus foxii* (Dinosauria, Ankylosauria) from England, from the Lower Cretaceous of Bexhill, Sussex: Proceedings of the Geologists Association, v. 125, p. 233–251.

Bodily, N.M., 1969, An armored dinosaur from the Lower Cretaceous of Utah: Brigham Young University Geology Studies, v. 16, p. 35–60, https://geology.byu.edu/0000017c-dde1-d27f-abfe-fde1f5f10001/an-amoured-dinosaur-from-the-lower-cretaceous-of-utah-norman-m-bodily-pdf.

Brown, B., 1908, The Ankylosauridae a new family of armored dinosaurs from the Upper Cretaceous: Bulletin of the American Museum of Natural History, v. 24, p. 187–201, http://hdl.handle.net/2246/1435.

Brown, C.M., 2017, An exceptionally preserved armored dinosaur reveals the morphology and allometry of osteoderms and their horny epidermal coverings: PeerJ, 39 p., https://peerj.com/articles/4066/.

Brown, C.M., Henderson, D.M., Vinther, J., Fletcher, I., Sistiaga, A., Herrera, J., and Summons, R.E., 2017, An exceptionally preserved three-dimensional armored dinosaur reveals insights into coloration and Cretaceous predator-prey dynamics: Current Biology, v. 27, p. 2514–2521, https://doi.org/10.1016/j.cub.2017.06.071.

Burns, M.E., 2008, Taxonomic utility of ankylosaur (Dinosauria, Ornithischia) osteoderms—*Glyptodontopelta mimus* Ford, 2000—a test case: Journal of Vertebrate Paleontology, v. 28, p. 1102–1109.

Burns, M.E., 2010, External and internal structure of ankylosaur (Dinosauria; Ornithischia) osteoderms: Edmonton, University of Alberta, M.S. thesis, 177 p.

Burns, M.E., 2015, Interspecific variation in armoured dinosaurs (Dinosauria: Ankylosauria): Edmonton, University of Alberta, Ph.D. dissertation, 285 p., https://era.library.ualberta.ca/items/7e770d19-2fe1-460d-8912-c027a18ce7c6.

Burns, M.E., and Currie, P., 2014, External and internal structure of ankylosaur (Dinosauria, Ornithischia) osteoderms and their systematic relevance: Journal of Vertebrate Paleontology, v. 34, p. 835–851, https://dx.doi.org/10.1080/02724634.2014.840309.

Burns, M.E., and Lucas, S.G., 2015, Biostratigraphy of Ankylosaur (Dinosauria: Ornithischia) osteoderms from New Mexico, *in* Sullivan, R.M., and Lucas, S.G., editors, Fossil record 4: New Mexico Museum of Natural History and Science Bulletin 67, p. 9–13, https://nmdigital.unm.edu/digital/collection/bulletins/id/4150/rec/2.

Burns, M.E., Currie, P.J., Sissons, R.L. and Arbour, V.M., 2011, Juvenile specimens of *Pinacosaurus grangeri* Gilmore, 1933 (Ornithischia: Ankylosauria) from the Late Cretaceous of China, with comments on the specific taxonomy of *Pinacosaurus*: Cretaceous Research, v. 32, p. 174–186, https://doi.org/10.1016/j.cretres.2010.11.007.

Carpenter, K., 1984, Skeletal reconstruction and life restoration of *Sauropelta* (Ankylosauria: Nodosauridae) from the Cretaceous of North America: Canadian Journal of Earth Science, v. 21, p. 1491–1498.

Carpenter, K.,1990, Ankylosaur systematics—an example using *Panoplosaurus* and *Edmontonia* (Ankylosauria: Nodosauridae), *in* Carpenter, K., and Currie, P.J., editors, Dinosaur systematics—perspectives and approaches: Cambridge University Press, p. 281–297.

Carpenter, K., 2001, Phylogenetic analysis of the Ankylosauria, *in* Carpenter, K., editor, The armoured dinosaurs: Bloomington, Indiana University Press, p. 455–483.

Carpenter, K., 2004, Redescription of *Ankylosaurus magniventris* Brown 1908 (Ankylosauridae) from the Upper Cretaceous of the Western Interior of North America: Canadian Journal of Earth Sciences, v. 41, p. 961–986, https://doi.org/10.1139/e04-043.

Carpenter, K., Bartlett, J., Bird, J., and Barrick, R., 2008, Ankylosaurs from the Price River quarries, Cedar Mountain Formation (Lower Cretaceous), east–central Utah: Journal of Vertebrate Paleontology, v. 28, p. 1089–1101.

Carpenter, K., DiCroce, T., Kinneer, B., and Simon, R., 2013, Pelvis of *Gargoyleosaurus* (Dinosauria: Ankylosauria) and the origin and evolution of the Ankylosaur pelvis: PLoS ONE v. 8, no. 11, https://doi.org/10.1371/journal.pone.0079887.

Carpenter, K., Dilkes, D., and Weishampel, D.B., 1995, The dinosaurs of the Niobrara Chalk Formation (Upper Cretaceous, Kansas): Journal of Vertebrate Paleontology, v. 15, p. 275–297, https://doi.org/10.1080/02724634.1995.10011230.

Carpenter, K., Hayashi, S., Kobayashi, Y., Maryańska, T., Barsbold, R., Sato, K., and Obata, I., 2011, *Saichania chulsanensis* (Ornithischia, Ankylosauridae) from the Upper Cretaceous of Mongolia: Palaeontographica, Abteilung A, v. 294, p. 1–61.

Carpenter, K., and Kirkland, J.I., 1998, Review of Lower and Middle Cretaceous ankylosaurs for North America: New Mexico Museum of Natural History and Science Bulletin 14, p. 249–270, https://econtent.unm.edu/digital/collection/bulletins/id/954.

Carpenter, K., Kirkland, J.I., Burge, D., and Bird, J., 1999, Ankylosaurs (Ankylosauria: Ornithischia) of the Cedar Mountain Formation, Utah, and their stratigraphic distribution, *in* Gillette, D.D., editor, Vertebrate paleontology in Utah: Utah Geological Survey Miscellaneous Publications 99-1, p. 243–251, https://doi.org/10.34191/MP-99-1.

Carpenter, K., Kirkland, J.I., Burge, D., and Bird, J., 2001, Disarticulated skull of a new primitive ankylosaurid from the Lower Cretaceous of eastern Utah, *in* Carpenter, K., editor, The armored dinosaurs: Bloomington, Indiana University Press, p. 211–238.

Carpenter, K., Miles, C., and Cloward, K., 1998, Skull of a Jurassic ankylosaur (Dinosauria): Nature, v. 393, p. 782–783.

Chin, K., and Kirkland, J.L., 1998, Probable herbivore coprolites from the Upper Jurassic Mygatt-Moore Quarry, western Colorado: Modern Geology, v. 23, p. 249–275.

Christiansen, E.H., Kowallis, B.J., Dorais, M.J., Hart, G.L., Mills, C.N., Pickard, M., and Parks, E., 2015, The record of volcanism in the Brushy Basin Member of the Morrison Formation—implications for the Late Jurassic of Western North America, *in* Anderson, T.H., Didenko, A.N., Johnson, C.L., Khanchuk, A.I., and MacDonald, J.H., Jr., editors, Late Jurassic margin of Laurasia—a record of faulting accommodating plate rotation: Geological Society of America Special Paper 513, https://doi.org/10.1130/2015.2513(11), https://www.researchgate.net/publication/281118079_The_record_of_volcanism_in_the_Brushy_Basin_Member_of_the_Morrison_Formation_Implications_for_the_Late_Jurassic_of_western_North_America.

Chure, D.J., 2000, A new species of *Allosaurus* from the Morrison Formation of Dinosaur National Monument (UT-CO) and a revision of the theropod family Allosauridae: New York, Columbia University, Ph.D. dissertation, 964 p.

Chure, D.J., and Loewen, M.A., 2020, Cranial anatomy of *Allosaurus jimmadseni*, a new species from the lower part of the Morrison Formation (Upper Jurassic) of Western North America: PeerJ 8, https://doi.org/10.7717/peerj.7803.

Colbert, E.H., 1968, Men and dinosaurs—the search in field and laboratory: New York, E.P. Hutton and Company, 283 p.

Coombs, W.P., 1971, The Ankylosauria: New York, Columbia University, Ph.D. dissertation, 487 p.

Coombs, W.P., 1978a, The families of the ornithischian dinosaur order Ankylosauria: Palaeontology, v. 21, p. 143–170, https://palass.org/sites/default/files/media/publications/palaeontology/volume_21/vol21_part1_pp143-170.pdf.

Coombs, W.P., 1978b, Forelimb muscles of the Ankylosauria (Reptilia, Ornithischia): Journal of Paleontology, v. 52, p. 642–657.

Coombs, W.P., 1979, Osteology and mycology of the hindlimb in the Ankylosauria (Reptilia, Ornithischia): Journal of Paleontology, v. 53 p. 666–684.

Coombs, W.P., 1990, Teeth and taxonomy in ankylosaurs, *in* Carpenter, K., and Currie, P., editors, Dinosaur systematics—approaches and perspectives: Cambridge University Press, p. 269–279.

Coombs, W.P., 1995, A nodosaurid ankylosaur (Dinosauria, Ornithischia) from the Lower Cretaceous of Texas: Journal of Vertebrate Paleontology, v. 15, p. 298–312.

Coombs, W.P., and Maryańska, T., 1990, Ankylosauria, *in* Weishampel, D.B., Dodson P., and Osmólska, H., editors, The Dinosauria, 1st edition: Berkeley, University of California Press, p. 456–483.

Currie, P.J., Badamgarav, D., Koppelhus, E.B., Sissons, R., and Vickaryous, M.K., 2011, Hands, feet, and behaviour in *Pinacosaurus* (Dinosauria: Ankylosauridae): Acta Palaeontologica Polonica, v. 56, p. 489–504, https://www.app.pan.pl/archive/published/app56/app20100055.pdf.

Delair, J.B., 1982, Notes on an armoured dinosaur from Barnes High, Isle of Wight: Proceedings Isle Wight Natural History and Archaeology Society, v. 7, p. 297–302.

Demko, T.M., Currie, B.S., and Nicoll, K.A., 2004, Regional paleoclimatic and stratigraphic implications of paleosols and fluvial/overbank architecture in the Morrison Formation (Upper Jurassic), Western Interior, USA: Sedimentary Geology, v. 167, p. 115–135.

Dong, Z.-M., 1993, An ankylosaur (ornithischian dinosaur) from the Middle Jurassic of the Junggar Basin, China: Vertebrata PalAsiatica, v. 31, p. 258–265, http://www.ivpp.cas.cn/cbw/gjzdwxb/xbwzxz/200812/W020090813370614393532.pdf.

Drumheller, S.K., McHugh, J.B., Kane, M., Riedel, A., and D'Amore, D.C., 2020, High frequencies of theropod bite marks provide evidence for feeding, scavenging, and possible cannibalism in a stressed Late Jurassic ecosystem: PLoS ONE, v. 15, no. 5, https://doi.org/10.1371/journal.pone.0233115.

Eaton, T.H., 1960, A new armoured dinosaur from the Cretaceous of Kansas: University of Kansas Paleontological Contributions, Vertebrata, v. 8, p. 1–24, https://kuscholarworks.ku.edu/entities/publication/63750429-0471-4092-9ec8-755d14dc3697.

Ford, T.L., 2000, A review of ankylosaur osteoderms from New Mexico and a preliminary review of ankylosaur armor: New Mexico Museum of Natural History Bulletin 17, p. 157–176.

Foster, J.R., 2003, Paleoecological analysis of the vertebrate fauna of the Morrison Formation (Upper Jurassic), Rocky Mountain region, USA: New Mexico Museum of Natural History Bulletin 23, 95 p.

Foster, J.R., Hunt-Foster, R.K., Gorman, M.A., Trujillo, K.C., Suarez, C., McHugh, J.B., Peterson, J.E., Warnock, J.P., and Schoenstein, H.E., 2018, Paleontology, taphonomy, and sedimentology of the Mygatt-Moore Quarry, a large dinosaur bonebed in the Morrison Formation, western Colorado—implications for Upper Jurassic dinosaur preservation modes: Geology of the Intermountain West, v. 5, p. 23–93, https://giw.utahgeology.org/giw/index.php/GIW/article/view/24.

Galton, P.M**.,** 1983a, *Sarcolestes leedsi* Lydeeker, an ankylosaurian dinosaur from the middle Jurassic of England: Neues Jahrbuch für Geologie und Paläontologie 1983, Heft. 3, p. 141–155, https://doi.org/10.1127/njgpm/1983/1983/141.

Galton, P.M**.,** 1983b, Armoured dinosaurs (Ornithischia: Ankylosauria) from the Middle and Upper Jurassic of Europe: Palaeontographica, Abteilung A, v. 182, p. 1–25, https://doi.org/10.1016/S0016-6995(80)80038-6.

Galton, P.M., and Upchurch, P., 2004, Stegosauria, *in* Weishampel, D.B., Dodson, P., and Osmólska, H., editors, The Dinosauria, 2nd edition: Berkeley, University of California Press, p. 342–361.

Garcia, G., and Pereda–Suberbiola, X., 2003, A new species of *Struthiosaurus* (Dinosauria: Ankylosauria) from the Upper Cretaceous of Villeveyrac (Southern France): Journal of Vertebrate Paleontology, v. 23, p. 156–165, https://www.jstor.org/stable/4524302.

Gasulla, J.M., Ortega, F., Pereda-Suberbiola, X., Escaso, F., and Sanz, L., 2011, Elementos de la armaduro dérmica del dinosaurio anquilosaurio *Polacanthus* Owen, 1865, en el Cretácico Inferior de Morella (Castellón, España): Ameghiniana, v. 48, p. 508–519, https://www.ameghiniana.org.ar/index.php/ameghiniana/article/view/276.

Gaston, R.W., Schellenbach, J., and Kirkland, J.I., 2001, Mounted skeleton of the polacanthine ankylosaur *Gastonia burgei*, *in* Carpenter, K., editor, The armored dinosaurs: Bloomington, Indiana University Press, p. 386–398.

Gilmore, C.W., 1914, Osteology of the armoured Dinosauria in the United States National Museum, with special reference to the genus *Stegosaurus*: Bulletin of the United States National Museum, v. 89, p. 1–137, https://repository.si.edu/items/188b80c0-c1d0-4ecc-89b7-5963a18a814e.

Gilmore, C.W., 1930, On dinosaurian reptiles from the Two Medicine Formation of Montana: Proceedings of the

United States National Museum, v. 77, p. 1–39, https://repository.si.edu/items/e577da3e-57dd-423a-94f8-8119ccdafc5c.

Haekel, O., 1910, Uber das system der Reptilien: Zoologischer Anzeiger, v. 35, p. 324–341, https://www.biodiversitylibrary.org/item/37586#page/7/mode/1up.

Hayashi, S., Carpenter, K., Scheyer, T.M., Watabe, M., and Suzuki, D., 2010, Function and evolution of ankylosaur dermal armor: Acta Palaeontologica Polonica, v. 55, p. 213–228.

Heckert, A.B., Zeigler, K.E., Lucas, S.G., Spielmann, J.A., Hester, P.M., Peterson, R.E., Peterson, R.E., and D'Andrea, N.V., 2003, Geology and paleontology of the Upper Jurassic (Morrison Formation: Brush Basin Member) Peterson Quarry, central New Mexico, *in* Lucas, S.G., Semken, S.C., Berglof, W., and Ulmer-Scholle, D., editors, Geology of the Zuni Plateau: New Mexico Geological Society Guidebook, 54th Field Conference, p. 315–324, https://libres.uncg.edu/ir/asu/f/Heckert_A_2003_Geology_and_Paleontology.pdf.

Hill, R.V., Witmer, L.M., and Norell, M.A., 2003, A new specimen of *Pinacosaurus grangeri* (Dinosauria: Ornithischia) from the Late Cretaceous of Mongolia—ontogeny and phylogeny of ankylosaurs: American Museum Novitates, v. 3395, 29 p., https://doi.org/10.1206/0003-0082(2003)395<0001:ANSOPG>2.0.CO;2.

Hulke, J.W., 1882, *Polacanthus foxii*, a large undescribed dinosaur from the Wealden Formation in the Isle of Wight: Philosophical Transactions of the Royal Society, v. 172, p. 653–662, https://royalsocietypublishing.org/doi/10.1098/rstl.1881.0015.

Hulke, J.W., 1888, Supplemental note on *Polacanthus foxii*, describing the dorsal shield and some parts of the endoskeleton imperfectly known in 1881: Philosophical Transactions of the Royal Society, v. 178 p. 169–172, https://royalsocietypublishing.org/doi/epdf/10.1098/rstb.1887.0007.

Kilbourne, B., and Carpenter, K., 2005, Redescription of *Gargoyleosaurus parkpinorum*, a polacanthid ankylosaur from the Upper Jurassic of Albany County, Wyoming: Neues Jahrbuch für Geologie und Paläontologie Abhandlungen v. 237, p. 111–160, https://doi.org/10.1127/njgpa/237/2005/111.

Kinneer, B., Carpenter, K., and Shaw, A., 2016, Redescription of *Gastonia burgei* (Dinosauria: Ankylosauria, Polacanthidae), and a description of a new species: Neues Jahrbuch für Geologie und Paläontologie Abhandlungen, v. 282, p. 37–80, https://doi.org/10.1127/njgpa/2016/0605.

Kirkland, J.I., 1998, A polacanthine ankylosaur (Ornithischia: Dinosauria) from the Early Cretaceous (Barremian) of eastern Utah: New Mexico Museum of Natural History and Science Bulletin 14, p. 271–281, https://nmdigital.unm.edu/digital/collection/bulletins/id/955/.

Kirkland, J.I., 2006, Fruita Paleontological Area (Upper Jurassic, Morrison Formation), western Colorado—an example of terrestrial taphofacies analysis, *in* Foster, J.R., and Lucas, S.G., editors, Paleontology and geology of the Upper Jurassic Morrison Formation: New Mexico Museum of Natural History and Science Bulletin 36, p. 67–95, https://nmdigital.unm.edu/digital/collection/bulletins/id/782.

Kirkland, J.I., and Carpenter, K., 1994, North America's first pre–Cretaceous ankylosaur (Dinosauria) from the Upper Jurassic Morrison Formation of western Colorado: Brigham Young University Geology Studies, v. 40, p. 25–42, https://geology.byu.edu/0000017c-f2bd-d0ec-a1fd-f7fd21140001/geo-stud-vol-40-kirkland-carpenter1-pdf.

Kirkland, J.I., Alcala´, L., Loewen, M.A., Espı´lez, E, Mampel, L., and Weirsma, J.P., 2013, The basal nodosaurid ankylosaur *Europelta carbonensis* n. gen., n. sp. from the Lower Cretaceous (Lower Albian) Escucha Formation of northeastern Spain: PLoS ONE, v. 8, no. 12, e80405, https://doi:10.1371/journal.pone.0080405.

Kirkland, J.I., Carpenter, K., Hunt, A.P., and Scheetz, R.D., 1998, Ankylosaur (Dinosauria) specimens from the Upper Jurassic Morrison Formation: Modern Geology, v. 23, p. 145–177.

Kirkland, J., DeBlieux, D., Hunt-Foster, R., Foster, J., Trujillo, K., and Finzel, E., 2020, The Morrison Formation and its bounding strata on the western side of the Blanding basin, San Juan County, Utah: Geology of the Intermountain West, v. 7, p. 137–195, https://doi.org/10.31711/giw.v7.pp137-195.

Kirkland, J.I., Scheetz, R.D., and Foster, J.R., 2005, Jurassic and Lower Cretaceous dinosaur quarries of western Colorado and eastern Utah, *in* Richard, G., compiler, Rocky Mountain Section of the Geological Society of America field trip guidebook: Grand Junction Geological Society Field Trip 402, p. 1–26.

Kirkland, J.I., Suarez, M., Suarez, C., and Hunt-Foster, R., 2016, The Lower Cretaceous in east-central Utah—the

Cedar Mountain Formation and its bounding strata: Geology of the Intermountain West, v. 3, p. 101–228, https://doi.org/10.31711/giw.v3i0.9.

Lambe, L.M., 1919, Description of a new genus and species (*Panoplosaurus mirus*) of armored dinosaur from the Belly River Beds of Alberta: Transactions of the Royal Society of Canada, Series Three, v. 13, p. 39–50.

Large, D.S., 2023, First occurrence of *Gargoyleosaurus* (Dinosauria: Ankylosauria) in Utah—the importance of osteoderms: Philadelphia, Pennsylvania, Drexel University, Ph.D. dissertation, 169 p., https://researchdiscovery.drexel.edu/esploro/outputs/graduate/First-Occurrence-of-Gargoyleosaurus-Dinosauria-Ankylosauria/991020340613604721.

Lee, Y.-N., 1996, A new nodosaurid ankylosaur (Dinosauria: Ornithischia) from the Paw Paw Formation (Late Albian) of Texas: Journal of Vertebrate Paleontology, v. 16, p. 232–245, https://doi.org/10.1080/02724634.1996.10011311.

Lull, R.S., 1921, The Cretaceous armoured dinosaur *Nodosaurus textilis* Marsh: American Journal of Science, Fifth Series, v. 1, p. 97–126.

Maidment, S.C.R, Brassey, C., Barrett, P.M., 2015, The postcranial skeleton of an exceptionally complete individual of the plated dinosaur *Stegosaurus stenops* (Dinosauria: Thyreophora) from the Upper Jurassic Morrison Formation of Wyoming, U.S.A.: PLoS ONE, v. 10, no. 10, https://doi.org/10.1371/journal.pone.0138352.

Main, R.P., de Risqlés, A., Horner, J.R., and Padian, K., 2005, The evolution and function of thyreophoran dinosaur scutes—implications for plate function in stegosaurs: Paleobiology, v. 31, p. 291–314.

Maleev, E.A., 1954, Armoured dinosaurs of the Upper Cretaceous of Mongolia (Family Syrmosauridae): Trudy Paleontologičeskogo Instituta [in Russian], v. 48, p. 142–170.

Maleev, E.A., 1956, Armoured dinosaurs of the Upper Cretaeous of Mongolia (Family Ankylosauridae: Trudy Paleoontologičeskogo Instituta [in Russian], v. 62, p. 51–91.

Martill, D.M., Batton, D.J., and Loydell, D. K., 2000, A new specimen of the thyreaophoran dinosaur cf. *Scelidosaurus* with soft tissue preservation: Palaeontology, v. 43, p. 549–559, https://palass.org/publications/palaeontology-journal/archive/43/3/article_pp549-559.

Maryańska, T., 1977, Ankylosauridae (Dinosauria) from Mongolia: Acta Palaeontologica Polonica, v. 37, p. 87–151, http://www.palaeontologia.pan.pl/Archive/1977-37_85-151_19-36.pdf.

Matthews, W.D., 1922, A super-dreadnaught of the animal world—the armored dinosaur *Palaeoscincus*: Natural History, v. 22, p. 333–342.

McHugh, J.B., Drumheller, S.K., Riedel, A., and Kane, M., 2020, Decomposition of dinosaurian remains inferred by invertebrate traces on vertebrate bone reveal new insights into Late Jurassic ecology, decay, and climate in western Colorado: PeerJ 8, https://doi.org/10.7717/peerj.9510.

McHugh, J.B., Drumheller, S.K., Kane, M., Riedel, A., and Nestler, J.H., 2023, Assessing paleoecological data retention among disparate field collection regimes—a case study at the Mygatt-Moore Quarry (Morrison Formation): Palaios, v. 38, p. 233–239, https://doi.org/10.2110/palo.2022.048.

Miller, W.E., Baer, J.L., Stadtman, K.L., and Britt, B.B., 1991, The Dry Mesa Dinosaur Quarry, Mesa County, Colorado, *in* Averett, W.R., editor, Guidebook for dinosaur quarries and tracksites tour, western Colorado and eastern Utah: Grand Junction Geological Society, p. 31–46.

Molnar, R.E., 1996, Preliminary report on a new ankylosaur from the Early Cretaceous of Queensland, Australia: Memoirs of the Queensland Museum, v. 39, p. 653–668, https://ia803209.us.archive.org/9/items/biostor-260397/biostor-260397.pdf.

Morgan, K., Kirkland, J.I., Suarez, C.A., and Pittman, J., 2016, First occurrence of an Arkansas ankylosaur [abs.]: Journal of Vertebrate Paleontology Abstracts with Program, p. 191.

Nopcsa, F., 1915, Die Dinosaurier der Seibenbürgischen Landesteile Ungarns: Mitteilungen aus dem Jahrbuche der Kniglich Ungarischen Geologischen Reichsanstalt, v. 23, p. 1–26, https://www.biodiversitylibrary.org/bibliography/11447.

Nopcsa, F.B., 1929, Dinosaurierresle aus Seibenburgen V: Geologica Hungarica, Series Palaeontologica, v. 4, p. 1–76, https://real-j.mtak.hu/17546/1/geologica_hungarica_ser_paleo_04_1929.pdf.

Norman, D.B., 2020a, *Scelidosaurus harrisonii* from the Early Jurassic of Dorset, England—cranial anatomy: Zoological Journal of the Linnean Society, v. 188, p. 1–81, https://doi.org/10.1093/zoolinnean/zlz074.

Norman, D.B., 2020b, *Scelidosaurus harrisonii* from the Early Jurassic of Dorset, England—postcranial skeleton: Zoo-

logical Journal of the Linnean Society, v. 189, p. 47–157, https://doi.org/10.1093/zoolinnean/zlz078.

Norman, D.B., 2020c, *Scelidosaurus harrisonii* from the Early Jurassic of Dorset, England—the dermal skeleton: Zoological Journal of the Linnean Society, v. 190, p. 1–53, https://doi.org/10.1093/zoolinnean/zlz085.

Norman, D.B., and Faiers, T., 1996, On the first partial skull of an ankylosaurian dinosaur from the Lower Cretaceous of the Isle of Wight, Southern England: Geological Magazine, v. 133, p. 299–310.

Ösi, A., 2005, *Hungarosaurus tormai*, a new ankylosaur (Dinosauria) from the Upper Cretaceous of Hungary: Journal of Vertebrate Paleontology, v. 25, p. 370–383.

Ösi, A., Botfolvai, G., Albert, G., and Hajdu, Z., 2019, The dirty dozen—taxonomical and taphonomical overview of a unique ankylosaurian (Dinosauria: Ornithischia) assemblage from the Santonian Iharkút locality, Hungary: Palaeobiodiversity and Palaeoenviroments, v. 99, p. 195–240, https://doi.org/10.1007/s12549-018-0362-z.

Ösi, A., and Makádi, L., 2009, New remains of *Hungarosaurus tormai* (Ankylosauria, Dinosauria) from the Upper Cretaceous of Hungary—skeletal reconstruction and body mass estimation: Paläontologische Zeitschrift, v. 83, p. 227–245.

Ösi, A., and Pereda-Suberbiola, X., 2017, Notes on the pelvic armor of European ankylosaurs (Dinosauria: Ornithischia), Cretaceous Research, v. 75, p. 11–22, https://doi.org/10.1016/j.cretres.2017.03.007.

Osborn, H.F., 1923, Two lower Cretaceous dinosaurs from Mongolia: American Museum Novitates, v. 95, p. 1–10, https://digitallibrary.amnh.org/items/ea6f092a-a5e4-4d4c-bc92-1e219e53bd70.

Ostrom, J.H., 1970, Stratigraphy and paleontology of the Cloverly Formation (Lower Cretaceous) of the Bighorn Basin area, Wyoming and Montana: Peabody Museum of Natural History Bulletin 35, 234 p., https://elischolar.library.yale.edu/peabody_museum_natural_history_bulletin/35/.

Owen, R., 1842, Report on British fossil reptiles, part II: Report of the British Association for the Advancement of Science, v. 1841, p. 60–204.

Parish, J.C., 2005, The evolution and palaeobiology of the armoured dinosaurs (Ornithischia: Ankylosauria): Oxford, England, University of Oxford, Ph.D. dissertation, 471 p.

Parish, J.C., and Barrett, P.M., 2004, A reappraisal of the ornithischian dinosaur *Amtosaurus magnus* Kurzanov and Tumanova 1978, with comments on the status of *A. archibaldi* Averianov 2002: Canadian Journal of Earth Sciences, v. 41 p. 299–306, https://cdnsciencepub.com/doi/10.1139/e03-101.

Park, J.Y., 2022, Cretaceous ankylosaurs of Mongolia—implications for paleobiogeography, paleoecology, and evolution, with a taxonomic review of Mongolian armored dinosaurs: Seoul, South Korea, Seoul National University, Ph.D. dissertation, 246 p., https://s-space.snu.ac.kr/handle/10371/188588?mode=full.

Park, J.Y., Lee, Y.-N., Kobayashi, Y., Jacobs, L.L., Barsbold, R., Lee, H.-J., Kim N., Song K.-Y., and Polcyn, M.J., 2021, A new ankylosaurid from the upper Cretaceous Nemegt Formation of Mongolia and implications for paleoecology of armoured dinosaurs: Nature Scientific Reports, v. 11, no. 22928, https://www.nature.com/articles/s41598-021-02273-4.

Parsons, W.L., and Parsons, K.M., 2009, A new ankylosaur (Dinosauria: Ankylosauria) from the Lower Cretaceous Cloverly Formation of central Montana: Canadian Journal of Earth Sciences, v. 46, p. 721–738, http://dx.doi.org/10.1139/E09-045.

Penkalski, P., 2001, Variation in specimens referred to *Euoplocephalus tutus*, *in* Carpenter, K., editor, The armored dinosaurs: Bloomington, Indiana University Press, p. 363–385.

Penkalski, P., and Blows, W.T., 2013, *Scolosaurus cutleri* (Ornithischia: Ankylosauria) from the Upper Cretaceous Dinosaur Park Formation of Alberta, Canada: Canadian Journal of Earth Sciences, v. 50, p. 171–182, https://cdnsciencepub.com/doi/10.1139/cjes-2012-0098.

Pereda-Suberbiola, X., 1993, *Hylaeosaurus*, *Polacanthus* and the systematics and stratigraphy of Wealden armoured dinosaurs: Geological Magazine, v. 130, p. 767–780.

Pereda-Suberbiola, X., 1994, *Polacanthus* (Ornithischia: Ankylosauria), a transatlantic armoured dinosaur from the Early Cretaceous of Europe and North America: Palaeontographica, Abteilung A, v. 232, p. 133–159.

Pereda-Suberbiola, X., and Galton, P.M., 2001, Reappraisal of the nodosaurid ankylosaur *Struthiosaurus austriacus* from the Upper Cretaceous Gosau Beds of Austria, *in* Carpenter, K., editor, The armored dinosaurs: Bloomington, Indiana University Press. p. 173-210.

Pereda-Suberbiola, X., Dantas, P., Galton, P.M., and Sanz, J.L., 2004, Autopodium of the holotype of *Dracopel-*

ta zbyszewskii (Dinosauria, Ankylosauria) and its type horizon and locality (Upper Jurassic, Tithonian), Western Portugal: Neues Jahrbuch für Geologie und Paläontologie Abhandlungen, v. 235, p. 175–196, https://doi.org/10.1127/njgpa/235/2005/175.

Peterson, F., and Turner, C.E., 1998, Stratigraphy of the Ralston Creek and Morrison Formations (Upper Jurassic) near Denver, Colorado: Modern Geology, v. 22, p. 3–38.

Raven, T.J., 2021, The taxonomic, phylogenetic, biogeographic and macroevolutionary history of the armoured dinosaurs (Ornithischia: Thyreophora): Brighton, United Kingdom, University of Brighton, Ph.D. dissertation, 649 p., https://cris.brighton.ac.uk/ws/portalfiles/portal/23893138/Raven_PhD_Thesis.pdf.

Raven, T.J., Barrett, P.M., Joyce, C.B., and Maidment, S.C.R., 2023, The phylogenetic relationships and evolutionary history of the armoured dinosaurs (Ornithischia: Thyreophora): Journal of Systematic Palaeontology, v. 21, no. 1, 2205433, https://doi.org/10.1080/14772019.2023.2205433.

Raven, T.J., Barrett, P.M., Pond, S.B., and Maidment, S.C.R., 2020, Osteology and taxonomy of British Wealden Supergroup (Berriasian–Aptian) ankylosaurs (Ornithischia, Ankylosauria): Journal of Vertebrate Palaeontology, v. 40, e1826956, https://doi.org/10.1080/02724634.2020.182695.

Russell, L.S., 1940, *Edmontonia rugosidens* (Gilmore), an armoured dinosaur from the Belly River Series of Alberta: University of Toronto Studies, Geology Series, v. 43, p. 3–28.

Russo, J.P.V.M., 2024, Evolution of polacanthid ankylosaurs and description of a new skeleton from the Late Jurassic of Portugal: Lisbon, Portugal, NOVA School of Science and Technology, Ph.D. dissertation, 305 p., https://run.unl.pt/bitstream/10362/183949/1/Russo_2024.pdf.

Russo, J., and Mateus, O., 2021, History of the discovery of the ankylosaur *Dracopelta zbyszewskii* (Upper Jurassic), with new data about the type specimen and its locality: Comunicações Geológicas, v. 108, p. 27–34, https://repositorio.lneg.pt/entities/publication/5e546e64-9ed0-4372-8b6f-c133f436e7f6.

Scheyer, T.M., and P.M., Sander, 2004, Histology of ankylosaur osteoderms—implications for systematics and function: Journal of Vertebrate Paleontology, v. 24, p. 874–893.

Schmude, D.E., and Weege, C.J., 1996, Stratigraphic relationship, sedimentology, and taphonomy of Meilyn, a dinosaur quarry in the basal Morrison Formation of Wyoming, *in* Morales, M., editor, The continental Jurassic: Museum of Northern Arizona Bulletin 60, p. 547–554.

Seeley, H.G., 1881, The reptile fauna from the Gosau Formation preserved in the geological museum of the University of Vienna—with a note on the geological horizon of the fossils of the Neue Welt, west of Werner Neustad: Quarterly Journal of the Geological Society of London, v. 37, p. 620–707, https://www.lyellcollection.org/doi/abs/10.1144/GSL.JGS.1881.037.01-04.49.

Seeley, H.G., 1887, On the classification of the fossil animals commonly named Dinosauria: Proceedings of the Royal Society of London, v. 43, p. 165–171, https://royalsocietypublishing.org/doi/epdf/10.1098/rspl.1887.0117.

Senter, P., 2011, Evidence for a sauropod-like metacarpal configuration in ankylosaurian dinosaurs: Acta Palaeontologica Polonica, v. 56, p. 221–224, https://www.app.pan.pl/archive/published/app55/app20091105.pdf.

Sereno, P.C., 1986, Phylogeny of the bird hipped dinosaurs (Ornithischia): National Geographic Research, v. 2, p. 234–256.

Stanford, R., Weishampel, D.B., and DeLeon, V.B., 2011, The first hatchling dinosaur reported from the Eastern United States—*Propanoplosaurus marylandicus* (Dinosauria: Ankylosauria) from the Early Cretaceous of Maryland, U.S.A.: Journal of Paleontology, v. 85, p. 916–924, https://doi.org/10.1666/10-113.1.

Tremaine, K., D'Emic, M., Williams, S., Hunt-Foster, R.K., Foster, J., and Mathews, J., 2015, Paleoecological implications of a new specimen of the ankylosaur *Mymoorapelta maysi* from the Hanksville-Burpee Quarry, latest Jurassic (Tithonian) Morrison Formation (Brushy Basin Member) [abs.]: Journal of Vertebrate Paleontology Program and Abstracts, p. 226.

Thompson, R.C., Parisch, J.C., Maidment, S.R., and Barrett, P.M., 2011, Phylogeny of the ankylosaurian dinosaurs (Ornithischia: Thyreophora): Journal of Systematic Paleontology, p. 1–12, https://www.tandfonline.com/doi/full/10.1080/14772019.2011.569091.

Trujillo, K.C., 2006, Clay mineralogy of the Morrison Formation (Upper Jurassic–?Lower Cretaceous), and its use in long distance correlation and paleoenvironmental analyses, *in* Foster, J., and Lucas, S.G., editors, Paleontology and geology of the Upper Jurassic Morrison Formation: Museum of Natural History and Science Bulletin 36, 249 p., https://nmdigital.unm.edu/digital/collection/bulletins/id/803/.

Trujillo, K.C., Foster, J.R., Hunt-Foster, R.K., and Chamberlain, K.R., 2014, A U/Pb age for the Mygatt-Moore Quarry, Upper Jurassic Morrison Formation, Mesa County, Colorado: Volumina Jurassica, v. 12, no. 2, p. 107–114, https://vjs.pgi.gov.pl/article/view/26613/18324.

Trujillo, K.C., and Kowallis, B.J., 2015, Recalibrated legacy $^{40}Ar/^{39}Ar$ ages for the Upper Jurassic Morrison Formation: Geology of the Intermountain West, v. 2, p. 1–8, https://giw.utahgeology.org/giw/index.php/GIW/article/view/6.

Turner, C.E., and Peterson, F., 1999, Biostratigraphy of dinosaurs in the Upper Jurassic Morrison Formation of the Western Interior, U.S.A., *in* Gillette, D.D., editor, Vertebrate paleontology in Utah: Utah Geological Survey Miscellaneous Publication 99-1, p. 77–114, https://ugspub.nr.utah.gov/publications/misc_pubs/mp-99-1.pdf.

Turner, C.E., and Peterson, F., 2004, Reconstruction of the Upper Jurassic Morrison Formation extinct ecosystem—a synthesis: Sedimentary Geology, v. 167, p. 309–355.

Vickaryous, M.K., 2001, Skull morphology of the Ankylosauria: Canada, University of Calgary, M.S. thesis, 269 p., https://www.collectionscanada.gc.ca/obj/s4/f2/dsk3/ftp05/mq64985.pdf.

Vickaryous, M.K., Maryańska, T., and Weishampel, D.B., 2004, Ankylosauria, *in* Weishampel, D.B., Dodson, P., and Osmólska, H., editors, The Dinosauria, 2nd edition: Berkeley, University of California Press, p. 363–392.

Vickaryous, M.K., Russell, A.P., and Currie, P.J., 2001, Cranial ornamentation of ankylosaurs (Dinosauria: Thyreophora)—reappraisal of developmental hypotheses, *in* Carpenter, K. editor, The armored dinosaurs: Bloomington, Indiana University Press, p. 318–340.

Yang, J.-T., You, H.-L., Li, D.-Q., and Kong, D.-L., 2013, First discovery of polacanthine ankylosaur dinosaur in Asia: Vertebrata PaAsiatica, v. 51, p. 17–30.